PB83-146340

Atmospheric Chemistry of Several Toxic Compounds

(U.S.) Environmental Sciences Research Lab.
Research Triangle Park, NC

Nov 82

U.S. Department of Commerce
National Technical Information Service
NTIS

EPA-600/3-82-092
November 1982

PB83-146340

ATMOSPHERIC CHEMISTRY OF SEVERAL TOXIC COMPOUNDS

by

Edward Edney
Steven Mitchell
Joseph J. Bufalini

Atmospheric Chemistry and Physics Division
Environmental Sciences Research Laboratory
Research Triangle Park, NC 27711

ENVIRONMENTAL SCIENCES RESEARCH LABORATORY
OFFICE OF RESEARCH AND DEVELOPMENT
U. S. ENVIRONMENTAL PROTECTION AGENCY
RESEARCH TRIANGLE PARK, NC 27711

REPRODUCED BY
NATIONAL TECHNICAL
INFORMATION SERVICE
U.S. DEPARTMENT OF COMMERCE
SPRINGFIELD, VA. 22161

TECHNICAL REPORT DATA *(Please read Instructions on the reverse before completing)*		
1. REPORT NO. EPA-600/3-82-092	2.	3. RECIPIENT'S ACCESSION NO. PB83 146340
4. TITLE AND SUBTITLE ATMOSPHERIC CHEMISTRY OF SEVERAL TOXIC CHEMICALS		5. REPORT DATE November 1982 6. PERFORMING ORGANIZATION CODE
7. AUTHOR(S) Edward Edney, Steven Mitchell, and Joseph Bufalini		8. PERFORMING ORGANIZATION REPORT NO.
9. PERFORMING ORGANIZATION NAME AND ADDRESS Environmental Sciences Research Laboratory Office of Research and Development U.S. Environmental Protection Agency Research Triangle Park, NC 27711		10. PROGRAM ELEMENT NO. CCUL1A/02-0050 (FY-82) 11. CONTRACT/GRANT NO.
12. SPONSORING AGENCY NAME AND ADDRESS Environmental Sciences Research Laboratory-RTP, NC Office of Research and Development U.S. Environmental Protection Agency Research Triangle Park, North Carolina 27711		13. TYPE OF REPORT AND PERIOD COVERED Final 14. SPONSORING AGENCY CODE EPA/600/09
15. SUPPLEMENTARY NOTES		

16. ABSTRACT

The hydroxyl radical initiated gas phase oxidation of several toxic compounds in nitrous acid, oxides of nitrogen, in air mixtures were investigated. The chemical species studied were: formaldehyde, acrylonitrile, vinylidine chloride, trichloroethylene, allyl chloride, acetaldehyde, and acrolein. Propylene and ethylene were also studied for comparative purposes. Experimental protocols were established for measuring hydroxyl rate constants. Product studies were also conducted. The results and their atmospheric implications are discussed.

17. KEY WORDS AND DOCUMENT ANALYSIS		
a. DESCRIPTORS	b. IDENTIFIERS/OPEN ENDED TERMS	c. COSATI Field/Group
18. DISTRIBUTION STATEMENT RELEASE TO PUBLIC	19. SECURITY CLASS *(This Report)* UNCLASSIFIED 20. SECURITY CLASS *(This page)* UNCLASSIFIED	21. NO. OF PAGES 120 22. PRICE

EPA Form 2220-1 (Rev. 4-77) PREVIOUS EDITION IS OBSOLETE

NOTICE

This document has been reviewed in accordance with U.S. Environmental Protection Agency policy and approved for publication. Mention of trade names or commercial products does not constitute endorsement or recommendation for use.

ABSTRACT

The hydroxyl radical-initiated gas-phase oxidation of several toxic compounds in mixtures of nitrous acid, oxides of nitrogen, and air were investigated. The chemical species studied were: formaldehyde, acrylonitrile, vinylidene chloride, trichloroethylene, allyl chloride, acetaldehyde, and acrolein. Propylene and ethylene were also studied for comparative purposes. Experimental protocols were established for measuring hydroxyl rate constants. Product studies were also conducted. The results and their atmospheric implications are discussed.

CONTENTS

Abstract. iii
Tables. vi
Figures vii

1. Introduction 1
2. Experimental 7
3. Data Analysis. 17
   Propylene 21
   Ethylene. 25
   Formaldehyde. 27
   Acrylonitrile 28
   Vinylidene chloride 31
   Trichloroethylene 35
   Allyl chloride. 38
   Acetaldehyde. 41
   Acrolein. 44
4. Results and Discussion 55

References. 60
Appendix: Preparation of HONO. 62

Preceding page blank

TABLES

Number		Page
1	Compounds Studied: Their Chemical Structure, Specific Gravity and Uses.	4
2	Concentration of Selected Toxic Compounds.	6
3	Manufacturers of Compounds	12
4	Reference Library.	15
5	Propylene, HONO, NO_x Data.	22
6	Ethylene, HONO, NO_x Data	27
7	Formaldehyde, HONO, NO_x Data	29
8	Acrylonitrile, HONO, NO_x Data.	30
9	Vinylidene chloride, HONO, NO_x Data.	33
10	Trichloroethylene, HONO, NO_x Data.	35
11	Allyl Chloride, HONO, NO_x Data	40
12	Acetaldehyde, HONO, NO_x Data	42
13	Predicted Weighted Contributions to $\Delta[NO]/\Delta[Acetaldehyde]$. . .	45
14	Acrolein, HONO, NO_x Data	46
15	Acrolein, Cl_2, NO_2 Data.	50
16	Experimental and Literature OH Rate Constants.	56
17	Atmospheric Lifetimes.	57

FIGURES

Number		Page
1	Long path cell and IR spectrometer.	64
2	Schematic of data handling system	65
3	HONO generating system.	66
4a	MCT spectrum of reactants of propylene/HONO/NO_x run	67
4b	MCT spectrum of propylene 5-min irradiation	67
5a	Five-min MCT propylene spectrum with HONO and propylene subtracted	68
5b	Five-min MCT propylene spectrum with HONO, propylene, and acetaldehyde subtracted.	68
6	Five-min MCT propylene spectrum with HONO, propylene, acetaldehyde, and HNO_3 subtracted.	69
7a	InSb spectrum of reactants of propylene/HONO/NO_x run.	70
7b	InSb spectrum of propylene 5-min irradiation.	70
8a	Five-min InSb propylene spectrum with water and propylene subtracted	71
8b	Five-min InSb propylene spectrum with water, propylene, acetaldehyde, and formaldehyde subtracted.	71
9a	InSb spectrum of initial NO_2.	72
9b	Left - MCT spectrum of initial NO, Right: 5-min MCT spectrum	72
10a	MCT spectrum of reactants of ethylene/HONO/NO_x run.	73
10b	MCT spectrum of ethylene 12-min irradiation	73
11a	Twelve-min MCT ethylene spectrum with HONO and ethylene subtracted	74

Number		Page
12a	InSb spectrum of reactants of ethylene/HONO/NO_x run.	75
12b	InSb spectrum of ethylene 12-min irradiation	75
13a	Twelve-min InSb ethylene spectrum with ethylene and water subtracted.	76
13b	Twelve-min InSb ethylene spectrum with ethylene, water, and formaldehyde subtracted	76
14a	InSb spectrum of ethylene 12-min irradiation	77
15a	InSb spectrum of reactants of formaldehyde/HONO/NO_x run.	78
15b	InSb spectrum of formaldehyde 12-min irradiation	78
16	InSb spectrum of formaldehyde 12-min irradiation	79
17a	MCT spectrum of reactants of acrylonitrile/HONO/NO_x run.	80
17b	MCT spectrum of acrylonitrile 20-min irradiation	80
18a	MCT spectrum of acrylonitrile spectrum with HONO, acrylonitrile, and water subtracted.	81
18b	Twenty-min MCT acrylonitrile spectrum with HONO, acrylonitrile, water, and HNO_3 subtracted.	81
19a	Twenty-min InSb acrylonitrile spectrum with water subtracted	82
19b	Twenty-min InSb acrylonitrile spectrum with water, acrylonitrile, and formaldehyde subtracted.	82
20	Twenty-min InSb acrylonitrile spectrum with NO subtracted.	83
21a	MCT spectrum of reactants of vinylidene chloride/HONO/NO_x run.	84
21b	MCT spectrum of vinylidene chloride 7-min irradiation.	84
22a	Seven-min MCT vinylidene chloride spectrum with HONO, vinylidene chloride, and water substracted.	85
22b	Seven-min MCT vinylidene chloride spectrum with HONO, vinylidene chloride, water phosgene, and HNO_3 subtracted.	85
23a	MCT spectrum of chloroacetyl chloride.	86

Number		Page
23b	Seven-min MCT vinylidene chloride spectrum with HONO, vinylidene chloride, water, phosgene, HNO_3, and chloroacetyl chloride subtracted.	86
24a	InSb spectrum of reactants of vinylidene chloride/HONO/NO_x run	87
24b	InSb spectrum of vinylidene chloride 7-min irradiation	87
25a	Seven-min InSb vinylidene chloride spectrum with vinylidene chloride and water subtracted	88
25b	Seven-min InSb vinylidene chloride spectrum with vinylidene chloride, water, and formaldehyde subtracted.	88
26a	MCT spectrum of reactants of trichloroethylene HONO/NO_x run. .	89
26b	MCT spectrum of trichloroethylene 15-min irradiation	89
27a	Fifteen-Min MCT trichloroethylene spectrum with trichloroethylene subtracted.	90
27b	MCT spectrum of dichloroacetyl chloride.	90
28a	Fifteen-min MCT trichloroethylene spectrum with trichloroethylene, HONO, water, and dichloroacetyl chloride subtracted.	91
28b	Fifteen-min MCT trichloroethylene spectrum with trichloroethylene, HONO, water, dichloroacetyl chloride, and phosgene subtracted	91
29a	MCT spectrum of formyl chloride.	92
29b	Fifteen-min MCT trichloroethylene spectrum with trichloroethylene, HONO, water, dichloroacetyl chloride, phosgene, and formyl chloride subtracted.	92
30a	MCT spectrum of reactants of allyl chloride/HONO/NO_x run . . .	93
30b	MCT spectrum of allyl chloride 5-min irradiation	93
31a	Five-min MCT allyl chloride spectrum with HONO, allyl chloride, and water subtracted.	94
32a	InSb spectrum of reactants of allyl chloride/HONO/NO_x run. . .	96
32b	InSb spectrum of allyl chloride 5-min irradiation.	96

Number		Page
33a	Five-min InSb allyl chloride spectrum with water and allyl chloride subtracted.	96
33b	Five-min InSb allyl chloride spectrum with water allyl chloride and formaldehyde subtracted	96
34a	MCT spectrum of reactants of acetaldehyde/HONO/NO_x run.	97
34b	MCT spectrum of acetaldehyde 10-min irradiation	97
35a	Ten-min MCT acetaldehyde spectrum with HONO subtracted.	98
35b	Ten-min MCT acetaldehyde spectrum with HONO, methyl nitrate, acetaldehyde, and water subtracted	98
36a	MCT spectrum of peroxy acetyl nitrate	99
36b	Ten-min MCT acetaldehyde spectrum with HONO, acetaldehyde, water, HNO_3, and peroxy acetyl nitrate subtracted.	99
37a	InSb spectrum of reactants of acetaldehyde/HONO/NO_x run	100
37b	InSb spectrum of acetaldehyde Ten-min irradiation	100
38a	MCT spectrum of reactants of acrolein/HONO/NO_x run.	101
38b	MCT spectrum of acrolein four-min irradiation	101
39a	Four-min MCT acrolein spectrum with acrolein, HONO, water, and HNO_3 subtracted.	102
39b	MCT spectrum of APAN.	102
40a	MCT spectrum of APAN, acrolein, NO_2, and peroxy nitric acid . .	103
41a	Four-min MCT acrolein spectrum with acrolein, HONO, water, HNO_3, and APAN subtracted.	104
41b	MCT spectrum of glycoaldehyde	104
42a	Four-min MCT acrolein spectrum with acrolein, HONO, water, HNO_3, APAN, and glycoaldehyde subtracted	105
43a	InSb spectrum of reactants of acrolein/HONO/NO_x run	106
43b	InSb spectrum of acrolein four-min irradiation.	106
44a	Four-min InSb acrolein spectrum with acrolein subtracted. . . .	107

Number		Page
44b	Four-min InSb acrolein spectrum with acrolein, water, and formaldehyde subtracted.	107
45a	InSb spectrum of acrolein four-min irradiation.	108

SECTION 1

INTRODUCTION

Because large amounts of toxic chemicals are being emitted into the atmosphere, fears have developed concerning their deleterious effects upon man and the rest of the ecosystem. A number of chemical species have been found to be carcinogenic and/or mutagenic. EPA's Environmental Sciences Research Laboratory has addressed this issue by conducting research programs to investigate the emission rates, ambient concentrations, and atmospheric fate of these species. This report examines the atmospheric fate of several toxic compounds.

Determining atmospheric fates of atmospheric pollutants has a long history in air pollution research (1). Much of the work has been associated with the formation of photochemical smog. Here, emphasis has not been on the detailed fate of the individual hydrocarbons as much as on their role in forming ozone (O_3). In fact, much of the earlier work has been conducted in smog chambers where one typically measures the hydrocarbon (HC), nitric oxide (NO), nitrogen dioxide (NO_2), and O_3 concentrations (2). In some experiments formaldehyde, peroxyacetyl nitrate (PAN), and carbon monoxide (CO) were measured (3). This type of information addresses questions like the O_3-forming potential of the HC, the influence of HC/oxides of nitrogen (NO_x) ratio on O_3 production, and the number of NO to NO_2 conversions per unit destruction of the HC. Only indirectly is one able to establish a chemical mechanism for the reaction of the HC. Confounding the problem in

the earlier studies was the poor sensitivity and specificity of the analytical equipment. Reaction products were usually observed by either gas chromatography or wet chemistry. Although both of these procedures can be made both sensitive and specific, there is a need to know the identity of the reaction products since many polar products will not be identified by g.c. or there may be interferences with the wet chemical procedures. Because of this, even now, propylene, the "grandfather" of HCs is still not understood completely in spite of the hundreds and perhaps thousands of propylene/NO_x runs conducted over the past 30 years.

New techniques are needed to elucidate the chemical mechanism of toxic chemicals when it is possible that the products themselves may be toxic. One new technique that has been employed in the last few years is long path Fourier transform infrared (FTIR) spectroscopy which has begun to shed light on the product distribution due to the photooxidation of propylene and other simple alkenes (4).

Besides identifying the individual products of the photodegradation processes, the time scale on which these events occur is also of interest. Chemicals emitted into the atmosphere can react with O_3, hydroxyl (OH), nitrogen trioxide (NO_3), RO_2, and other free radicals as well as photolyze. Evidence suggests that photolysis, O_3, and OH attack dominate as homogeneous gas phase removal processes. In general, HCs will not photolyze in the troposphere. For non-alkene HCs one can neglect O_3 attack. In the case of carbonyl compounds both photolysis and OH attack must be considered. Ozone attack is also important if the compound is not saturated. We have chosen, in this study, to examine the OH rate constants with the organic compounds and the subsequent products formed in an NO_x containing system.

A number of techniques have been developed to measure OH rate constants. Examples of these are flash photolysis-resonance fluoresence, discharge flow-resonance fluoresence, discharge flow electron spin resonance detection, discharge flow-laser magnetic resonance, discharge flow-mass spectrometry, and relative rate methods (5). Most of these techniques are conducted at low pressure (less than 10 Torr) and little information is gained concerning the products formed.

The goal of this study was to establish the OH-initiated chemical mechanism for seven organic chemicals. We attempted to develop techniques which yield both rate constants and details of the reaction mechanism. The chemicals studied in this report are vinylidene chloride, trichloroethylene, formaldehyde, acetaldehyde, acrylonitrile, acrolein, and allyl chloride. Propylene and ethylene were used as the test compounds to check the method. A long path FTIR spectrometer facility was employed as the analytical tool for this study. The development of a technique for generating copious amounts of OH radicals via the photolysis of nitrous acid (HONO) has served as an important starting point. Methods have been developed to analyze complicated product spectra. It has been found that by utilizing these methods that the results from one FTIR experiment can be used to obtain both the OH rate constant and the product distribution.

The choice of the particular compounds studied was based on two facts: that they are high-volume-production chemicals and that they either have been shown to be carcinogenic and/or mutagenic, or there are strong indications that they are. Table 1 lists these compounds as well as their chemical structure, specific gravity and uses. Typical and maximum urban concentrations are presented in Table 2.

TABLE 1. COMPOUNDS STUDIED: THEIR CHEMICAL STRUCTURE, SPECIFIC GRAVITY, AND USES

Compound	Chemical Structure	Specific Gravity	Uses
Acrylonitrile	CH_2=CHCN	0.80	Raw material for synthetic fibers, synthetic resins, synthetic rubbers, antioxidants, pharmaceuticals, dyes and surfactants.
Acrolein	CH_2=CHCHO	0.84	Intermediate for synthetic glycerine, polyurethane, polyester resin, methionine, pharmaceuticals, and herbicides; material for treatment of textile fibers, manufacture of colloidal forms of osmium, rhodium, and ruthenium.
Acetaldehyde	CH_3CHO	0.78	Manufacture of acetic acid, acetic anhydride, n-butanol, 2-ethyl-hexanol, peracetic acid, pentaerythritol, pyridine, chloral, 1,3-butyleneglycol and trimethylolpropane; intermediate for various chemicals.
Formaldehyde	HCHO	0.82	Phenolic, urea, and melamine resins; organic synthesis, fertilizer, medicine, reducing agent, hardening agent, dyes, and perservatives.
Trichloroethylene	CCl_2=CHCl	1.465	Metal degreasing, extraction solvent for oils, fats, and waxes; solvent dyeing, dry cleaning, refrigerant, and exchange liquid; organic synthesis fumigant; medicine, cleaning and drying electronic parts.

TABLE 1. (CONTINUED)

Compound	Chemical Structure	Specific Gravity	Uses
Allyl chloride	$CH_2=CHCH_2Cl$	0.94	Manufacture of allyl alcohol and other allyl compounds. (Base material for varnishes, plastics, adhesives, pharmaceuticals, glycerin, perfumes, and insecticides.)
Vinylidene Chloride	$CH_2=CCl_2$	1.213	Intermediate for vinylidene polymers.

TABLE 2. CONCENTRATION OF SELECTED TOXIC COMPOUNDS

Compound	Typical Urban	Max Urban
Acetaldehyde[a]	1 to 2 ppb	37 ppb
Acrolein[b]	1 to 2 ppb	12.8 ppb
Acrylonitrile[c,d]	--	--
Allyl Chloride[c]	5 ppt	5 ppt
Formaldehyde[c]	10 to 20 ppb	41 ppb
Trichloroethylene[c]	0.1 to 0.2 ppb	224 ppt

[a]Grosjean, D. Environ. Sci. Technol., 16, 254 (1982).

[b]Cohen, I.R. and A.P. Altshuller, Anal. Chem. 33, 726 (1961).

[c]Singh, H.B., L.J. Salas, A. Smith, R. Stiles, and H. Shigeishi, EPA Interim Report, U.S. Environmental Protection Agency, Research Triangle Park, NC, November 1980.

[d]Measurement method not available for ambient air analysis.

In the next section we describe the experimental apparatus, the technique employed to generate HONO and the details of the experimental technique established to measure both reaction rates and products. The Data Analysis section explains how the data was analyzed in order to extract the OH rate constants and the chemical mechanisms. We also examine the results from irradiations of all of the chemicals. Finally in the last section we discuss our results and their atmospheric implications.

SECTION 2

EXPERIMENTAL

All experiments were conducted in a 9-m borosilicate glass reaction chamber. The chamber consists of 6 cylinders 1.5 m in length, 0.31 m in diameter, and having a total of 700 l volume. Aluminum spacers 1.91 cm wide with 0.32 cm Teflon gaskets are used to join the sections. Each spacer has three ports used to introduce and remove the gases. Gases are blown into the chamber through ports in all five spacers from a central manifold system to insure proper mixing. An eight mirror multiple-reflection long path optical system is used to provide the 216-m path length for the experiments (6). A large displacement vacuum pump is attached to one end plate through a ball vacuum valve and can evacuate the chamber to less than one Torr in about five min. Gas samples are introduced into the chamber from the mixing manifold which consists of multiple inlet valves, a mixing bulb of known volume, and two MKS Baratron pressure gauges covering the range from 10^{-3} Torr to 10^{3} Torr.

Each section of the chamber is surrounded by a bank of 16 40W ultraviolet fluorescent lamps. Twelve of the lamps are "black lamps" with maximum spectral intensity near 365 nm and four are "sun lamps" with the intensity maximum near 310 nm. Since the radiation is filtered through the Pyrex pipe, only a negligible amount of radiation with wavelengths below 300 nm reaches the reacting gas mixture. The photolysis rate (k)

for NO_2 in the chamber is 0.60 min^{-1}. This was obtained in N_2.

A Digilab FTIR spectrometer which includes a glow bar as the IR radiation source, a computer-controlled scanning Michelson interferometer coupled to the optical system of the long path cell, and a pair of IR-sensitive detectors serve as a detection system for the reacting gas phase mixture. The mercury-cadmium-telluride (MCT) and indium-antimonide (InSb) liquid nitrogen-cooled detectors can cover the spectral region from 700 cm^{-1} to 3400 cm^{-1} which enables detection of most hetero-nuclear gases. A NOVA 1200 computer controls the system. Data was stored in digitized form on both an Alpha Data 128K fixed head disk and a Kennedy Magnetic Tape Unit. Data can be displayed on either a Digiscope CRT display or a Houston Instruments x-y plotter. Typically 30 to 200 interferograms are collected for signal averaging purposes. The transmission spectra were obtained by Fourier transforming the co-added interferograms. The spectra were taken at 1.0 cm^{-1} resolution and the transform uses triangular apodization. A diagram of the long path cell and the Michelson interferometer is shown in Figure 1. A schematic diagram of the data handling system is shown in Figure 2.

HONO has been found to be a convenient source of OH radicals. In the presence of radiation between 3000 Å and 4000 Å, HONO readily photolyzes into OH radicals and NO. The technique used in this study is an adaptation of the method developed by Nash and Cox (7,8). A 1.2 x 10^{-2} M solution of sodium nitrite ($NaNO_2$) and a 5% by volume solution of sulfuric acid (H_2SO_4) are prepared. A 100 ml $NaNO_2$ solution was added dropwise to 150 ml of the H_2SO_4 solution in a 2 l mixing bulb. The mixture was slowly stirred by a magnetic stirring bar. The dissolved H^+ ions combine with the NO_2^- ions to

produce HONO which goes into the gas phase. The HONO gas was flushed into the long path cell with N_2, at the same time as some NO, NO_2, and H_2O. The drop rate for the $NaNO_2$ was about two drops/s and the N_2 flow rate is approximately 8 l/min. An icewater bath was used to trap some of the water vapor. Figure 3 shows the HONO generating system.

We determined the amount of HONO generated by this technique by using an apodization-corrected IR absorption coefficient from Calvert (9). We also checked this result by performing N_2 balances on irradiated HONO/NO/NO_2 mixtures in N_2 and O_2. We found an absorption coefficient (base 10) = 4.15 x 10^{-4} $ppm^{-1}min^{-1}$ for $\bar{\nu}$= 1250 cm^{-1}. This absorption coefficient is for the total HONO concentration, including both the cis-and trans-isomers.

The technique as described generates about 4 ppm HONO in the cell, comparable amounts of NO, and about 1.5 ppm NO_2. Substantial amounts of water were also introduced into the cell. Modifications of this method have enabled reducing both the NO and NO_2 concentrations relative to HONO, however we needed excess NO for the experiments. A detailed description of the HONO production technique appears in Appendix A.

An important element of this study was establishing an experimental protocol for measuring OH rate constants as well as establishing detailed chemical mechanisms for certain chemicals using the long path cell. Above we described the chamber, the detection system, and the method for HONO production. Next we describe in detail the actual experimental procedure.

All data was calculated in the absorbance mode and stored on magnetic tape. The absorbance mode is defined by the following relationship:

$$\text{Absorbance} = -\log \frac{T_1(\bar{\nu})}{T_2(\bar{\nu})} \qquad \text{(I-1)}$$

$$T_j(\bar{\nu}) = F_j(\bar{\nu})I_j(\bar{\nu})\exp - \left(\sum_{i=1}^{N_j} k_{ji}(\bar{\nu})\rho_{ji}\ell\right) \qquad \text{(I-2)}$$

where

$T_j(\bar{\nu})$ = Transmission spectrum j

$F_j(\bar{\nu})$ = Response function of IR detector for spectrum j

$I_j(\bar{\nu})$ = Intensity function of the IR source for spectrum j

$k_{ji}(\bar{\nu})$ = Absorption coefficient for species i in spectrum j

ρ_{ji} = Density of absorbing species i in spectrum j

ℓ = Path length

$\bar{\nu}$ = Wavenumber

N_j = Total number of absorbing species in spectrum j

$T_2(\bar{\nu})$ was chosen to be a spectrum of 700 Torr cylinder air (< 1 ppm total HC). Carbon dioxide was not removed from the air. Thus, the CO_2 could not be measured in the experiments. If we assume that the intensity function and the response function are the same for the spectrum of interest and the air reference spectrum we find:

$$\text{Absorbance} = \sum_{i=1}^{N} \kappa_i(\bar{\nu})\rho_i\ell \qquad \text{(I-3)}$$

where

$$\kappa_i(\bar{\nu}) = (1/2.3)k_i(\bar{\nu})$$

In this expression we have dropped the subscript 1. If the intensity function changes, it will offset the absorbance spectrum. For graphical convenience we define the absorbance to be 100 times the result shown in Equation I-3.

An HONO/NO_x/organic chemical experiment was conducted by first obtaining a reference spectrum of 700 Torr cylinder air. Usually 200 scans at 1 cm^{-1} resolution were taken. To cover the range between 700 cm^{-1} to 3400 cm^{-1} it was necessary to obtain spectra with both the MCT and the InSb detectors. Each spectrum took approximately 15 min to collect. The cell was evacuated to about 300 Torr and the HONO was put into the cell as described. A total of 100 l of N_2 was employed to flush the HONO into the cell bringing the total pressure to 400 Torr. Approximately 11 ppm of NO were then added, flushed into the cell with N_2 to avoid NO_2 formation. The total pressure was brought to 500 Torr. Absorbance spectra for both detectors were then taken. These spectra permitted evaluation of the initial HONO, NO, and NO_2. Finally the organic chemical was introduced into the cell. Species which are liquids at room temperatures were injected into a gas stream of cylinder air with either a 10 or 100 µl syringe. The gas phase species propylene and ethylene were metered into the cell using the dilution manifold. Formaldehyde was produced by slowly heating paraformaldehyde into the mixing bulb of the dilution manifold and, after the appropriate dilutions, flushing into the long path cell. Acetaldehyde was introduced into the cell by placing a small amount of the liquid in a glass vial which was located at one of the ports of the dilution manifold. The acetaldehyde was cooled to liquid N temperatures and all vapor above the frozen acetaldehyde was removed. This distillation process was repeated a number of times. Finally the vapor produced above the liquid was diluted and introduced into the cell. In all cases the total pressure in the cell was brought to 700 Torr with cylinder air. A list of the manufacturers of the toxic compounds used is given in Table 3.

TABLE 3. MANUFACTURERS OF COMPOUNDS

Compounds	Manufacturer
Paraformaldehyde	Matheson Coleman and Bell
Acetaldehyde	Eastman Kodak Company
Acrolein	Eastman Kodak Company
Acrylonitrile	Mallinckrodt Chemical Works
Vinylidene Chloride	Fisher Scientific Company
Allyl chloride	Eastman Kodak Company
Trichloroethylene	Fisher Scientific Company
Propylene	Union Carbide Corporation*
Ethylene	Union Carbide Corporation
Nitrogen Dioxide	Union Carbide Corporation
Nitric Oxide	Union Carbide Corporation

*Linde Division

Because many of these species are considered hazardous, all transfers from bottles to syringes were conducted under a hood.

After introducing the organic compound, reference spectra scans were taken, which constituted the reactant spectra and displayed the IR bands of HONO, NO, NO_2, and the chemical under investigation.

In the process of producing HONO, substantial amounts of H_2O were introduced into the cell, relative humidity ~5%, which made it difficult to interpret the IR spectrum between 1300 cm^{-1} to 2000 cm^{-1}. Next the fluorescent lights were turned on and the mixture was irradiated from

between 4 and 20 min. The lights were then turned off and the products were scanned 200 times, which was also calculated in the absorbance mode. This data, as all previous data, was stored on magnetic tape for future analysis. All experiments were conducted at room temperature (~23 $\pm$ 1.5^{o}C).

The initial HONO and NO_2 concentrations were determined from the 500 Torr spectrum. The IR bands used to determine these concentrations were 1250 cm^{-1} and 2890 cm^{-1}, respectively. The H_2O interference prevented the use of the strong 1600 cm^{-1} band for NO_2. By repeatedly introducing known amounts of NO into the cell an absorption coefficient of 0.83 x 10^{-4} ppm^{-1} m^{-1} was determined. The amount of NO present was determined using the spike at 1876 cm^{-1}. The high wave number side was used to establish a baseline. Care must be exercized when using this band because there is a small H_2O interference. In this case calibration curves were established by using known amounts of NO and H_2O. The above mentioned coefficient is only good if the NO concentration is greater than 3 ppm. The reactant concentration of the compound of interest was checked against reference spectra.

A major effort was spent analyzing product spectra. These spectra are complicated and at many points in the spectrum a number of newly formed products as well as remaining reactants contribute to the absorbance. To accurately identify and measure the concentration of the products it is necessary to systematically subtract the absorbances due to the remaining reactants and the known products to uncover the absorbances of other products. This operation is available via the Digilab arithmetic software package. If we spectrally subtract two spectra we see from I-3 that

$$\text{Absorbance (A)-Absorbance(B)} = \sum_{i-1}^{N} \kappa_i(\bar{\nu})\ell(\rho_i{}^{A} - \rho_i{}^{B})$$

With the Digilab package one can subtract a constant times the absorbance, a powerful technique and numerous examples will be shown. However, the applicability of this technique is limited by the size of the reference library. Because of this, much of the past year was spent establishing a reference library on magnetic tape. Table 4 displays a list of the compounds in the library. Not only are stable species included in this library, but also a number of unstable species such as PAN, dinitrogen pentoxide (N_2O_5), and peroxy nitric acid appear. Spectra of compounds such as dichloroacetyl chloride and glycoaldehyde are also in the library. The library of spectra were obtained by making the species in the long path cell and subtracting the contribution of the remaining reactants and other compounds formed. While spectral subtraction is effective, problems arise when attempting to subtract either two large absorbances, or very narrow bands. The method is most effective when subtracting two moderately absorbing broad bands.

When evaluating an MCT-product spectrum, we found it convenient to first subtract the remaining HONO absorbance, then the remaining toxic compound contribution, followed by the H_2O contribution. Subtracting the H_2O cleared up the region between 1100 cm^{-1} and 1400 cm^{-1} and sometimes enabled seeing some general features in the carbonyl region. The absorbance due to HONO in the InSb was small and isolated to a region where one rarely sees any absorbances (approximately 2495 cm^{-1}). To avoid needlessly introducing any noise into the spectra no HONO spectral subtraction was conducted. Water was the first species subtracted in the InSb, followed by removal of the remaining absorbance due to the organic compound. The remaining spectral subtractions depended on which particular compound was

TABLE 4. REFERENCE LIBRARY

Hydrocarbons	Carbonyls	NO_x	Others
Ethylene	Benzaldehyde	Nitrous acid	Ozone
Propylene	Methacrolein	Nitrogen dioxide	Hydrogen chloride
Cis-2-butene	Methyl vinyl ketone	Meta-nitrotoluene	Water
Toluene	Methyl glyoxal	Nitric acid	Carbon monoxide
Ortho-xylene	Glyoxal	Nitric oxide	
Ortho-cresol	Biacetyl	Peroxy acetyl nitrate	
Para-cresol	Acetaldehyde	Peroxy nitric acid	
Meta-cresol	Formaldehyde	Dinitrogen pentoxide	
Isoprene	Formic acid	Nitrous oxide	
Alpha-pinene	Ortho-tolualdehyde		
Methanol	Meta- tolualdehyde		
Allyl alcohol	Para-tolualdehyde		
Ethylene oxide	Methyl ethyl ketone		
Methane	Phosgene		
Acrylonitrile	Acrolein		
Cis 1,2-dichloroethylene	Chloroacetyl chloride		
Vinylidene chloride	Dichloroacetyl chloride		
Chloroform	Formyl chloride		
Allyl chloride	Glycoaldehyde		
Trichloroethylene			

irradiated.

For a number of species with very distinct IR spectra the concentrations could be obtained directly from investigation of the product spectra. This was always the case with CO, NO, and many times one could read the absorbance due to formaldehyde without any subtraction. The absorbances of these kinds of species were converted into concentrations by using calibration curves. The magnetic tape library contains many spectra of commonly found products such as formaldehyde and CO at various concentrations. For nearly all product compounds identified in this study, correlations between the concentrations and IR absorbances were established by repeatedly injecting known amounts of product into the cell and measuring the IR absorbance.

In many cases the spectral subtraction technique ended with a number of unidentified bands appearing in the spectra. As the reference library is enlarged many more compounds will be identified.

SECTION 3

DATA ANALYSIS

The reaction mechanisms for alkenes irradiated in the presence of a $HONO/NO_x$ mixture in synthetic air can be expressed (10):

$$HONO + h\nu \rightarrow OH + NO \qquad (1\text{-}1)$$

$$OH + HONO \rightarrow H_2O + NO_2 \qquad (1\text{-}2)$$

$$OH + NO \rightarrow HONO \qquad (1\text{-}3)$$

$$OH + NO_2 \rightarrow HNO_3 \qquad (1\text{-}4)$$

$$OH + HC \xrightarrow{O_2} RO_2 \qquad (1\text{-}5)$$

$$RO_2 + NO \rightarrow NO_2 + RO \qquad (1\text{-}6)$$

$$RO \xrightarrow{O_2} HO_2 + CARB_1 \qquad (1\text{-}7)$$

$$RO \xrightarrow{O_2} CARB_2 + CARB_3 + HO_2 \qquad (1\text{-}8)$$

$$HO_2 + NO \rightarrow OH + NO_2 \qquad (1\text{-}9)$$

HC represents the parent HC while $CARB_j$ stands for a carbonyl compound. Reaction (1-5) is an OH addition reaction. Reactions (1-7) and (1-8) represent two possible channels for the decay of the alkoxy radical. In Reaction (1-7), a single hydroxy aldehyde or ketone is formed, whereas in (1-8) two aldehydes are produced. As an example consider propylene. Here reactions (1-7) and (1-8) are:

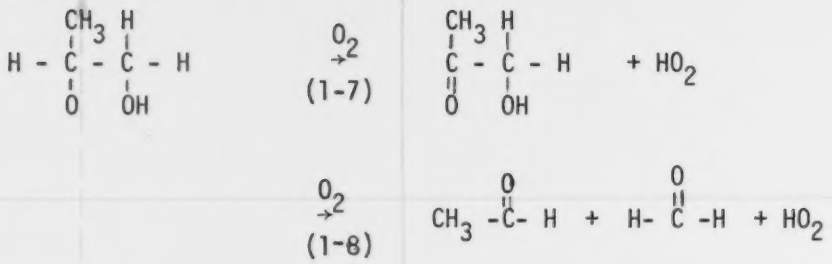

(1-7)

(1-8)

The split between these two channels has been the source of much controversy in the literature (11). Recent results suggest that Reaction 1-8 is the dominant channel (12). However no information in the literature suggests that this is any type of universal result. In general, both channels must be considered since both channels produce an HO_2 radical.

We have not considered the photolysis of NO_2 in this reaction scheme. While NO_2 is being photolyzed in this system, the excess NO present prevents any net change in the NO or NO_2, i.e., the fate of the O atom is:

$$NO_2 + h\nu \rightarrow NO + O \qquad (1\text{-}10)$$

$$O + O_2 + M \rightarrow O_3 + M \qquad (1\text{-}11a)$$

$$O + NO \rightarrow NO_2 + M \qquad (1\text{-}11b)$$

$$O_3 + NO \rightarrow NO_2 + O_2 \qquad (1\text{-}12)$$

The competing reaction $O + NO_2 \rightarrow NO + O_2$ has only a very small effect on this system. However, this would not be the case without excess NO. Excess NO also makes it possible to ignore both the O atom, O_3 attack on the HC, as well as NO_3 radical attack. Within the time scale of the experiments conducted there is no photolytic decay of any of the compounds studied. Therefore we can ascribe all decay of the parent HC to OH attack.

If we assume steady state conditions for the OH, HO_2, and RO_2 radicals we obtain the following result for the steady state OH concentration (10):

$$[OH] = \frac{k_1[HONO]}{k_2[HONO] + k_3[NO] + k_4[NO_2]} \qquad (I\text{-}4)$$

The OH concentration is independent of the HC concentration. This arises because the OH radical destroyed due to reaction with HC is regenerated when the HO_2 radical, produced by the decomposition of the alkoxy radical (Reactions 1-7 or 1-8), is converted back to an OH radical via Reaction 1-9. The time derivative of the HC concentration is :

$$(d/dt)\,[HC(t)] = -k_5[OH(t)]\,[HC(t)] \qquad (I\text{-}5)$$

If we assume that the OH radical concentration is independent of time we find:

$$\frac{[HC(t)]}{[HC(0)]} = \exp\,(-k_5\ t[OH]) \qquad (I\text{-}6)$$

Equation I-6, serves as the foundation for all OH rate constants measured in this study. The NO_x system establishes the OH concentrations. Introducing the HC only modifies this concentration slightly due to the HC-related modifications of the relative distribution of HONO, NO, NO_2, and HNO_3. Conventional relative rate measurements introduce two HCs into an NO_x system. One of these species serves as a reference compound and enables obtaining the rate constant of the second compound relative to the first one. Here we use only one HC.

Inspection of I-4 shows that the absolute OH concentration is dependent on the values of a number of rate constants. All of these values, except k_1 the photolysis rate, of HONO are available in the literature. This rate constant must be measured since it is a function of the intensity

spectrum of the radiation employed in this study. It is also possible to establish this rate constant by employing a reference compound and assuming a particular value for the rate constant. From the measured time rate of change of the reference compound in conjunction with the experimentally determined values for HONO, NO, and NO_2 and the values for k_2, k_3, and k_4 we determine k_1. In this study we chose propylene as the reference compound.

As mentioned above we assume that the OH concentration is independent of time. But this is obviously an oversimplification since all the species vary with time. To include this one would have to integrate all the concentration-determining equations numerically on a computer. We have examined this problem through the study of computer simulation and do not believe that the precision to be gained from an exact numerical solution alters the rate constants enough to warrant abandoning the above analytical method. In this study we examined a number of compounds which have OH rate constants in the literature. The accuracy of our method depends on agreement with these results. As we show later in this report, the agreement is good giving credibility to the simplified approach.

Another important parameter which aids in the establishment of the chemical mechanism is the number of NO conversions to products per unit destruction of the parent HC (ε), i.e.

$$\varepsilon = \frac{[NO]}{[HC)} \qquad \text{(I-7)}$$

where

$$[A] = [A]_{initial} - [A]_{final}$$

In our reaction mechanism ε=2. This is true independent of whether the hydroxyl alkoxy radical decomposition is via the channel of reaction

1-7 or 1-8. Therefore one would expect that given experimental uncertainty, all the alkenes studied in this report should yield a value of ε=2. Strong deviations from this suggest that the proposed mechanism is incorrect.

To extract the value of ε from the experimental results, one must include the fact that not only are NO molecules destroyed in these experiments, but are also produced. Note that any decrease in HONO must be accompanied by an increase in NO_2, NO, or HNO_3. Combining Reactions 1-1 with 1-2, and 1-1 with 1-4 we obtain the following effective reactions:

(Channel A) $$2HONO + h\nu \rightarrow H_2O + NO + NO_2 \qquad (1\text{-}13)$$

(Channel B) $$HONO + NO_2 + h\nu \rightarrow NO + HNO_3 \qquad (1\text{-}14)$$

Both channels produce NO molecules, whose production can be expressed:

$$\Delta_p[NO] = 0.5\ |\Delta[HNO_3] + \Delta[HONO]| \qquad (I\text{-}8)$$

The apparent decrease in NO ($\Delta_a[NO]$) is read directly from the experimental results. Combining $\Delta_p[NO]$ with $\Delta_a[NO]$ one finds:

$$\varepsilon = \frac{\Delta_a[NO] + \Delta_p[NO]}{\Delta[HC]} \qquad (I\text{-}9)$$

The final aspect of the analysis involves a study of the products. Important considerations here are the N and C balances. Before any concrete conclusions are reached concerning the chemical mechanism one must be able to obtain a reasonable carbon balance. These balances are addressed in the analysis of the chemical fate of the various compounds studied.

PROPYLENE

The results of the propylene/HONO/NO_x irradiation are shown in

Figures 4a to 9b. The initial concentrations are shown in Table 5. Figures 4a and 4b show the IR MCT spectrum of the reactants and products, respectively. In Figure 5a we have subtracted the remaining propylene and HONO. Figure 5b shows the results after also removing the acetaldehyde produced in the irradiation. In Figure 6a we have removed the contribution due to HNO_3.

TABLE 5. PROPYLENE, HONO, NO_x DATA

Propylene

t(min)	[HONO]	[NO]	$[NO_2]$	$[HNO_3]$	$\frac{[NO_x]_f}{[NO_x]_i}$
0	4.29	13.15	1.56	0.00	--
5	3.05	7.28	8.70	0.46	1.03

t(min)	[Prop]	[Acetaldehyde]	[Formaldehyde]	$\frac{\Delta[C]_+}{\Delta[C]_-}$
0	17.10	0.00	0.00	--
5	14.00	2.93	2.72	0.92

$k_{lit} = 25 \times 10^{-12} \frac{cm^3}{sec}$

$\frac{\Delta[NO]}{\Delta[Prop]} = 2.17$

Computer subtractions have also been conducted for the product spectrum obtained from the InSb detector. Figures 7a and 7b show the reactant and product spectra. In Figure 8a we have subtracted the contributions due to H_2O and remaining propylene. Figure 8b shows the NO_2 contents of the products, and here the formaldehyde and acetaldehyde contributions were

also removed. Finally Figures 9a and 9b show the initial NO and NO_2 as well as the final NO. From these spectra the concentrations[a] of both products and reactants can easily be calculated. These results are also shown in Table 5. Also included in this table are two parameters to measure C and N balances. The ratio $\Delta[C]_p/\Delta[C]_r$ is simply the sum of the C in the products divided by the reactants loss in C due to consumption of the parent HC propylene. The ratio $[NO_x]_f/[NO_x]_i$ is the total final N compound concentration (excluding N_2) divided by the initial N-containing compounds, i.e.

$$[NO_x]_i = [HONO]_i + [NO]_i + [NO_2]_i$$

and

$$[NO_x]_f = [HONO]_f + [NO]_f + [NO_2]_f + [HNO_3]_f$$

In all cases the initial NO_x is the sum shown above but in some cases the final NO_x will include other species such as PAN, methyl nitrate, etc.

Propylene was employed as a reference compound to normalize all the other OH rate constants. Equations I-4 and I-6 can be combined since: $k_3 = k_4 = 1.7\ k_2$ (10), equation I-10 can be written as:

$$-\frac{1}{t}\ln\frac{[HC(t)]}{[HC(0)]} = k_5\frac{k_1}{k_2}\frac{[HONO]}{[HONO] + 1.7\ [NO + NO_2]} \qquad \text{(I-10)}$$

A value for the ratio k_1/k_2 is found by substituting in the initial NO_x concentrations, and the reactant and five-min concentrations for propylene as well as the propylene literature value for k. Once a value for k_1/k_2 is established one obtains the simple general relationship:

---

[a]All concentrations appearing in this report are in ppm unless otherwise indicated.

$$k = 5.47 \times 10^{-9} \frac{\alpha}{\beta} \left(\frac{cm^3}{molecule}\right) \qquad \text{(I-11)}$$

$$\alpha = -\frac{1}{t} \ln \frac{[HC(t)]}{[HC(0)]} \qquad \text{(I-12)}$$

$$\beta = \frac{[HONO]_i}{[HONO]_i + 1.7\,([NO]_i + [NO_2]_i)} \qquad \text{(I-13)}$$

These expressions are used throughout the remainder of this section to calculate various OH rate constants.

From Table 5 we see that $\frac{\Delta[NO]}{\Delta[Propylene]} = 2.17$ and that $\frac{\Delta[Acetaldehyde]}{\Delta[Propylene]} = 0.95$ and $\frac{\Delta[Formaldehyde]}{\Delta[Propylene]} = 0.88$. These results are consistent with the recent findings of Niki and suggest that the OH-initiated reaction mechanism is (11)

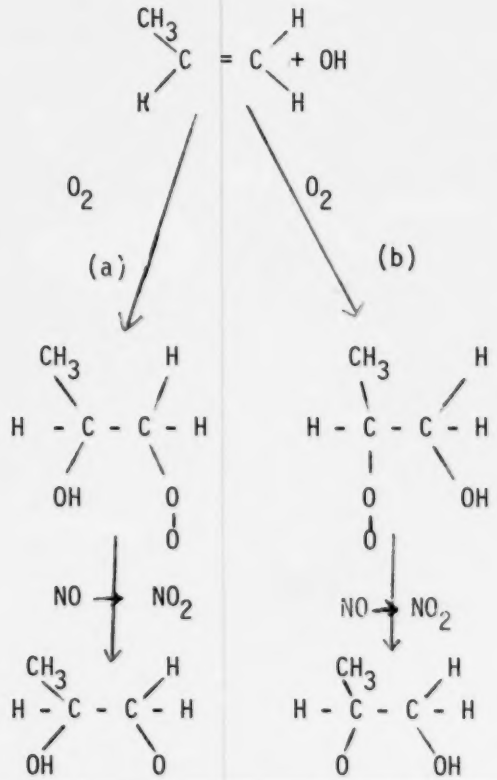

(I-14)

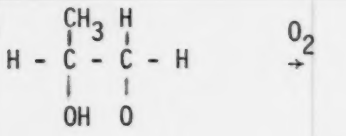

$$\xrightarrow{O_2} \quad HCHO + CH_3CHO + HO_2 \qquad (1\text{-}15)$$

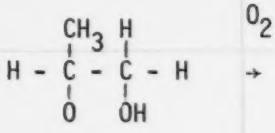

$$\xrightarrow{O_2} \quad HCHO + CH_3CHO + HO_2 \qquad (1\text{-}16)$$

$$HO_2 + NO \rightarrow \quad OH + NO_2 \qquad (1\text{-}17)$$

Independent of the attacked by the OH this mechanism gives $\frac{\Delta[\text{Formaldehyde}]}{\Delta[\text{Propylene}]} = 1$, $\frac{\Delta[\text{Acetaldehyde}]}{\Delta[\text{Propylene}]} = 1$, and $\frac{\Delta[\text{NO}]}{\Delta[\text{Propylene}]} = 2.0$, which agree with our experimental results. As stated earlier there has been some speculation that the alkoxy radicals formed in Reaction 1-14a might directly react with O_2 to form hydroxy aldehydes. If this occurs it must be a minor channel because of the good C balance obtained just including the acetaldehyde and formaldehyde. However inspection of Figure 6 indicates that some residual absorbance remains after subtracting acetaldehyde and formaldehyde but we have not identified these bands. Reference spectra for the hydroxy aldehydes are not available. We cannot rule out that perhaps a small fraction of the time this hydroxy compound is formed. Note that $\varepsilon = 2$ even if the hydroxy compound is formed. The remaining bands may also represent a trace amount of 1,2-propanedioldinitrate which forms when nitrogen trioxide (NO_3) radicals react with propylene (12).

ETHYLENE

To be certain that the technique was working properly ethylene was irradiated in a $HONO/NO_x$ mixture. Figures 10a to 14a show some of the IR spectra obtained in these runs and their subsequent subtractions.

The concentrations of the reactants and products are shown in Table 6. The experimentally determined rate constant agrees well with the literature value. Both the C and N balances are quite good. These results are essentially consistent with the following mechanism:

$$CH_2 = CH_2 + OH \xrightarrow{O_2} H - \underset{\underset{OH}{|}}{\overset{H}{\overset{|}{C}}} - \underset{\underset{O}{|}}{\overset{H}{\overset{|}{C}}} - H \xrightarrow{NO} H - \underset{\underset{OH}{|}}{\overset{H}{\overset{|}{C}}} - \underset{\underset{O}{|}}{\overset{H}{\overset{|}{C}}} - H \qquad (1\text{-}18)$$
$$\qquad\qquad\qquad

TABLE 6. ETHYLENE, HONO, NO_x DATA

Ethylene

t(min)	[HONO]	[NO]	$[NO_2]$	$[HNO_3]$	$\frac{[NO_x]_f}{[NO_x]_i}$
0	4.83	13.83	2.73	0.00	--
13	2.59	10.43	8.65	0.81	1.05

t(min)	[Ethylene]	[HCHO]	[CO]	$\frac{\Delta[C]_+}{\Delta[C]-}$
0	19.40	0.00	0.00	--
13	16.67	4.70	0.80	1.01

$k_{exp} = 7.3 \times 10^{-12} \frac{cm^3}{sec}$

$k_{lit} = 8.0 \times 10^{-12} \frac{cm^3}{sec}$

$\frac{\Delta[NO]}{\Delta[Ethylene]} = 1.77$

corrected value, 1.51, seems low compared to the experimental value of 1.77. However no other obvious sources for CO are apparent. Also, the CH_2O yield is 0.76 ppm less than predicted by the amount of ethylene reacted suggesting that the CH_2O did indeed degrade to CO.

FORMALDEHYDE

Formaldehyde results are shown in Figures 15a to 16a and the results are tabulated in Table 7. A value of 14.1×10^{-12} cm^3/sec was obtained for the rate constant and $\frac{\Delta[NO]}{\Delta[Formaldehyde]} = 1.03$. Both N and C balances

are reasonable. These results are consistent with the expected mechanism, Reaction 1-21 and 1-22. From this mechanism we expect $\frac{\Delta[CO]}{\Delta[Formaldehyde]}$ = 1.0 and ε = 1.0. The experimental results yield $\frac{\Delta[CO]}{\Delta[Formaldehyde]}$ = 0.88 while ε = 1.03. The above mechanistic scheme is obviously not the same as an alkene scheme.

ACRYLONITRILE

The spectra obtained in the acrylonitrile run are shown in Figures 17a to 20a. The tabulated reactants and products are shown in Table 8. A rate constant of 3.2×10^{-12} cm^3/sec was found and $\frac{\Delta[NO]}{\Delta[Acrylonitrile]}$ = 2.13. From the table we see that $\frac{\Delta[HCHO]}{\Delta[Acrylonitrile]}$ = 0.95. This suggests that the OH-initiated reaction mechanism can be represented as

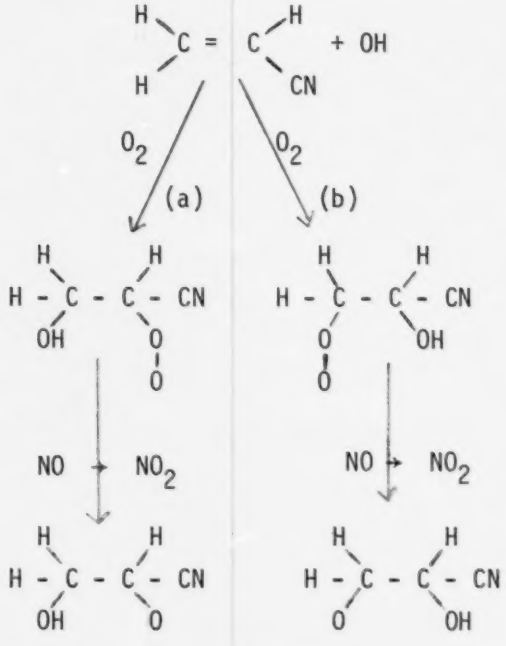

(1-23)

TABLE 7. FORMALDEHYDE, HONO, NO_x DATA

Formaldehyde

t(min)	[HONO]	[NO]	$[NO_2]$	$[HNO_3]$	$\frac{[NO_x]_f}{[NO_x]_i}$
0	5.18	14.32	2.73	0.00	--
12	2.67	12.16	5.13	0.40	0.88

t(min)	[HCHO]	[CO]	$\frac{\Delta[C]_+}{\Delta[C]-}$
0	14.20	0.00	--
12	10.70	3.07	0.88

$k_{exp} = 14.1 \times 10^{-12} \frac{cm^3}{sec}$

$k_{lit} = 10 \times 10^{-12} \frac{cm^3}{sec}$

$\frac{\Delta[NO]}{\Delta[HCHO]} = 1.03$

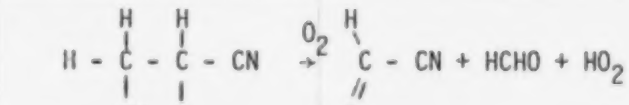

(1-24a)

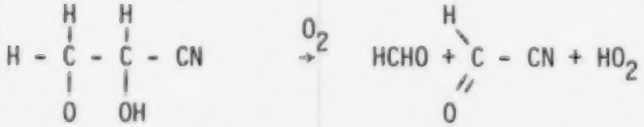

(1-24b)

$$HO_2 + NO \rightarrow OH + NO_2 \qquad (1\text{-}25)$$

We have not included in this mechanism the possibility for hydroxyl aldehyde formation which seems ruled out because of the formaldehyde yield.

TABLE 8. ACRYLONITRILE, HONO, NO_x DATA

Acrylonitrile

t(min)	[HONO]	[NO]	$[NO_2]$	$[HNO_3]$	$\frac{[NO_x]_f}{[NO_x]_i}$
0	3.95	12.84	1.78	0.00	--
20	1.67	10.06	6.97	0.69	1.04

t(min)	[Acrylonitrile]	[HCHO]	[CO]	$\frac{\Delta[C]_+}{\Delta[C]-}$
0	21.74	0.00	0.00	--
20	19.74	1.90	0.55	--

$k_{exp} = 3.2 \times 10^{-12} \frac{cm^3}{sec}$

k_{lit} = Unknown

$\frac{\Delta[NO]}{\Delta[Acrylonitrile]} = 2.13$

Examination of Figures 18b and 20a indicates the presence of two unknown bands. The band centered at 915 cm^{-1} may be associated with the C-C≡N group and the band at 2235 cm^{-1} is representative of a nitrile group (13). Because of the formaldehyde yield and the ε value we believe that these bands may be associated with formyl cyanide (CH(O)CN). Unfortunately the carbonyl group is masked by H_2O and it is not possible to check for a carbonyl stretch. We also see hydrogen cyanide (HCN) and CO in the product spectra. HCN could arise from either OH attack on formyl cyanide or its thermal decomposition. We have not been able to calibrate an IR spectrum

of HCN and have not measured the thermal decomposition of the compounds whose bands we described above. The product spectrum also contains CO, whose source is not certain, but which may come from either formyl cyanide (if this compound is actually formed) or the OH attack on formaldehyde. Because of the presence of at least one unknown no C balance was possible, but the N balance is good.

VINYLIDENE CHLORIDE

The results of the vinylidene chloride run are shown in Figures 21a to 25b. Interpretation of this data is complicated because of an apparent chain reaction involving vinylidene chloride and chlorine (Cl) atoms. Sanhueza et al. have shown that when any Cl atoms are in the presence of vinylidene chloride in an O_2 containing environment the following chain reaction occurs (14):

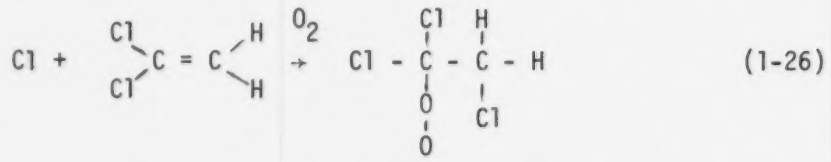

(1-26)

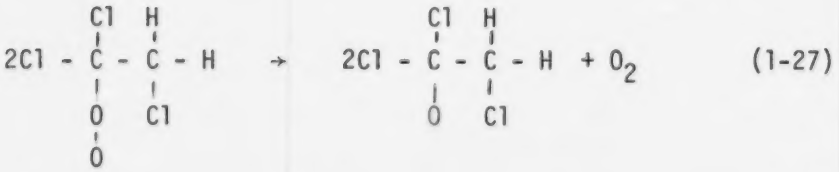

(1-27)

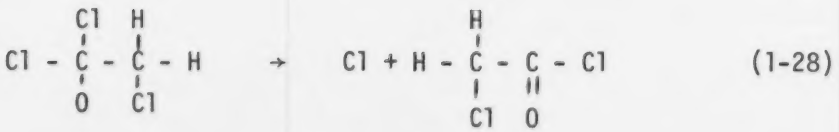

(1-28)

chloroacetyl chloride

Figure 21b shows the presence of chloroacetyl chloride in the product spectrum. We believe that this chloride arises from a Cl chain reaction and not from direct reaction with OH. Hisatsune et al. have demonstrated that the chain length is quite long, and therefore as a first approximation, one can assume that the Cl-producing channels in the OH vinylidene chloride reaction mechanism are quite small and can be ignored (15). However one must correct for the role this reaction plays when determining the rate constant as well as the normalized NO to NO_2 conversion ratio ε.

A reference spectrum of chloroacetyl chloride was prepared by irradiating vinylidene chloride and Cl in air and subtracting the remaining vinylidene and a trace of phosgene from the product spectrum. The amount of chloroacetyl chloride present was found by assuming that the decrease in the vinylidene chloride equalled the increase in chloroacetyl chloride with a correction made for the phosgene. The reference spectrum is shown in Figure 23a.

The reactant and product concentrations are shown in Table 9. To calculate the change in vinylidene chloride used in the OH rate constant measurement equation we must remove the amount of vinylidene chloride which is destroyed by Cl attack, i.e. we find:

$$[VDC]_{OH} = [VDC]_7 + [CAC]_7$$

where

$[VDC]_{OH}$ = concentration of vinylidence chloride which would be present after seven min irradiation if there was no Cl attack.

$[VDC]_7$ = measured concentration of vinylidene chloride after seven min irradiation.

TABLE 9. VINYLIDENE CHLORIDE, HONO, NO_x DATA

Vinylidene chloride

t(min)	[HONO]	[NO]	$[NO_2]$	$[HNO_3]$	$\frac{[NO_x]_f}{[NO_x]_i}$
0	4.48	12.65	2.18	0.00	--
7	2.88	7.72	8.31	0.75	1.02

t(min)	[VDC]	[Chloroacetyl chloride]	[ClC(O)Cl]	[HCHO]	[CO]	$\frac{\Delta[C]_+}{\Delta[C]-}$
0	14.28	0.00	0.00	0.00	0.00	--
7	9.93	2.50	1.66	1.05	0.50	0.94

$k_{exp} = 12.0 \times 10^{-12} \frac{cm^3}{sec}$

k_{lit} = Unknown

$\frac{\Delta[NO]}{\Delta[VDC]} = 1.68$

$[CAC]_7$ = concentration of chloroacetyl chloride after seven min irradiation.

With this adjusted value for the product concentration of vinylidene chloride we obtained a value of 12.0×10^{-12} cm^3/sec for the OH rate constant. To calculate ε due to OH attack, we must again factor out the chain reaction effect. Each time Cl reacts with vinylidene chloride one molecule of NO will be converted to NO_2. In the OH-initiated NO to NO_2 conversion rate, these NO to NO_2 conversions subtract out and only the change in vinylidene chloride due to OH attack is included, which equals 1.85 ppm. With these qualifications we find ε= 1.95. From Table 9 we

see that $\frac{\Delta[\text{Phosene}]}{\Delta[\text{Vinylidene chloride}]} = 0.90$ and $\frac{\Delta[\text{Formaldehyde}]}{\Delta[\text{Vinylidene chloride}]} = 0.57$.

A possible reaction mechanism is:

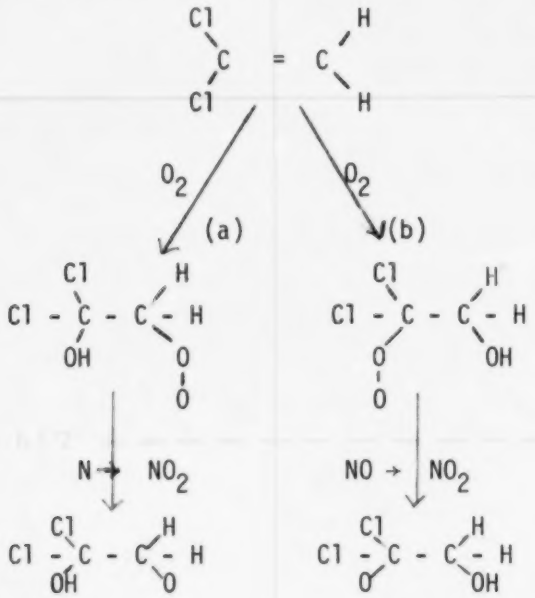

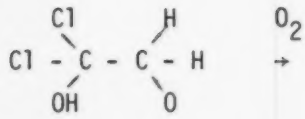

(1-30)

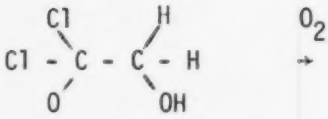

(1-31)

(1-32)

In both cases we find $\frac{\Delta[\text{Formaldehyde}]}{\Delta[\text{Vinylidene chloride}]} = 1.0$, $\frac{\Delta[\text{Phosgene}]}{\Delta[\text{Vinylidene chloride}]} = 1.0$ and $\varepsilon = 2.0$. The latter two values agree well with the experimental values. The formaldehyde results differ by about 43%. However we also

found that 0.50 ppm of CO is produced and likely arises from Cl attack on formaldehyde. Assuming this, we find that if there was no attack by Cl on formaldehyde, $\frac{\Delta [\text{Formaldehyde}]}{\Delta[\text{Vinylidene chloride}]} = 0.83$. Since the secondary attack on formaldehyde also produces one NO to NO_2 conversion, the adjusted value of 1.68 ppm disagrees with the predicted value by 16%. We found good balances for both N and C species.

TRICHLOROETHYLENE

The results for the trichloroethylene/HONO/NO_x irradiations are displayed in Figures 26a to 29a and tabulated in Table 10. This run was more

TABLE 10. TRICHLOROETHYLENE, HONO, NO_x DATA

Trichloroethylene

t(min)	[HONO]	[NO]	[NO_2]	[HNO_3]	$\frac{[NO_x]_f}{[NO_x]_i}$
0	3.91	13.15	1.73	0.00	--
15	1.56	7.78	6.69	0.85	0.93

t(min)	[TCE]	[$COCl_2$]	[Dichloroacetyl chloride]	[CHOCl]	[CO]	$\frac{\Delta[C]_+}{\Delta[C]-}$
0	19.19	0.00	0.00	0.00	0.00	--
15	14.05	1.50	3.68	1.71	0.41	0.92

$k_{exp} = 3.6 \times 10^{-12} \frac{cm^3}{sec}$

$k_{lit} = 2.2 \times 10^{-12} \frac{cm^3}{sec}$

$\frac{\Delta[NO]}{\Delta[TCE]} = 2.25$

difficult to analyze than most of the others because of complications due to a chain reaction, and the subtracted spectra are very noisy in some of the important regions of the IR spectrum. Examination of the product spectra shows that the main products are dichloroacetyl chloride, phosgene, and formyl chloride. As in the case of vinylidene chloride, dichloroacetyl chloride probably arises from a chain reaction involving Cl atoms. The effect of this chain reaction was removed from the analysis in the same way done for vinylidene chloride.

The dichloroacetyl chloride reference spectrum which appears in Figure 27b, was obtained by irradiating trichloroethylene and molecular Cl in air and subtracting the absorption due to the remaining trichloroethylene. It was also necessary to generate a reference spectrum for formyl chloride which appears in Figure 29a. This was accomplished by irradiating methyl chloride and molecular Cl in air and again subtracting the absorption due to the remaining methyl chloride. Since formyl chloride is unstable and its products are CO and hydrogen chloride, in this run we assume that the presence of CO indicates decomposition of formyl chloride (15).

We assume that the dichloroacetyl chloride is formed via the set of reactions.

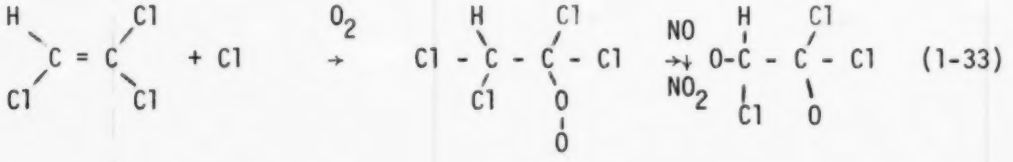

(1-33)

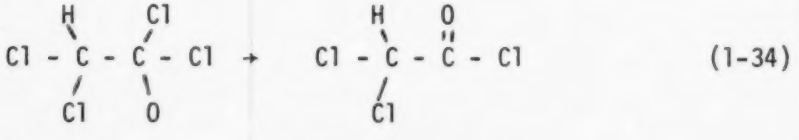

(1-34)

Dichloroacetyl chloride

From Cl attack alone we find $\frac{\Delta [NO]}{\Delta[\text{Trichloroethylene}]} = 1.0$

As with vinylidene chloride, we assumed that the percentage of the time that OH attack liberates Cl atoms is small, but due to the long chain length the effect can be large. The rate constant measurement and ε we corrected for the Cl chain reaction effect in the same manner as was done for vinylidene chloride. The resulting rate constant and ε are 3.6×10^{-12} cm^3/sec and 2.25 respectively. We also found $\frac{\Delta[\text{Phosgene}]}{\Delta[\text{Trichloroethylene}]} = 1.03$ and $\frac{\Delta[\text{Formyl chloride}] + \Delta[CO]}{\Delta[\text{Trichloroethylene}]} = 1.45$. It seems likely the dominant channels for the OH-initiated attack on trichloroethylene are represented.

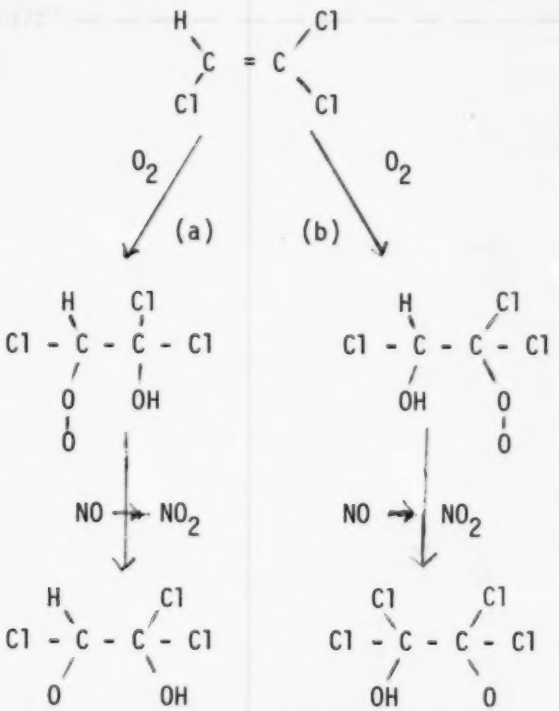

(1-35)

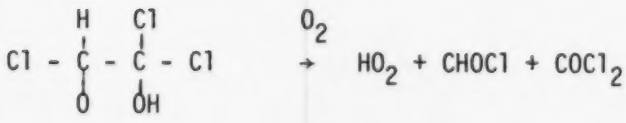

(1-36)

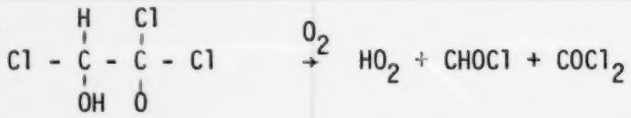

(1-37)

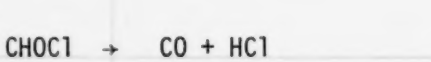

(1-38)

This mechanism predicts (independent of the position of the initial OH attack is) that $\frac{\Delta[\text{Formyl chloride}] + [\text{CO}]}{\Delta[\text{Trichloroethylene}]} = 1.0$, $\frac{\Delta[\text{Phosgene}]}{\Delta[\text{Trichloroethylene}]} = 1.0$, and $\frac{\Delta[\text{NO}]}{\Delta[\text{Trichloroethylene}]} = 2.0$. The phosgene results agree well which may be fortuitous since substantial error is probable in the reading of the phosgene concentration seen from inspection of Figure 28a. The experimental value for $\frac{\Delta[\text{Formyl chloride}] + [\text{CO}]}{\Delta[\text{Trichloroethylene}]}$ is much larger than expected and may arise because of the compounding of errors involved with both the calibration of formyl chloride and accurately accounting for its thermal decomposition. Perhaps CO arises from a Cl reaction.

ALLYL CHLORIDE

The allyl chloride IR results are shown in Figures 30a to 33b and tabulated data is in Table 11. A value of 19.8×10^{-12} cm^3/sec is found for the OH rate constant and $\frac{\Delta[\text{NO}]}{\Delta[\text{Allyl chloride}]} = 1.80$. We also see $\frac{\Delta[\text{Formaldehyde}]}{\Delta[\text{Allyl chloride}]} = 0.52$. These results indicate allyl chloride does not react with OH as does propylene, which suggests that the dominant reaction channel would be

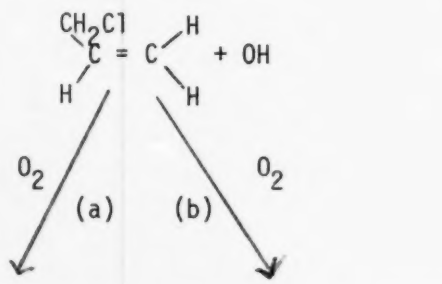

(1-39)

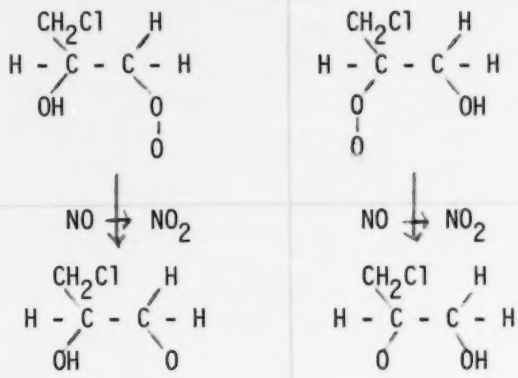

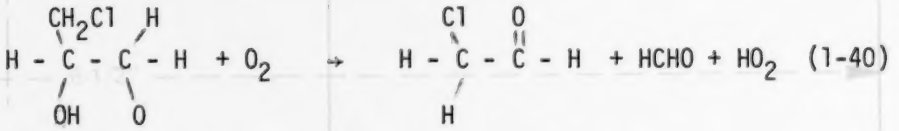

(1-40)

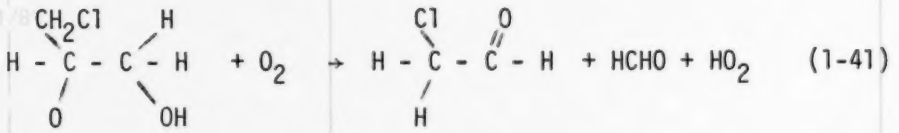

(1-41)

This mechanism yields $\frac{\Delta[\text{Formaldehyde}]}{\Delta[\text{Allyl chloride}]} = 1.0$ and $\frac{\Delta[\text{NO}]}{\Delta[\text{Allyl chloride}]} = 2.0$.

Another mechanism possible involves H abstraction by an O molecule on one of the hydroxy alkoxy radicals, i.e.,

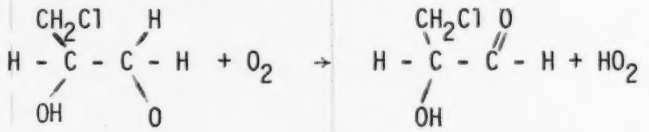

and

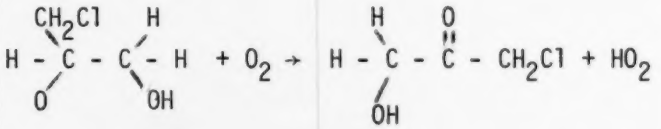

Any reaction which proceeds via these channels will although reduce the formaldehyde yield, still $\varepsilon = 2$. Examination of Figures 31a and 33b reveals

TABLE 11. ALLYL CHLORIDE, HONO, NO_x DATA

Allyl Chloride

t(min)	[HONO]	[NO]	$[NO_2]$	$[HNO_3]$	$\frac{\Delta[NO_x]_f}{\Delta[NO_x]_i}$
o	4.83	13.58	2.29	0.00	--
5	3.87	9.01	7.03	0.32	0.98

t(min)	[allyl chloride]	[HCHO]	$\frac{[C]_+}{[C]_-}$
0	19.10	0.00	--
5	16.20	1.50	--

$k_{exp} = 19.8 \times 10^{-12} \frac{cm^3}{sec}$

k_{lit} = Unknown

$\frac{\Delta[NO]}{\Delta[\text{allyl chloride}]} = 1.80$

the presence of a number of unidentified bands, both in the MCT and InSb spectra. Because reference spectra were not available for any of the previously discussed chlorinated carbonyls, the reaction mechanism is open to speculation. The experimental evidence available indicates that both decomposition of the hydroxy alkoxy radicals and direct reaction with O_2 occur.

Since there are a number of unknown bands in the IR product spectra performing a C balance was impossible. The N balance was quite good. Note that we have assumed that no Cl atoms are produced.

ACETALDEHYDE

IR spectra are displayed in Figures 34a to 37b. The tabulated data is in Table 12. Using Equation I-11 we obtain a value of $9.6 \times 10^{-12} cm^3/sec$ for the OH rate constant. However examination of the product spectrum shows the formation of compounds such as PAN, methyl nitrate ($MeONO_2$), and methyl nitrite (MeONO). If these species are produced, the OH radical which attacks the acetaldehyde is not recycled and the method used in calculating the OH rate constant is incorrect. In general, we expect the OH-initiated attack on acetaldehyde can be expressed as:

$$OH + CH_3CHO \xrightarrow{O_2} CH_3COO_2 + H_2O \qquad (1\text{-}42a)$$

$$CH_3COO_2 + NO_2 \rightarrow PAN \qquad (1\text{-}42b)$$

$$CH_3COO_2 + NO \xrightarrow{O_2} CH_3O_2 + CO_2 + NO_2 \qquad (1\text{-}42c)$$

$$CH_3O_2 + NO \rightarrow CH_3O + NO_2 \qquad (1\text{-}42d)$$

$$CH_3O + O_2 \rightarrow HO_2 + HCHO \qquad (1\text{-}42e)$$

$$CH_3O + NO \rightarrow CH_3ONO \qquad (1\text{-}42f)$$

$$CH_3O + NO_2 \rightarrow CH_3ONO_2 \qquad (1\text{-}42g)$$

$$HO_2 + NO \rightarrow OH + NO_2 \qquad (1\text{-}42h)$$

We have ignored the thermal decomposition of PAN. From the reaction scheme we see that the OH radical is recycled only if the methoxy (CH_3O) radical reacts with O_2 via Reaction e. From Table 12 we find the results:

TABLE 12. ACETALDEHYDE, HONO, NO_x DATA

Acetaldehyde

t(min)	[HONO]	[NO]	$[NO_2]$	$[HNO_3]$	[PAN]	[MeONO]	$[MeONO_2]$	$\frac{\Delta[NO_x]_i}{\Delta[NO_x]_f}$
0	4.20	13.83	2.29	0.00	0.00	0.00	0.00	--
10	2.46	10.68	6.14	0.36	0.23	0.84	0.57	1.05

t(min)	$[CH_3CHO]$	[HCHO]
0	20.00	0.00
10	17.38	1.04

$k_{exp} = 21 \times 10^{-12} \frac{cm^3}{sec}$

$k_{lit} = 16 \times 10^{-12} \frac{cm^3}{sec}$

$\frac{\Delta[NO]}{\Delta[CH_3CHO]} = 1.60$

$$\frac{\Delta[\text{Formaldehyde}]}{\Delta[\text{Acetaldehyde}]} = 0.40,$$

$$\frac{\Delta[\text{Methyl nitrate}]}{\Delta[\text{Acetaldehyde}]} = 0.57,$$

$$\frac{\Delta[\text{Methyl nitrite}]}{\Delta[\text{Acetaldehyde}]} = 0.84,$$

$$\frac{\Delta[\text{PAN}]}{\Delta[\text{Acetaldehyde}]} = 0.23.$$

The methyl nitrite measurement may involve considerable error since the absorption coefficient was not obtained by calibration, but rather was calculated from the earlier work of Gay et al. (16). The above results demonstrate that recycling does not dominate the reaction channels. However, we can still easily calculate the steady state OH concentration. We find:

$$[OH] = 1.095 \times 10^{10} \frac{[HONO]}{[HONO] + 1.7([NO]+[NO_2])+(k_5/k_2)(1-\gamma)[\text{Acetaldehyde}]} \quad \text{(I-14)}$$

where

$$\gamma = \frac{k_e[CH_3O][O_2]}{k_5[\text{Acetaldehyde}]} \quad \text{(I-15)}$$

Unfortunately k_e is not known within a factor of two (17). However we can calculate these ratios by noting that γ is approximately equal to the fraction of acetyl peroxy radicals which eventually form formaldehyde, i.e.,

$$\gamma = \frac{\Delta[\text{Formaldehyde}]}{\Delta[\text{Acetaldehyde}]} \quad \text{(I-16)}$$

Using Equations I-6, 11, 12, 13, and 14, we can easily show that

$$k_5 = k_5^{(0)}\left(1 - \beta \frac{k_5}{k_2}^{(0)} (1-\gamma)\frac{[\text{Acetaldehyde}]}{[HONO]}\right)^{-1} \quad \text{(I-17)}$$

where $k_5^{(0)}$ is the rate constant obtained from I-11. We chose a value of 6.6×10^{-12} cm^3/sec for k_2 (10). Substituting the appropriate values into

I-17 we find $k_5 = 21.4 \times 10^{-12}$ cm^3/sec and see that the nonrecycling effect plays an important role in establishing the rate constant.

The reason so much methyl nitrate and methyl nitrite formed is the large NO and NO_2 concentrations which compete readily with O for the methoxy radicals. Lowering these NO and NO_2 concentrations, would raise the formaldehyde yield and would diminish the importance of the non-recycling channel. Because we are not able to detect the CO_2 produced, we did not do a C balance. However, despite the possibly large errors in the methyl nitrite concentration we found:

$$\Delta[MeONO] + \Delta[MeONO_2] + \Delta[HCHO] + \Delta[PAN = 2.68 \text{ ppm}$$

whereas Δ[acetaldehyde] = 2.62 ppm.

A value of 1.60 was obtained for ε. From the assumed mechanism we can predict the $\frac{\Delta [NO]}{\Delta[Acetaldehyde]}$ as a function of product formed. These results are shown in Table 13. The predicted weighted $\frac{\Delta[NO]}{\Delta[Acetaldehyde]} = 1.96$, which differs from the experimental result by 18%.

The quality of the subtracted spectra is not good. In Figure 36b it was not clear whether the bands between 110 cm^{-1} and 1200 cm^{-1} are real, or artifacts produced during the subtraction.

ACROLEIN

IR spectra for the acrolein run are shown in Figures 38a to 44b. Tabulated data appears in Table 14. Using Equation I-11 a value of 22.1 x 10^{-12} cm^3/sec was found for the OH rate constant. However note that a peroxy nitrate forms which prevents the recycling of the OH radical. Once the nitrate yield is known, its effect can be accounted for in a way similar to that done for acetaldehyde. The corrected rate constant is

TABLE 13. PREDICTED WEIGHTED CONTRIBUTIONS TO $\Delta[NO]/\Delta[ACETALDEHYDE]$

Product Formed	$\frac{\Delta[Prod]}{\Delta[Acetaldehyde]}$	$\frac{\Delta[NO]}{\Delta[Acetaldehyde]}$	$\frac{\Delta[Product]}{\Delta[Acetaldehyde]}$	$\frac{\Delta[NO]}{\Delta[Acetaldehyde]}$
HCHO	0.40	3	1.20	
PAN	0.09	00	0.00	
MeONO	0.32	1[a]	0.32	
$MeONO_2$	0.22	2	0.44	
Total			1.96	

[a]The production of MeONO produces two conversions of NO to NO_2, but also serves as a sink for one NO. Therefore $\frac{\Delta[NO]}{\Delta[Acetaldehyde]} = 1$.

34.3×10^{-12} cm^3/sec. A value of 1.71 was obtained for ε. CO_2, formaldehyde, and ketene were among the products formed during the irradiation. In the subtracted product spectrum, Figure 39a, bands are located at approximately 800 cm^{-1}, 1075 cm^{-1}, and 1300 cm^{-1}. The positions of these bands are characteristic of a peroxy nitrate (18). Bands are also seen at 860 cm^{-1} and around 1100 cm^{-1} and the latter band frequently indicates the presence of an aldehydic species (19).

Developing a mechanism for acrolein is complicated because both addition and abstraction by the OH radical should be considered. To discuss our results, consider three mechanisms and Reactions 1-54 through 1-58:

TABLE 14. ACROLEIN, HONO, NO_x DATA

Acrolein

t(min)	[HONO]	[NO]	[NO_2]	[HNO_3]	[APAN]	$\frac{[NO_x]_f}{[NO_x]_i}$
0	4.83	13.15	2.29	0.00	0.00	--
4	3.51	8.76	6.86	0.31	0.46	0.98

t(min)	[Acrolein]	[HCHO]	[GALD]	[CO]	$\frac{\Delta[C]_+}{\Delta[C]_-}$
0	21.91	0.00	0.00	0.00	--
4	18.86	1.80	1.08	2.50	--

$k_{exp} = 34.3 \times 10^{-12} \frac{cm^3}{sec}$

$k_{lit} = 27.0 \times 10^{-12} \frac{cm^3}{sec}$

$\frac{\Delta[NO]}{\Delta[Acrolein]} = 1.71$

Mechanism A (addition)

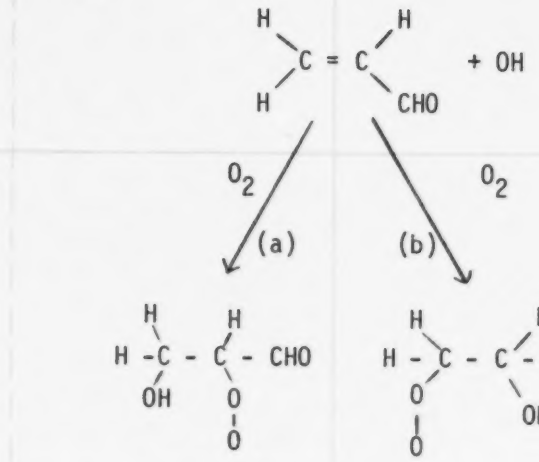

(1-43)

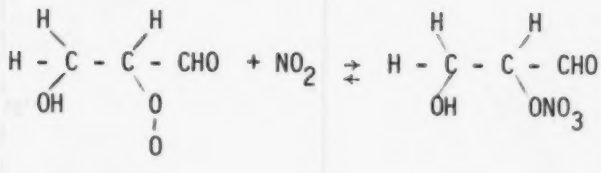

(1-44)

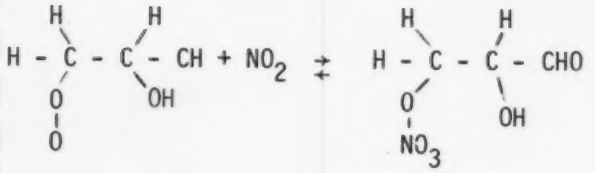

(1-45)

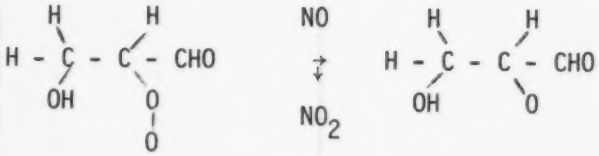

(1-46)

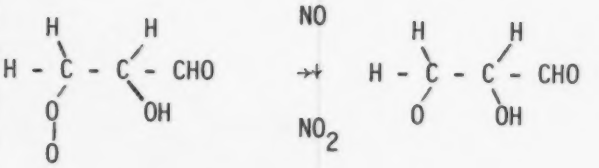

(1-47)

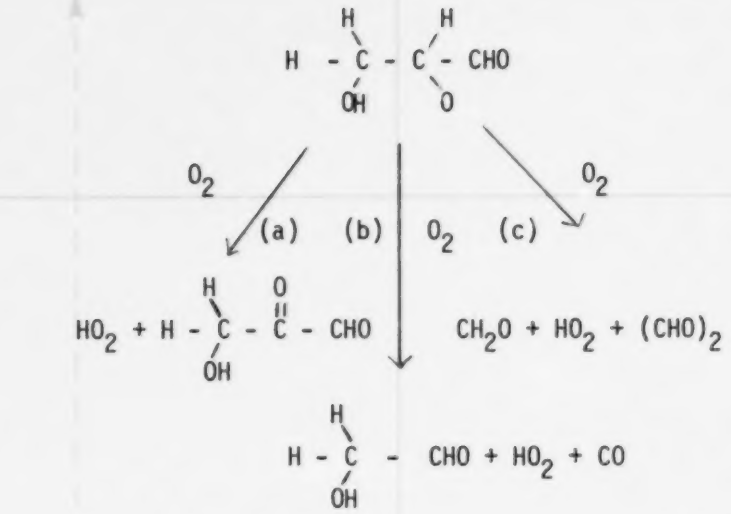

(1-48)

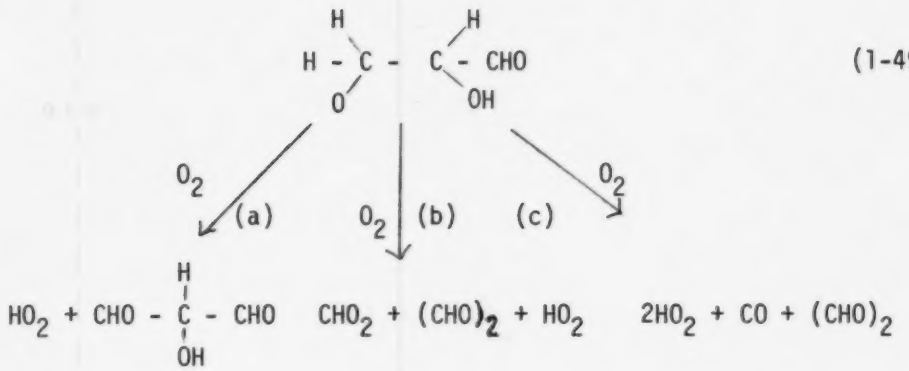

(1-49)

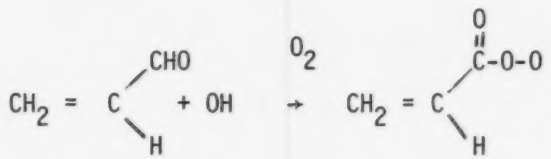

(1-50)

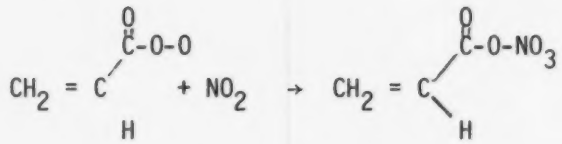

(1-51)

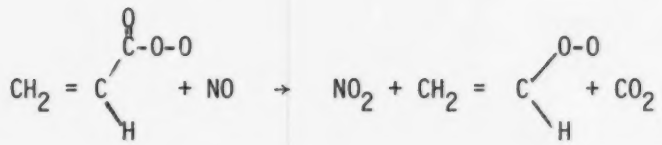

(1-52)

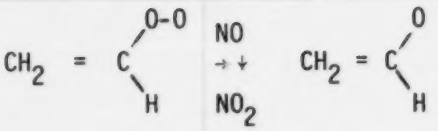

(1-53)

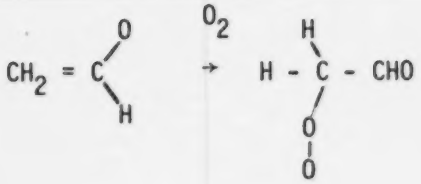

(1-54)

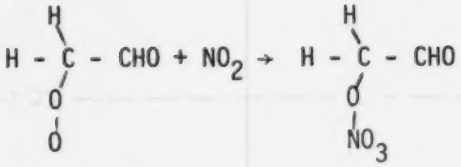

(1-55)

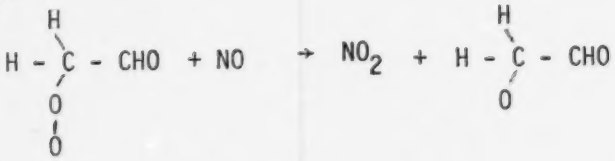

(1-56)

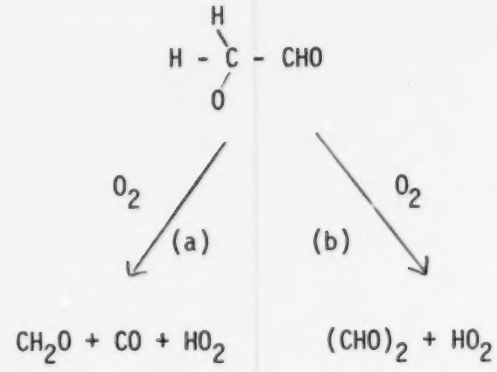

(1-57)

Mechanism C (abstraction)

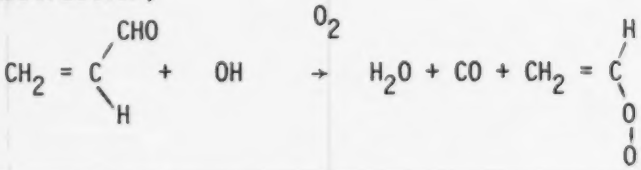

(1-58)

In each mechanism at least one type of peroxy nitrate (RO_2NO_2) is formed. To establish the absorption coefficient for the IR bands we attempted to synthesize this peroxy nitrate by irradiating ppm levels of acrolein, molecular Cl, and NO_2 in air. The Cl easily photolyzed and served as a free radical to extract the H atom from acrolein. The resulting concentrations of the reactants and products are shown in Table 15. In MCT IR spectrum, shown in Figure 39b, the absorbances due to acrolein, HNO_3, peroxy nitric acid, and N_2O_5 have been subtracted. The dominant peaks labeled in the figure were ascribed to the peroxy nitrate which we call APAN. By comparing Figures 39a and 39b we see that the same peroxy nitrate is formed in the HONO run. By performing a N balance on the reaction system, absorption coefficients for the peroxy nitrate can be found. Also, a carbonyl band is seen in the spectrum (Figure 40a). Recent information suggests that carbonyl-containing peroxy nitrates are quite stable (20, 21, 22). We determined the thermal stability of the new peroxy nitrate by adding excess NO into the cell and measuring the decay of the band at 1075 cm^{-1}. At T = 24°C the thermal half-life was about 15 min.

TABLE 15. ACROLEIN, Cl_2, NO_2 DATA

t(min)	[Acrolein]	$[NO_2]$	$[HNO_3]$	$[N_2O_5]$	$[HO_2NO_2]$	$[O_3]$
0	10.71	6.00	0.00	0.00	0.00	0.00
5	7.30	2.10	0.38	0.62	0.84	1.45
t(min)	[CO]	[HCHO]				
0	0.00	0.00				
5	3.50	0.39				

An obvious precursor for this peroxy nitrate is a carbonyl-containing peroxy radical, whose possible candidates are seen in Reaction Schemes 1-45, 46, 52, and 56. Since the same species is formed in the Cl system, the OH addition-initiated free radical attack would seem unlikely. Though probably true, from Table 14 we see that O_3 is formed, indicating that some NO is oxidized back to NO_2 by species other than O_3. If this is accomplished by HO_2 radicals an OH radical is formed. A second strong candidate for this radical is the one displayed in Reaction 1-52. Indeed this might be the case, but it is difficult to explain why [acrolein] = [CO] in the Cl-initiated reaction. The third possibility involves a novel step where one of the double bonds is broken to form a carbonyl bond (Reaction 1-52). The Cl/acrolein/NO_2 run was successful in that it produced the same peroxy nitrate, established that it contained a carbonyl group and enabled measuring its thermal stability. But while it suggested that the peroxy radical was formed after H abstraction it was not proven, and even if true, it is not clear which peroxy carbonyl radical produces the peroxy nitrate. Possibly more information can be obtained by examining other products formed in the reaction.

In Figure 41a we subtracted the peroxy nitrate from the product spectrum. In Figure 41b we show a spectrum of glycoaldehyde. This spectrum was obtained by irradiating a mixture of allyl alcohol, HONO, NO, and NO_2 in an O_2/N_2 mixture. It is expected that the glycoaldehyde and formaldehyde are produced in equal amounts and that the decrease in allyl alcohol is equal to the increase in formaldehyde. The latter assumption appears to be correct. By equating the formaldehyde and glycoaldehyde concentrations it is possible to obtain an absorption coefficient for glycoaldehyde. In

Figure 41b we subtracted the IR contributions due to allyl alcohol, HONO, and HNO_3, and hopefully we have a pure spectrum of glycoaldehyde. A better reference spectrum would have been obtained if the pure compound was available, however, we were unable to obtain one. By comparing this reference spectrum with Figure 41a, it appears that there may be some glycoaldehyde in the product spectrum, but it is by no means conclusive. If this is glycoaldehyde, our IR absorption coefficient suggests that it is a major product and that OH addition is an important component of the OH rate constant. In Figure 42a we have subtracted the glycoaldehyde, but the remaining bands could not be identified. In Figure 45a, we identified ketene (CH_2CO), although we had no reference spectrum. From our previous work we know that it is a very strong absorber, and therefore the amount of ketene is probably quite small. It is probably formed via

$$CH_2 = \underset{\underset{O}{|}}{C} - H + O_2 \rightarrow \quad HO_2 + CH_2CO \qquad (1\text{-}59)$$

Although we expect that this is a minor pathway, it does indicate that some abstraction is occurring.

From Table 15 we obtained the yields:

$$\frac{\Delta[CO]}{\Delta[\text{acrolein}]} = 0.82,$$

$$\frac{\Delta[\text{formaldehyde}]}{\Delta[\text{acrolein}]} = 0.59,$$

$$\frac{\Delta[\text{glycoaldehyde}]}{\Delta[\text{acrolein}]} = 0.35,$$

$$\frac{\Delta[\text{APAN}]}{\Delta[\text{acrolein}]} = 0.15,$$

$$\frac{\Delta[NO]}{\Delta[\text{acrolein}]} = 1.71.$$

If we assume that 15% of the acrolein is converted into the peroxy nitrate we find the following results for the three mechanisms:

Mechanism	$\frac{\Delta[NO]}{\Delta[\text{Acrolein}]}$
A	1.70*
B	3.40
C	2.45

In Mechanism B we assume that the 15% nitrate yield is formed via Reaction 1-52 only. Mechanism A agrees with the experimental results for ε. The result from mechanism B gives much too high value of ε which suggests that it is only a minor route. Mechanism C also gives high results. Formaldehyde can be produced by either addition or abstraction mechanisms. Glyoxal and formaldehyde are formed in equal amounts in Mechanism A. We have not been able to detect glyoxal, but because it is very difficult to detect in the IR, some may be present. Its absorbances may be buried under some of the glycoaldehyde bands. Formaldehyde is also produced in Mechanism C, and in this case was accompanied by CO. If we assume that glycoaldehyde is associated with addition and formaldehyde and the peroxy nitrate arise via abstraction we can divide the mechanisms as follows:

Mechanism A (addition) = 32%

Mechanism B (abstraction) + Mechanism C (abstraction) = 68%

The large value for ε found from Mechanisms B and C suggests an error in these routes.

*We have ignored reaction 1-49c

Our results at this time suggest that we can account for some of the major acrolein products. If we assume that when an OH radical attacks acrolein either formaldehyde, glycoaldehyde, or the peroxy nitrate is produced then we seem to account for most of the reacted acrolein. However we did not establish the specific reaction mechanism, and hope this will be obtained through future experiments.

SECTION 4

RESULTS AND DISCUSSION

In Table 16 the experimentally determined rate constants are compared with literature values. Assigning error bars to our experimental results was difficult because these experiments were not repeated, and the appropriate error bar was determined by the propagation of the individual errors in the rate constant measurement. Instead we assumed a base error of 25% in our rate constants because the reference compound has an uncertainty of $\pm$25% (13). We assumed other errors add up to another 25%, yielding an uncertainty of $\pm$50%. However, comparing the known OH rate constants with our experimentally determined rate constants suggests that the uncertainty is less than this. The measured ethylene OH rate constant agrees well with the literature value. The acetaldehyde results differ, but if an uncertainty of 25% is associated with the experimental results, the two values overlap. Again a 25% error bar on formaldehyde makes the results agree. Morris et al. and Niki et al. have obtained $(14 \pm 3.5) \times 10^{-12}$ cm^3/sec and $(14.4 \pm 0.8) \times 10^{-12}$ cm^3/sec for this OH rate constant (23, 24). Atkinson, in his recent review, has decided to give more weight to the two recent flash photolysis resonance fluorescence studies which yielded the values $(9.4 \pm 1.0) \times 10^{-12}$ cm^3/sec and $(9.9 \pm 1.1) \times 10^{-12}$ cm^3/sec (17, 25, 26). The acrolein results agree within experimental error if we choose an error bar of 25%. For trichloroethylene three literature values are clustered (27, 28, 29). The high value of 4.5×10^{-12} cm^3/sec was obtained by Winer using a relative

rate method (30). The previously described Cl chain reaction may explain why our result is high, but with a 50% error bar it overlaps with the clustered values. Both in the trichloroethylene and vinylidene chloride experiments a large uncertainty is expected for the rate constant because of the errors introduced when removing the Cl chain reaction effect.

TABLE 16. EXPERIMENTAL AND LITERATURE OH RATE CONSTANTS

Compound	T = 25°C Literature $k \times 10^{12}$ ($\frac{cm^3}{sec}$)	T = 23°C Experimental $k \times 10^{12}$ ($\frac{cm^3}{sec}$)
Propylene	25 ± 20% (17)	--
Ethylene	8 ± 25%	7.3
Acetaldehyde	16 ± 25% (17)	21
Formaldehyde	10 ± 25% (17)	14
Acrylonitrile	N.M	3.2
Trichloroethylene	2.0 ± 20% (27), 2.35 ± 17% (28), 2.34 (29) 4.5 ± 30% (30)	3.6
Vinylidene chloride	N.M.	12
Allyl chloride	N.M.	20
Acrolein	27 ± 13% (2)	34

N.M. = not measured

We calculated a half life for the various compounds using the equation ($t_{1/2} = \frac{\ell n 2}{[OH]\, k_{OH}}$) at approximately 23°C by assuming an average OH concentration of 10^6 cm^{-3}. These results are displayed in Table 17. Since all of the half lives are less than 3 days, we would not expect these species to accumulate in the atmosphere. However, before we can assess the significance of those short lifetimes, the lifetime and toxicity of the products must be considered.

TABLE 17. ATMOSPHERIC LIFETIMES

Compound	$\tau_{1/2}$ (h)
Propylene	7.7
Ethylene	2.6
Acetaldehyde	9.0
Formaldehyde	13.6
Acrylonitrile	60.3
Trichloroethylene	53.6
Vinylidene chloride	16.1
Allyl chloride	9.7
Acrolein	5.6

The experimentally determined mechanisms for propylene and ethylene agree with those suggested by Niki (11). A question remains as to the source of CO in the ethylene run. The mechanism for the OH-initiated photooxidation of formaldehyde yields the expected result. We conducted a detailed study of acrylonitrile oxidation, and tentatively identified

formyl cyanide. The ultimate fate of the CN radical is likely HCN. The initial species formed in the OH attack on vinylidene chloride are formaldehyde and phosgene. We believe that the other major product, chloroacetyl chloride, is produced via a Cl chain reaction. Trichloroethylene produces phosgene and formyl chloride and, via a Cl chain route, dichloroacetyl chloride. It is questionable whether the chlorine reaction mechanism is important in the free troposphere. We expect that any free chlorine atom that is produced would quickly react with other organic molecules and the chain sequence would quickly terminate. Gay et al. conducted product studies for these two chlorinated HCs, irradiating these compounds in air in the presence of NO_2 (31). Separating the effects of OH attack from those due to reaction with O_3 is difficult in these experiments and therefore directly comparing detailed results is impossible. The formation of the chlorinated chlorides is likely due to a Cl chain attack rather than the rearrangement of a hot epoxide suggested by Gay et al. (31).

Our study of the atmospheric chemistry allyl chloride is the first we have conducted. Unfortunately the lack of reference spectra of chlorinated aldehydes has prevented the establishment of a mechanism. Our acetaldehyde experiment is the first to directly study the OH-initiated mechanism for photooxidation which examines the products in detail. Our results are compatible with the reaction mechanism in the literature, but our verification is indirect because the reaction is short circuited by the presence of large amounts of NO_x which intercept the methoxy radical. This would not occur in the atmosphere. The last compound we studied was acrolein, studied previously by Altshuller et al. (32). In acrolein/NO and acrolein/NO_2 irradiations, they found formaldehyde a major product and indications of

the presence of glyoxal. However, our results indicate that formaldehyde and CO are major products, and we also tentatively identified glycoaldehyde. We did not observe glyoxal, but because of the poor quality of our reference spectrum, we cannot rule it out. If the ratio of NO_2 to NO is high, it seems likely that the peroxy nitrate will form but this species has not been detected before. We have found that it has a half-life of approximately 15 min at T = 26°C.

The FTIR technique clearly generates much interesting information concerning the removal rate of chemical due to OH attack. The identification of products is of special interest because of their potential toxicity. The species studied all have short OH-initiated half lives. The chlorinated HCs cannot be transported into the stratosphere and a buildup of these species in the troposphere is not expected. But an estimate of their concentration would be a factor in the emission rates as well as other removal rates such as O_3 attack and photolysis.

REFERENCES

1. Altshuller, A.P. and J.J. Bufalini, Environ. Sci. Technol., 5, 39 (1971).

2. Maldotti, A., C. Chionboli, C.A. Bignozzi, C. Bartocci, and V. Carassiti, Int. J. Chem. Kinet., 12, 905 (1980).

3. Carter, W.P.L., A.C. Lloyd, J.L. Sprung, and J.N. Pitts, Jr., Int. J. Chem. Kinet., 11, 45 (1979).

4. Niki, H., P.D. Maker, C.M. Savage, and L.P. Breitenbach, J. Phys. Chem., 82, 135 (1978).

5. Atkinson, R., In: "Chemical Kinetic Data Needs for Modeling the Lower Troposphere," NBS special publication 557, August 1979.

6. Hanst, P.L., A. S. Lefohn, and B.W. Gay, Jr., Appl. Spectrosc., 27, 188 (1973).

7. Nash, T., Ann. Occup. Hyg., 11, 235 (1968).

8. Cox, R.A., J. Photochem., 3, 175 (1974).

9. Chang, Y.S., J.H. Shaw, E. Niple, J.G. Calvert, W.H. Chan, S.Z. Levine, and W.M. Uselman, EPA-600/3-78-057, U.S. Environmental Protection Agency, Research Triangle Park, NC (1978).

10. Cox, R.A., R.G. Derwent, and M.R. Williams, Environ. Sci. Technol., 14, 57 (1980).

11. Niki, H., In: "Chemical Kinetic Data Needs for Modeling the Lower Troposphere," NBS special publication 557, August 1979.

12. Bandow, H., M. Okuda, and H. Akimoto, J. Phys. Chem. 84, 3604 (1980).

13. Alpert, N.L., W.E. Keiser, and H.A. Szymanski In: IR Theory and Practice in Infrared Spectroscopy, 2nd. ed., Plenum Press, New York (1970).

14. Sanhueza, E., I.C. Hisatsume, and J. Heicklen, Amer. Chem. Soc. Meeting, Philadelphia, Pennsylvania. April 1975.

15. Hisatsune, I.C. and Heicklen, J., Can. J. Spectrosc., 18, 77 (1973).

16. Gay, B.W., Jr., R.C. Noonan, P.L. Hanst, and J.J. Bufalini, In Removal of Trace Contaminants from the Air" ACS Symposium Series, 17, 132 (1975).

17. Atkinson, R. and A.C. Lloyd, Submitted to J. Phys. Chem. Ref. Data.

18. Edney, E.O., J.W. Spence, and P.L. Hanst, In: Nitrogeneous Air Pollutants, D. Grosjean, ed. Ann Arbor Press, Ann Arbor, Michigan. (1979).

19. Aldrich Chemical Company, Milwaukee, Wisconsin (1975).

20. Spence, J.W., E.O. Edney, and P.L. Hanst, Chem. Phys. Lett. 56, 478 (1978).

21. Hendry, D.G. and R.A. Kenley, J. Amer. Chem. Soc., 99, 3198 (1977).

22. Cox, R.A. and M. J. Roffey, Environ. Sci. Technol., 11, 900 (1977).

23. Morris, E.D., Jr. and H. Niki, J. Chem. Phys. 55, 1991 (1971).

24. Niki, H., P.D. Maker, C.M. Savage, and L.P. Breitenbach, J. Phys. Chem., 82, 132 (1978).

25. Atkinson, R. and J.N. Pitts, Jr., J. Chem. Phys. 68, 3581 (1978).

26. Stief, L.J., D.F. Nava, W.A. Payne, and J. V. Michael, Amer. Chem. Soc. Meeting, Washington, DC, September 1979.

27. Howard, C.J., J. Chem. Phys., 65, 4771 (1976).

28. D.D. Davis, U. Machado, G. Smith, S. Wagner, and R.T. Watson (unpublished results).

29. Chang, J.S. and F. Kaufman, J. Chem. Phys., 66, 4989 (1977).

30. Winer, A.M., A.C. Lloyd, K.R. Darnall, and J.N. Pitts, Jr., J. Phys. Chem. 80, 1635 (1976).

31. Gay, B.W., Jr., P.L. Hanst, J.J. Bufalini, and R.C. Noonan, Environ. Sci. Technol. 10, 58 (1976).

32. Altshuller, A.P. and I.R. Cohen, J. Air Wat. Pollut., 7, 1043 (1963).

APPENDIX A

Preparation of HONO

I. Equipment needed:

1. Magnetic stirrer with stirring bar
2. One Two neck 2-l (or l-l) mixing flask
3. Two l-l volumetric flasks
4. One U-shaped tube
5. One 125-ml pear-shaped separatory funnel with stopcock
6. Adaptor for separatory funnel
7. Fritted bubbler top
8. One l-l beaker for ice
9. Ringstand with clamp
10. Tank of nitrogen gas
11. Flowmeter
12. Connecting hoses and tubes
13. Distilled water
14. Bottle of sodium nitrite ($NaNO_2$)
15. Bottle of sulfuric acid (H_2SO_4)

II. Preparations:

A. Sodium nitrite solution: The 1.2×10^{-2} Molar solution of $NaNO_2$ must be made fresh daily since it will not keep overnight. Each run uses 100 ml of solution. To prepare, add 0.17 g of $NaNO_2$ per 100 ml of distilled water in one of the volumetric flasks and shake gently to mix.

B. Sulfuric acid solution: The 5% by volume H_2SO_4 solution is prepared by slowly adding 40 ml of reagent grade H_2SO_4 to 800 ml of distilled water in the other volumetric flask. Shake the flask gently to mix and be careful to avoid overheating.

C. Fill the l-l beaker with ice and add water.

D. Evacuate the cell to 300 torr air and assemble the apparatus as shown in the diagram.

E. Add 150 ml of H_2SO_4 solution to the 2-l mixing flask and add 100 ml of $NaNO_2$ solution to the separatory funnel. Attach all tubes and hoses and prepare to start.

III. Making HONO:

Open all valves in the N-line to begin the flow at about 8 l/min. Turn magnetic stirrer on at the lowest speed. Turn the separatory funnel stopcock until the $NaNO_2$ solution begins to drop into the H_2SO_4 solution. Adjust the drop rate to about 2 drops/sec. It should take about 10 min to use all of the $NaNO_2$ solution and the stopcock should be closed immediately at the end of this operation and the stirrer turned off. Allow about 10 l more of N_2 to flow through the apparatus to insure that all residual HONO is flushed from the mixing flask. Turn off the N_2 and close the inlet port to the cell.

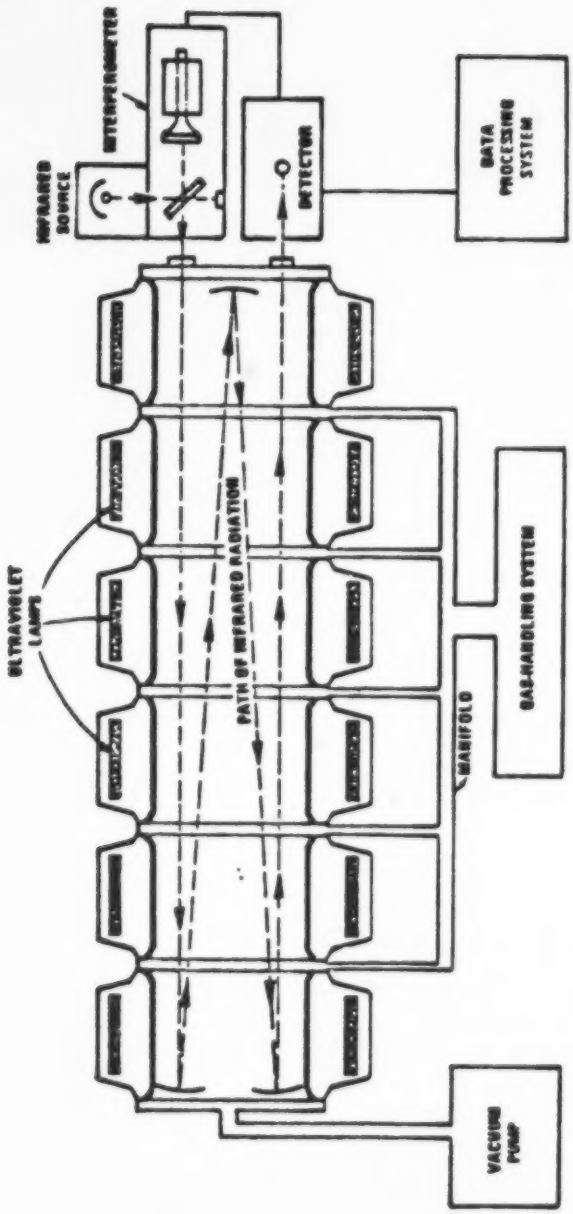

Figure 1. Long path cell and IR spectrometer

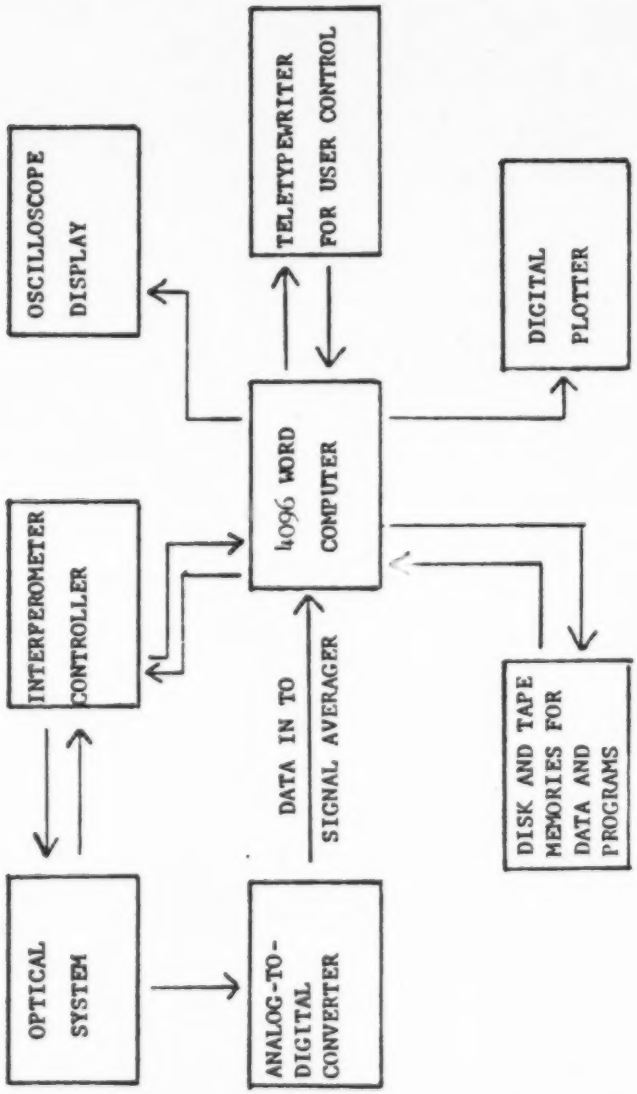

Figure 2. Schematic of data handling system

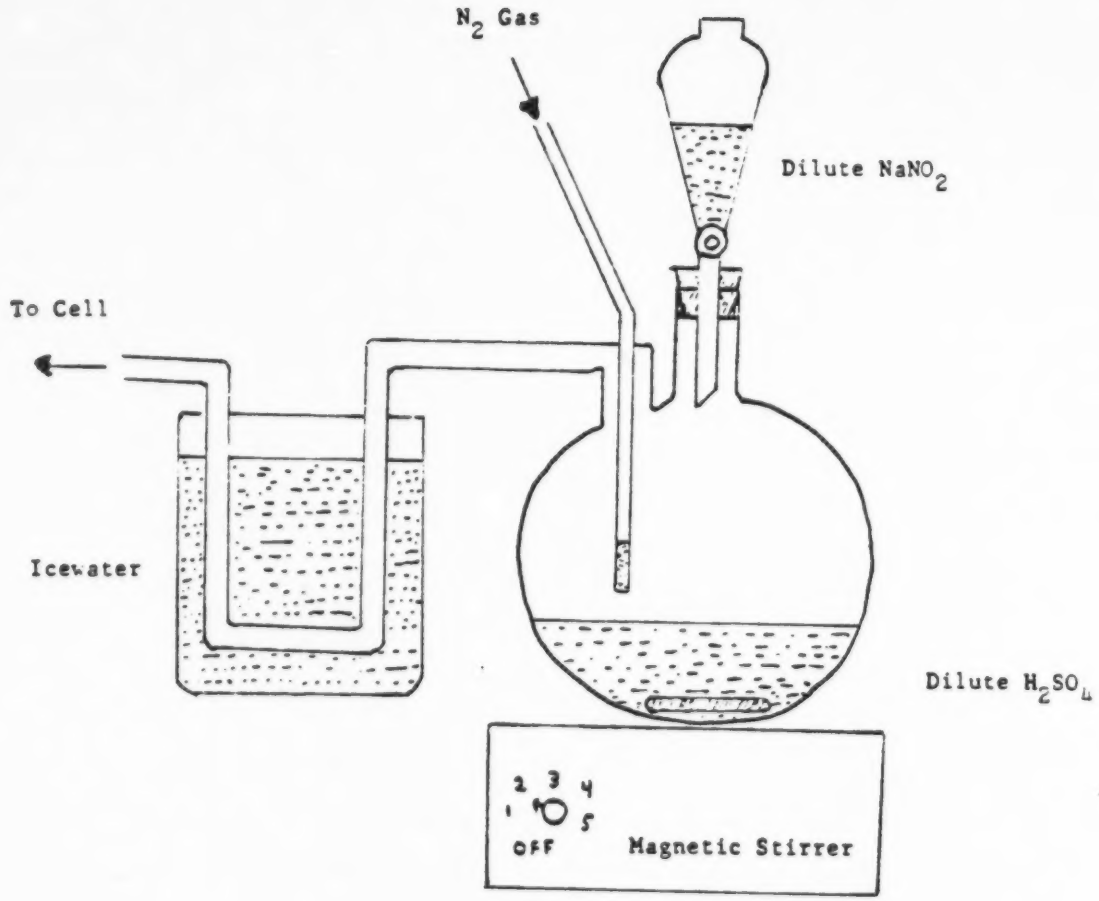

Figure 3. HONO generating system

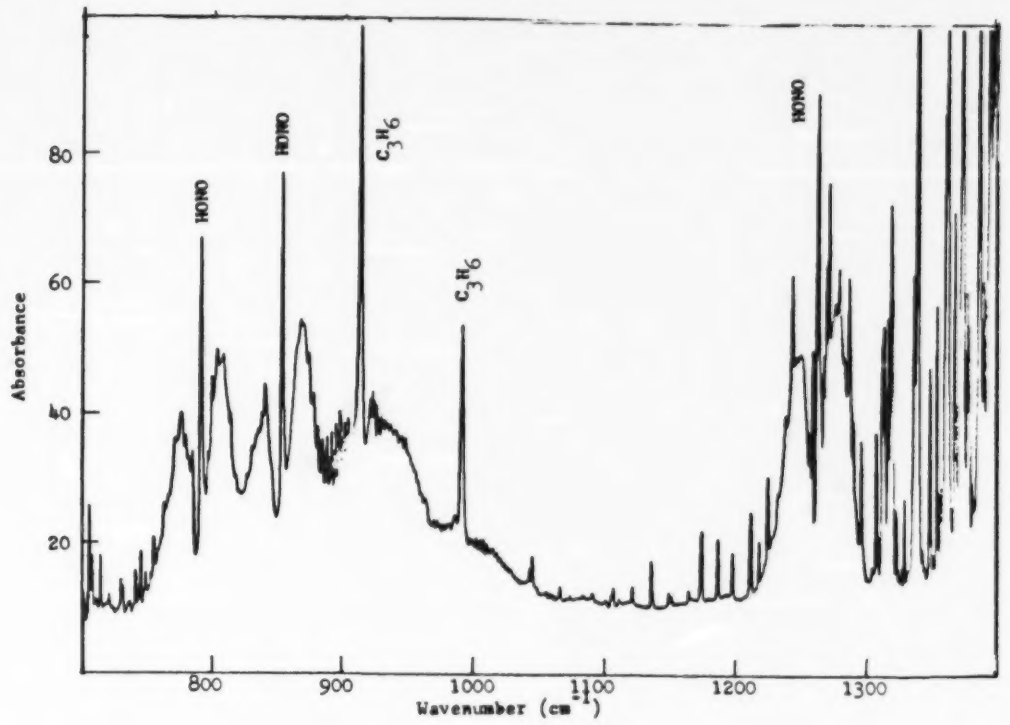

Figure 4a. MCT spectrum of reactants of propylene/HONO/NO_x run

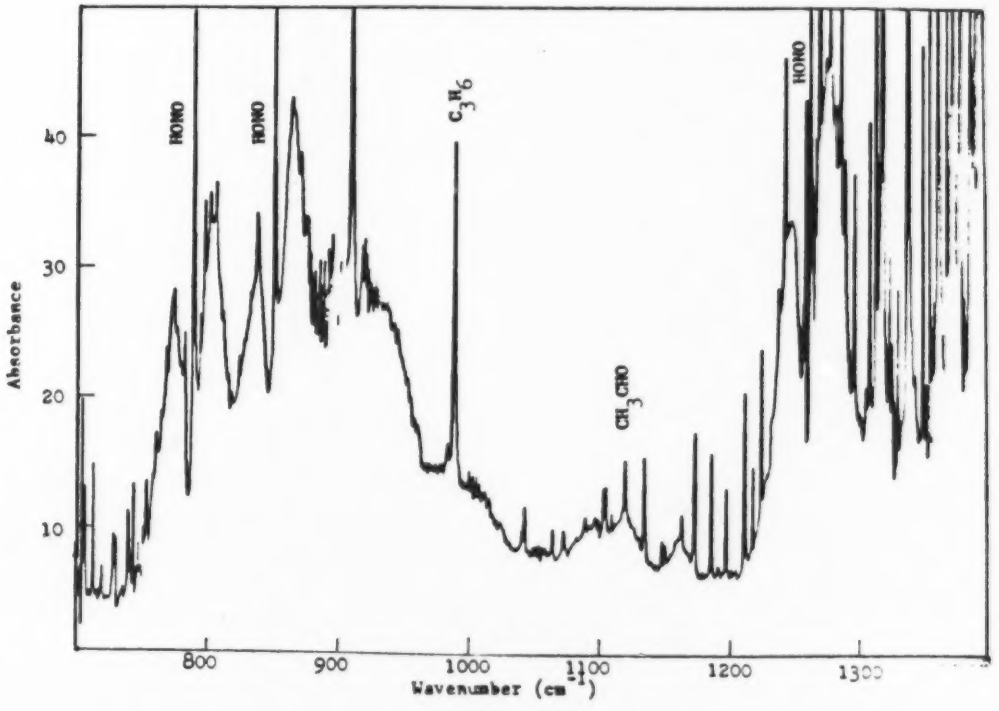

Figure 4b. MCT spectrum of propylene 5-min irradiation

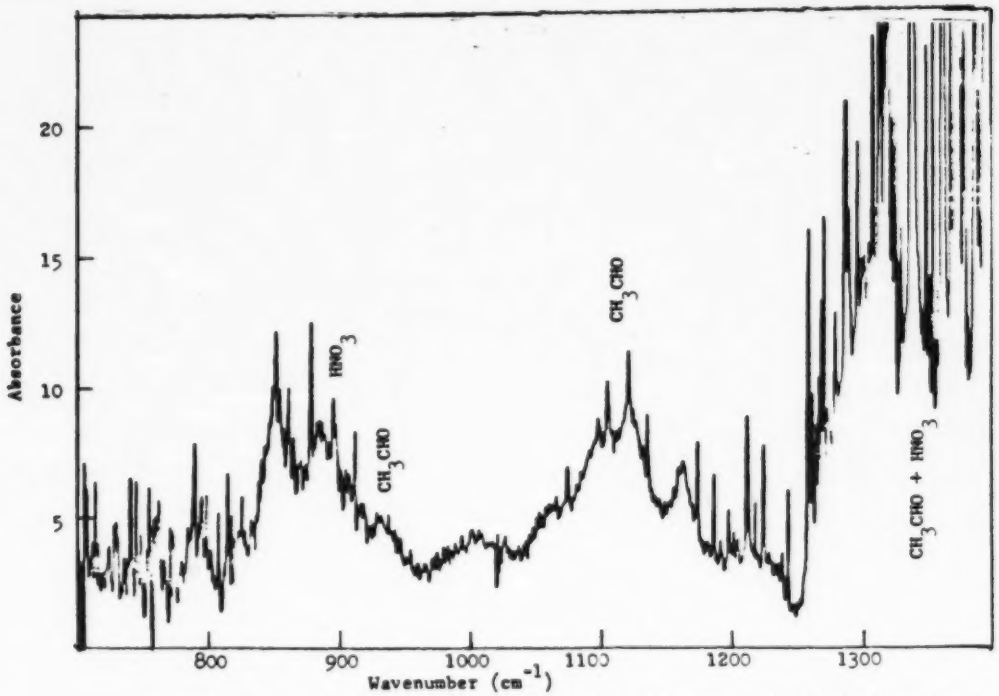

Figure 5a. Five-min MCT propylene spectrum with HONO and propylene subtracted

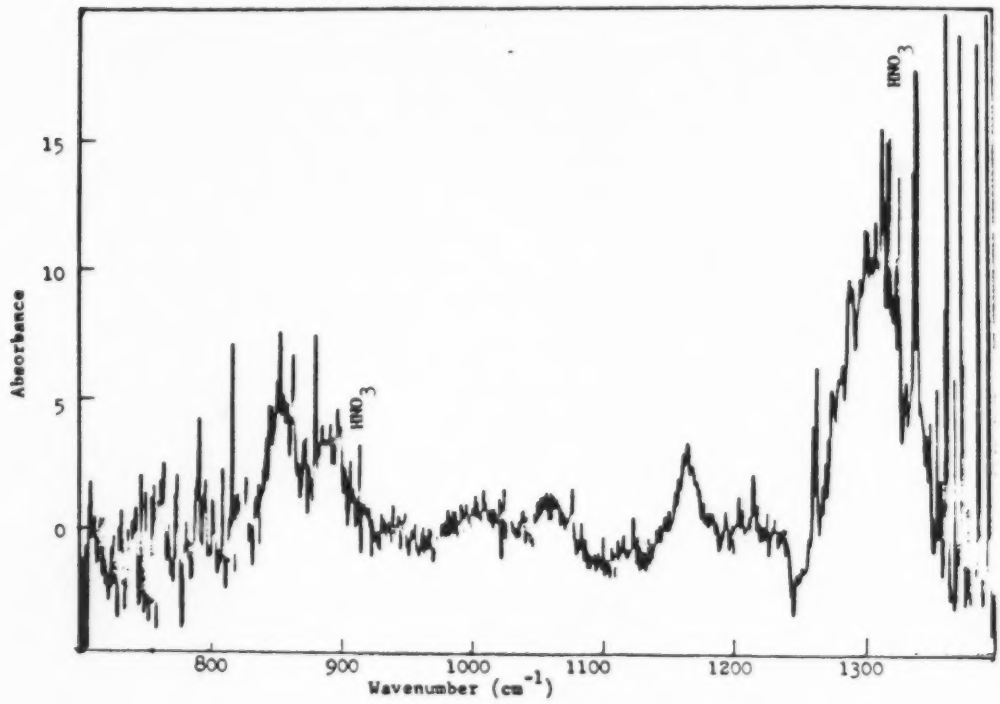

Figure 5b. Five-min MCT propylene spectrum with HONO, propylene, and acetaldehyde subtracted

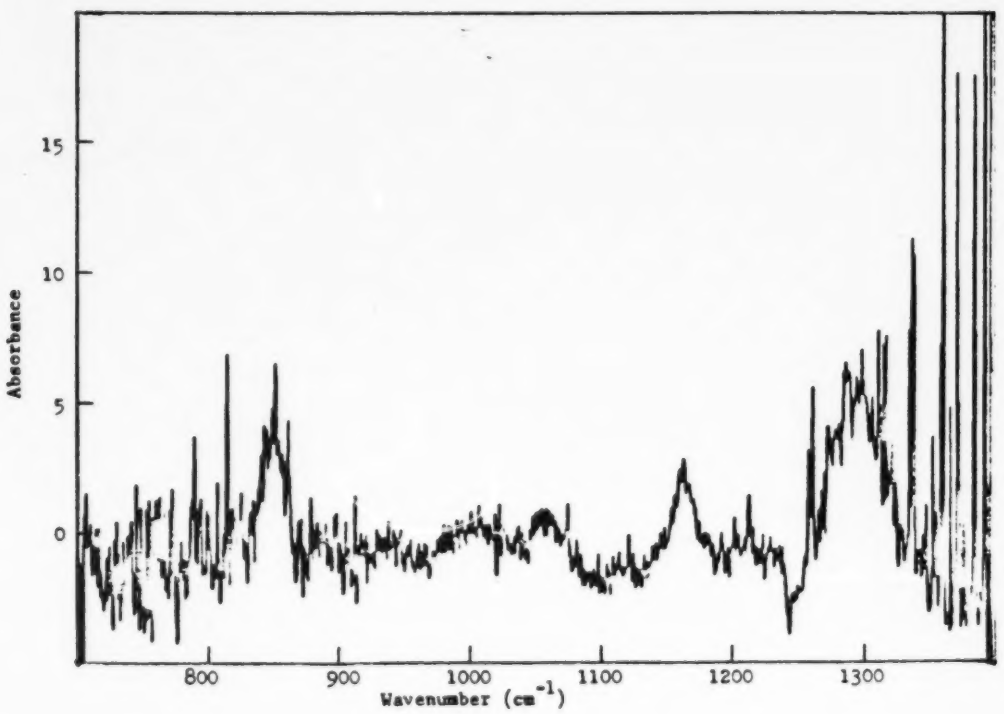

Figure 6a. Five-min MCT propylene spectrum with HONO, propylene, acetaldehyde, and HNO_3 subtracted

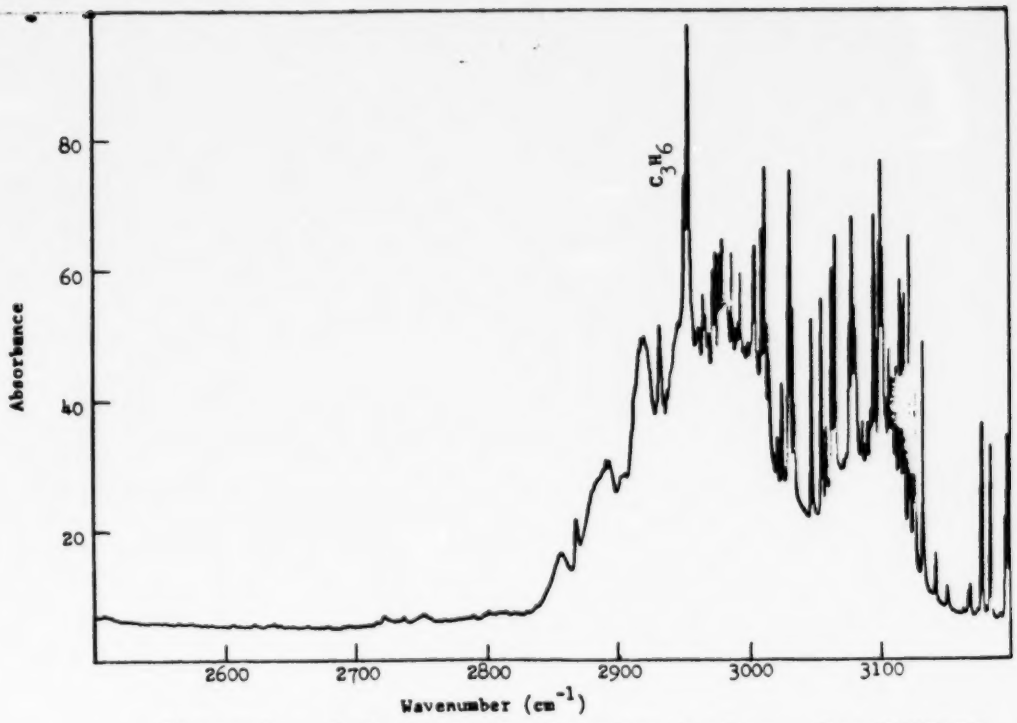

Figure 7a. InSb spectrum of reactants of propylene/HONO/NO_x run

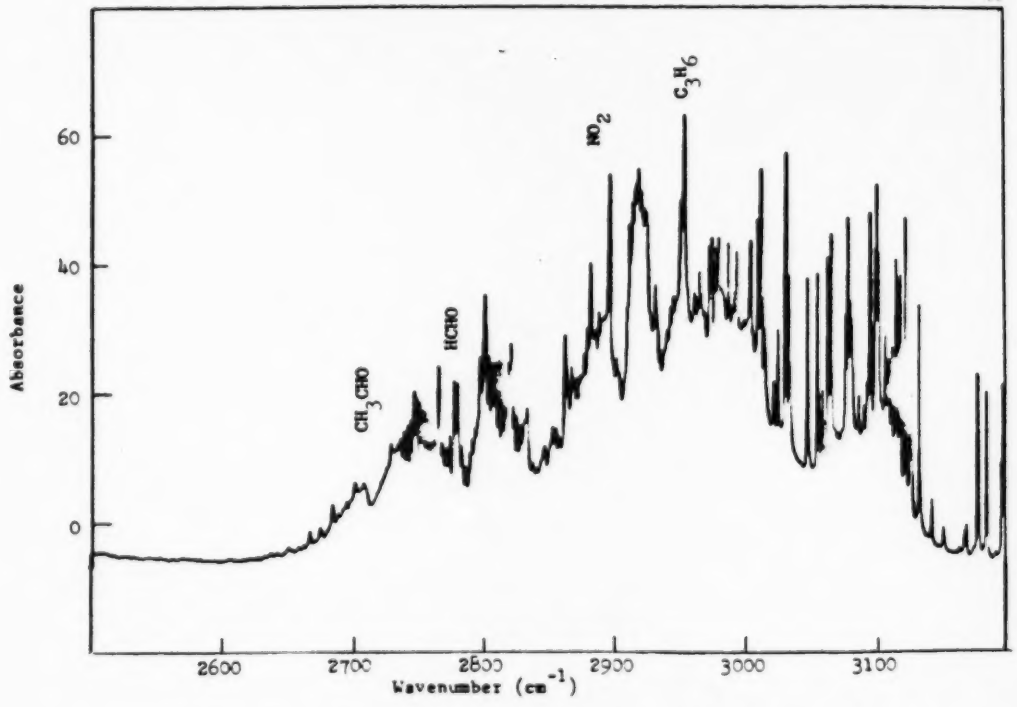

Figure 7b. InSb spectrum of propylene 5-min irradiation

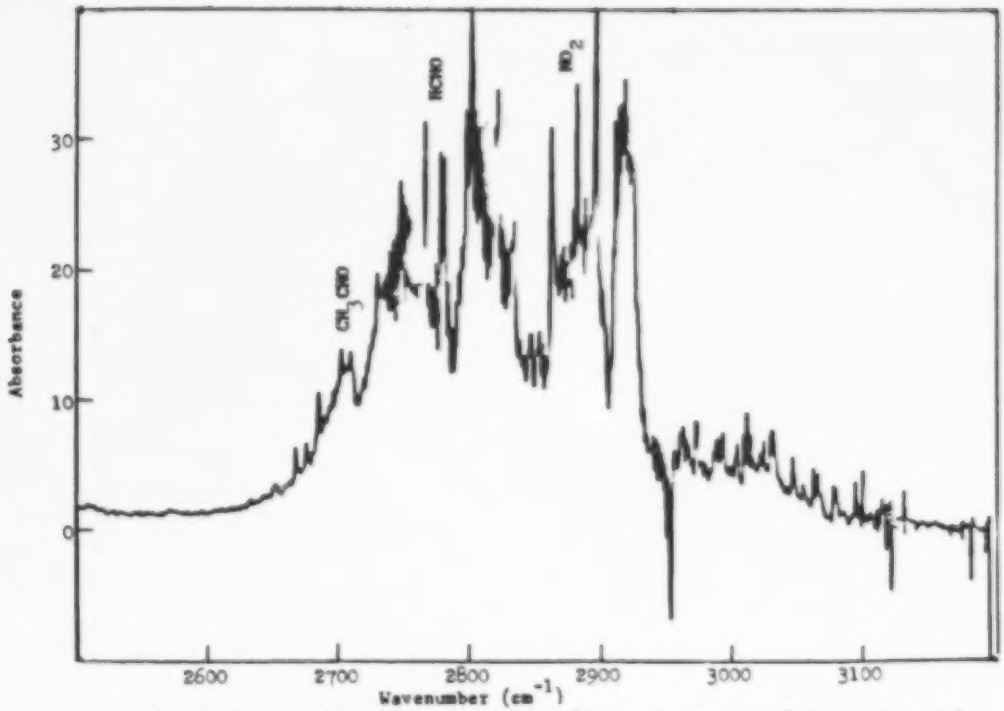

Figure 8a. Five-min InSb propylene spectrum with water and propylene subtracted

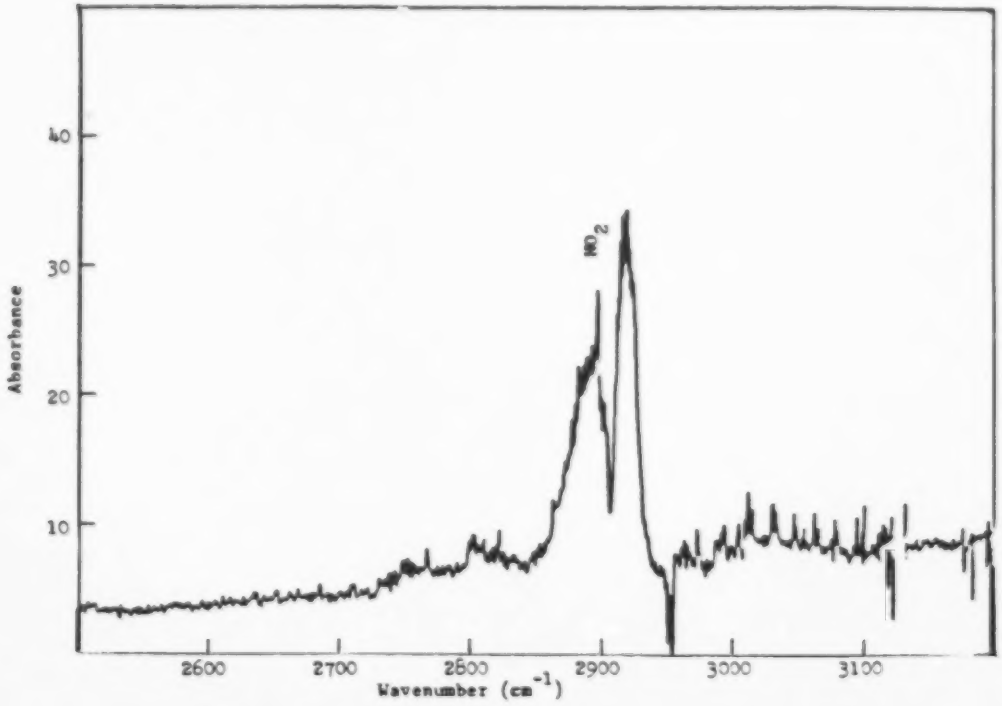

Figure 8b. Five-min InSb propylene spectrum with water, propylene, acetaldehyde, and formaldehyde subtracted

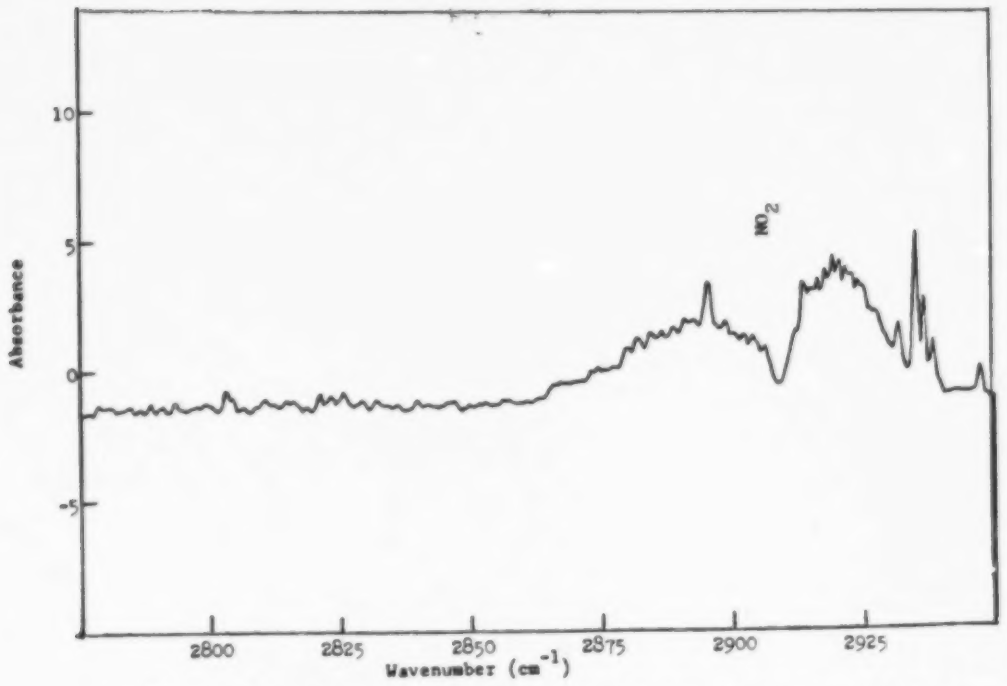

Figure 9a. InSb spectrum of initial NO, Right: 5-min MCT spectrum

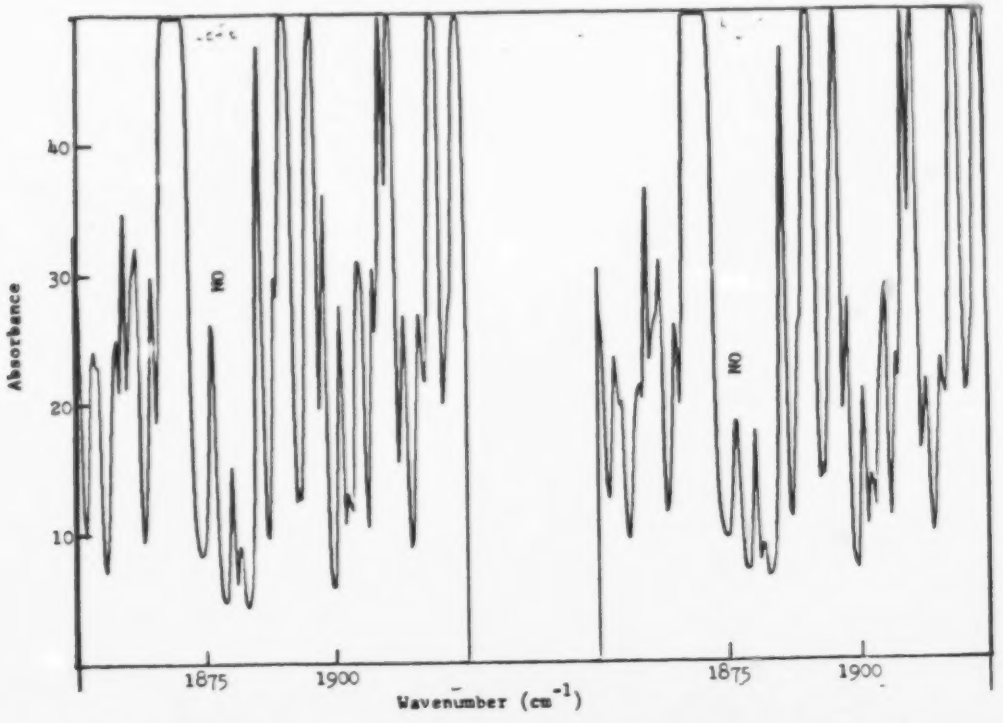

Figure 9b. Left - MCT spectrum of initial NO, Right: 5-min MCT spectrum

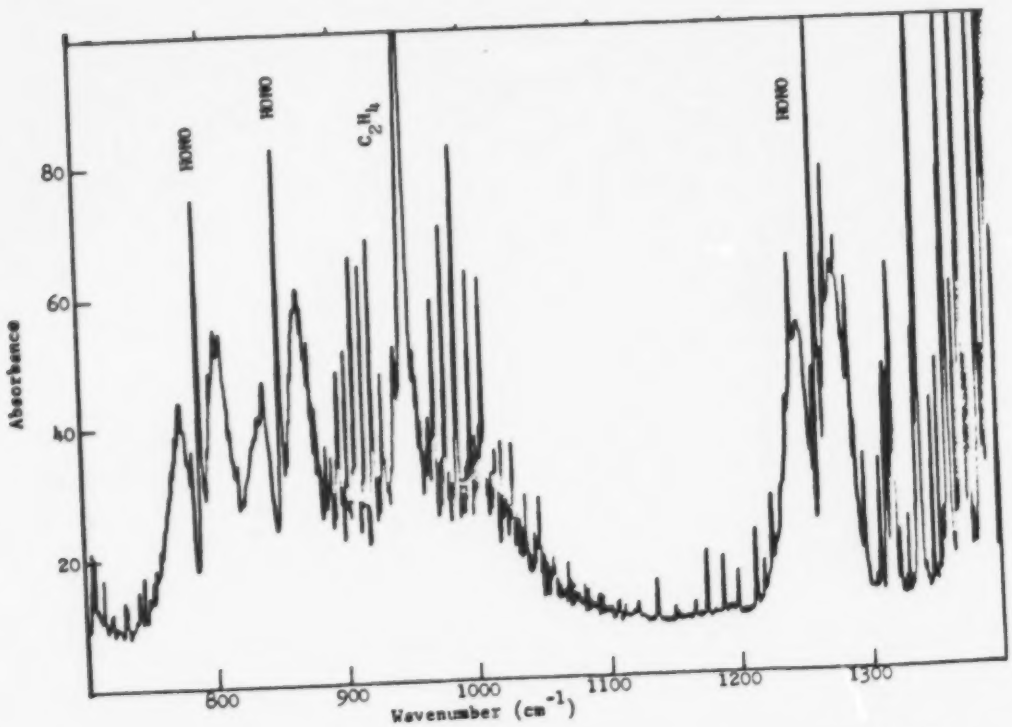

Figure 10a. MCT spectrum of reactants of ethylene/HONO/NO_x run

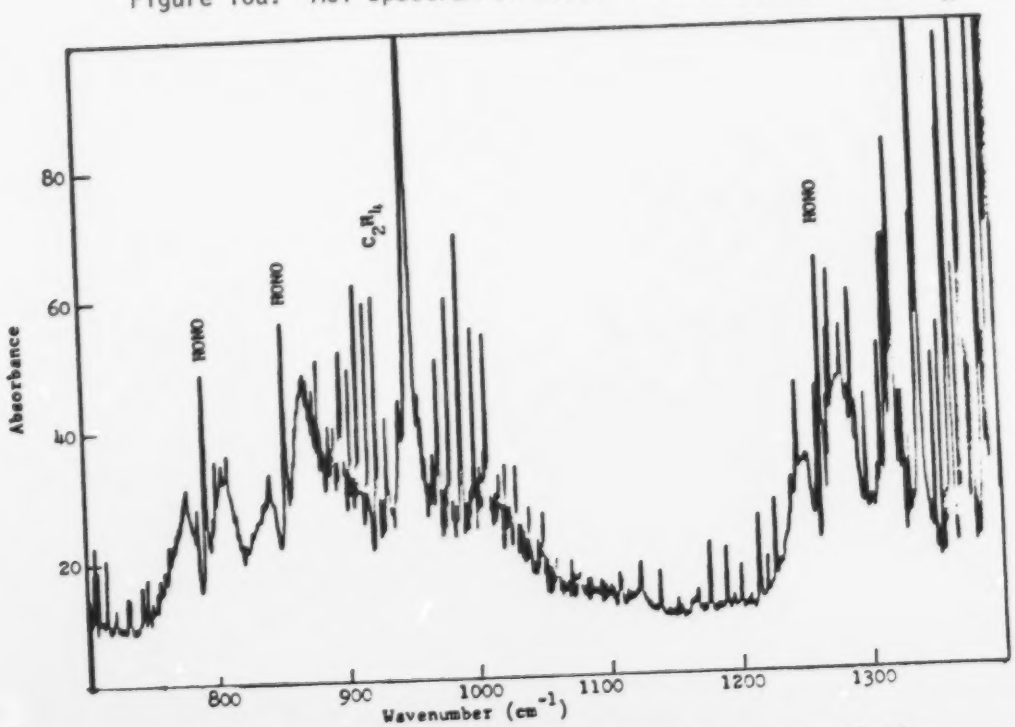

Figure 10b. MCT spectrum of ethylene 12-min irradiation

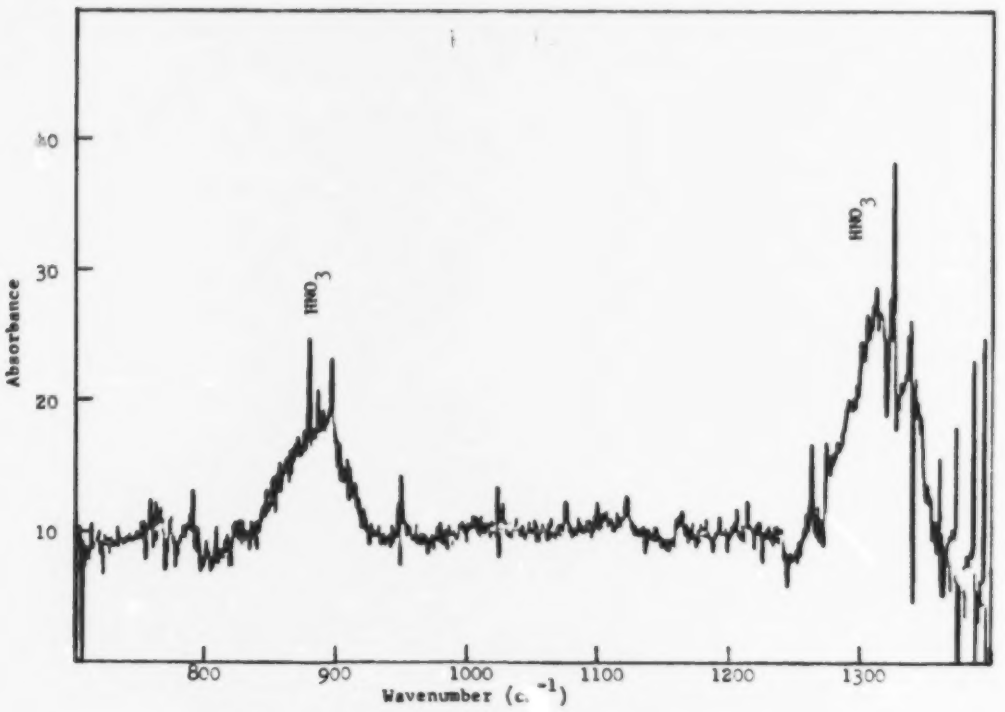

11a. Twelve-min MCT ethylene spectrum with HONO and ethylene subtracted

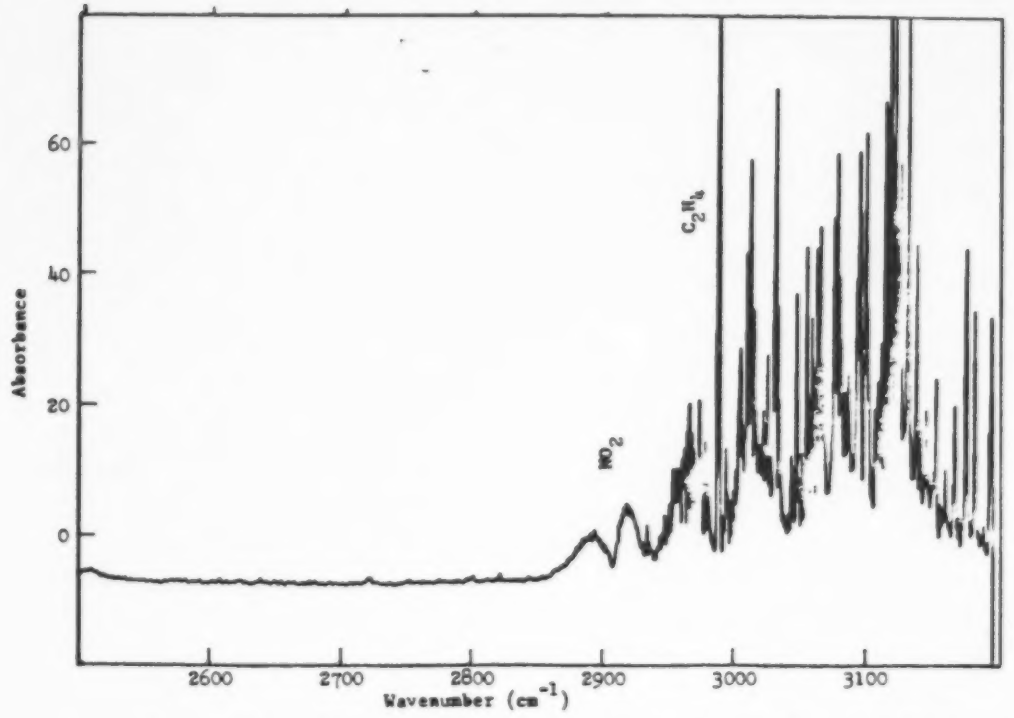

Figure 12a. InSb spectrum of reactants of ethylene/HONO/NO_x run

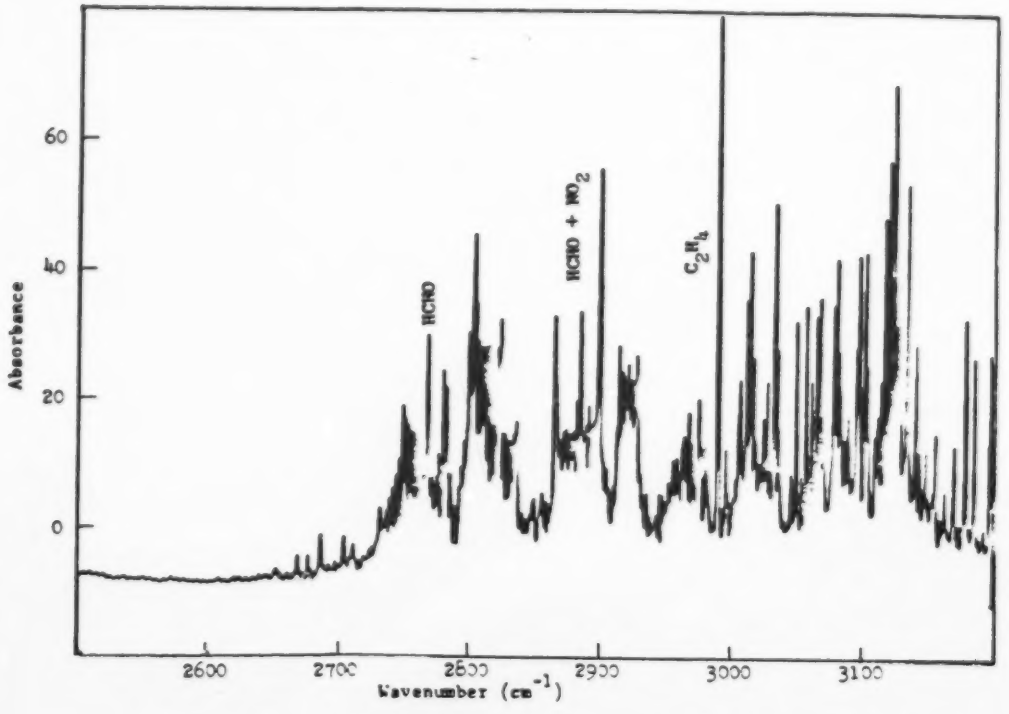

Figure 12b. InSb spectrum of ethylene 12-min irradiation

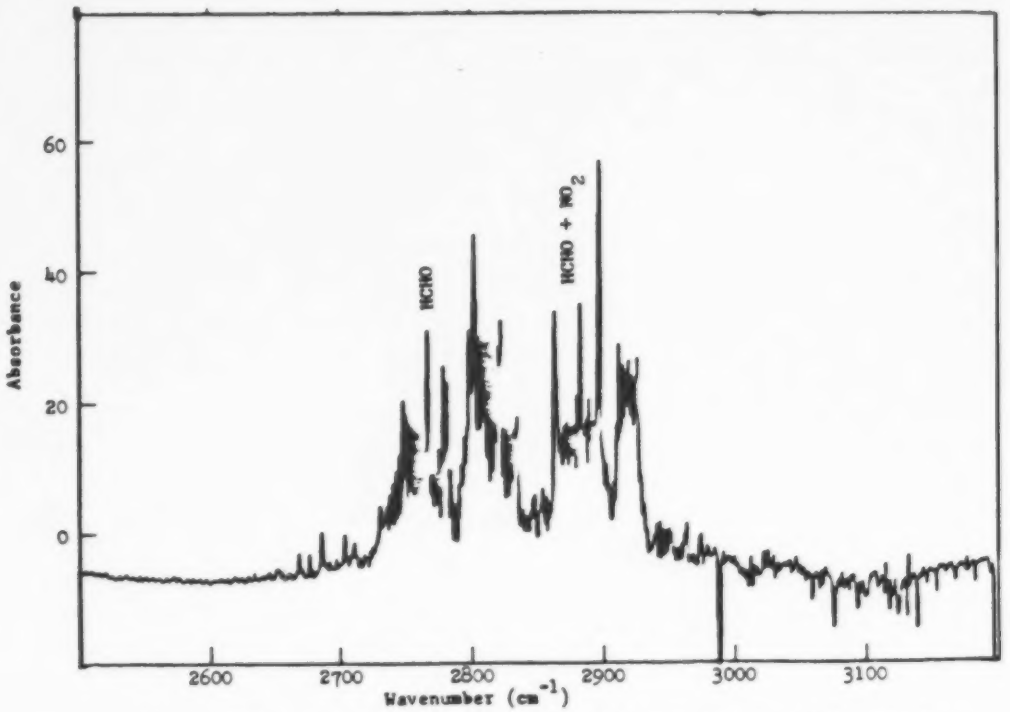

Figure 13a. Twelve-min InSb ethylene spectrum with ethylene and water subtracted

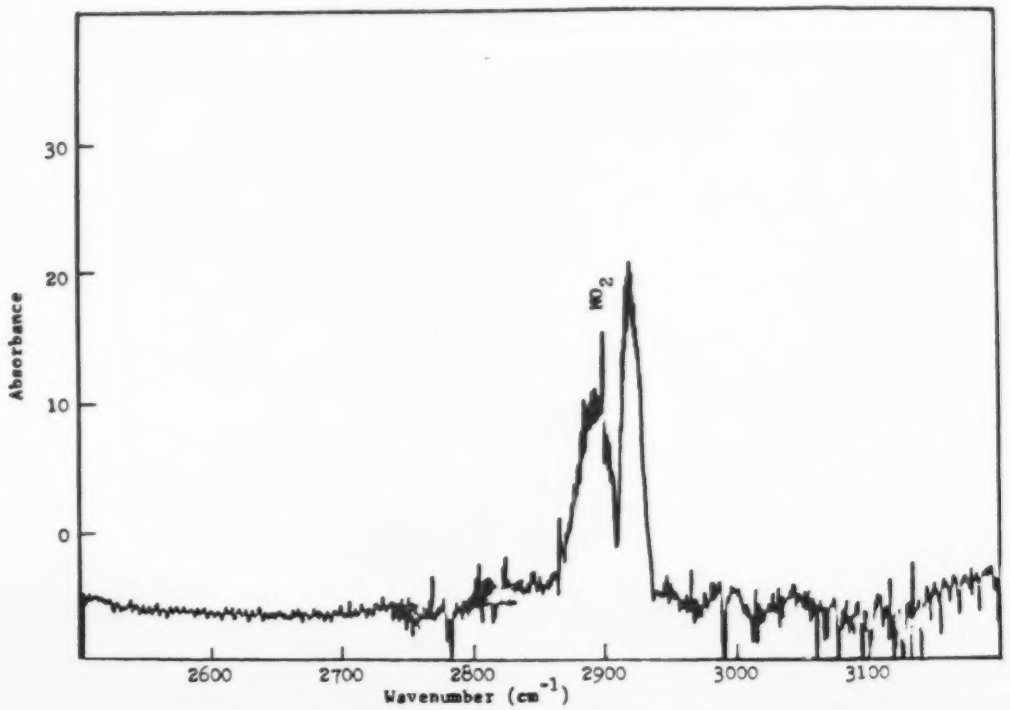

Figure 13b. Twelve-min InSb ethylene spectrum with ethylene, water, and formaldehyde subtracted

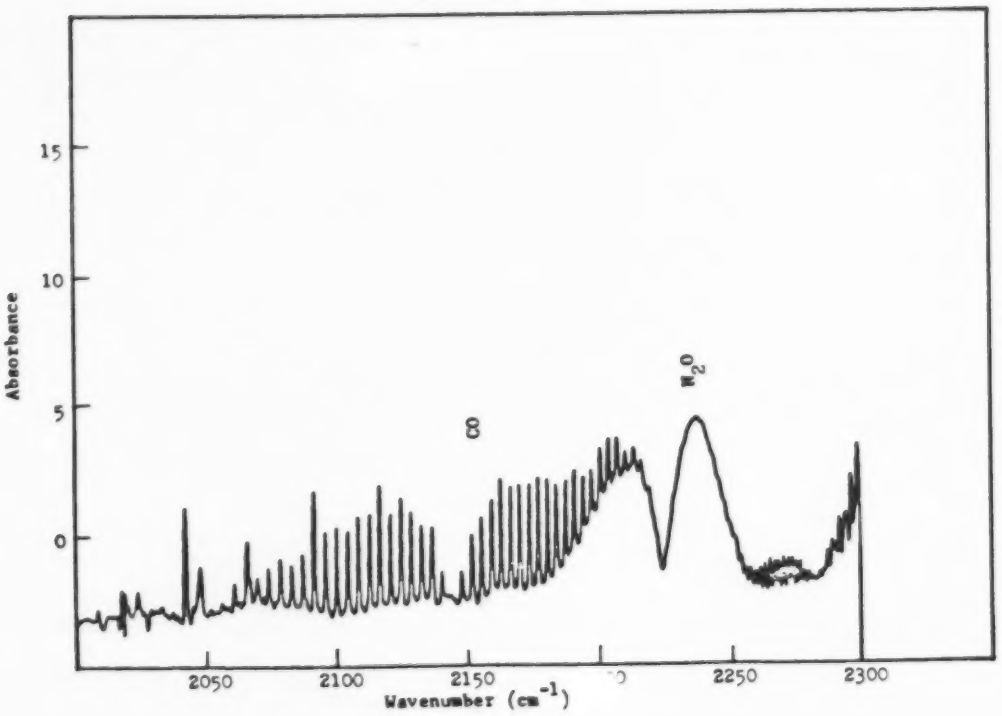

Figure 14a. InSb spectrum of ethylene 12-min irradiation

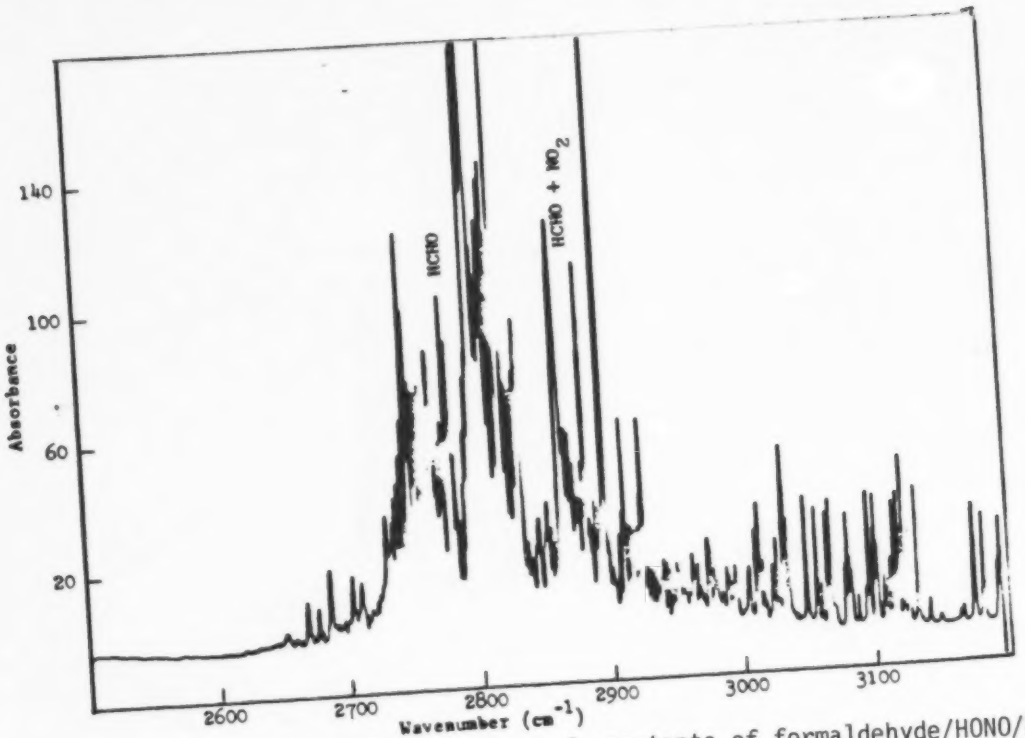

Figure 15a. InSb spectrum of reactants of formaldehyde/HONO/NO_x run

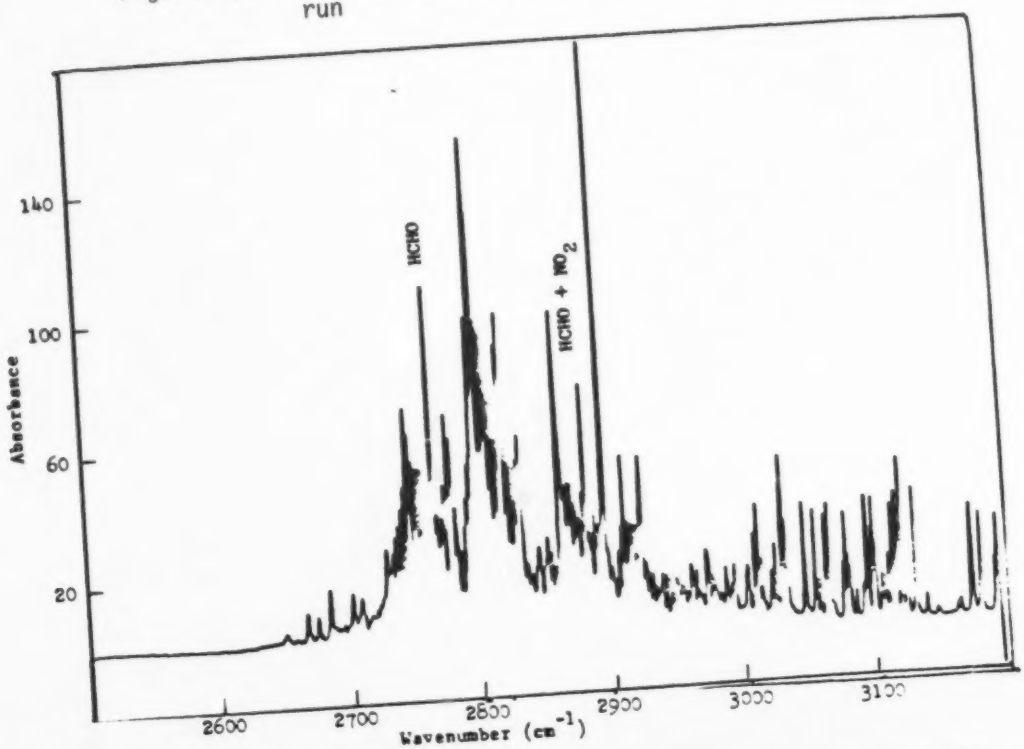

Figure 15b. InSb spectrum of formaldehyde 12-min irradiation

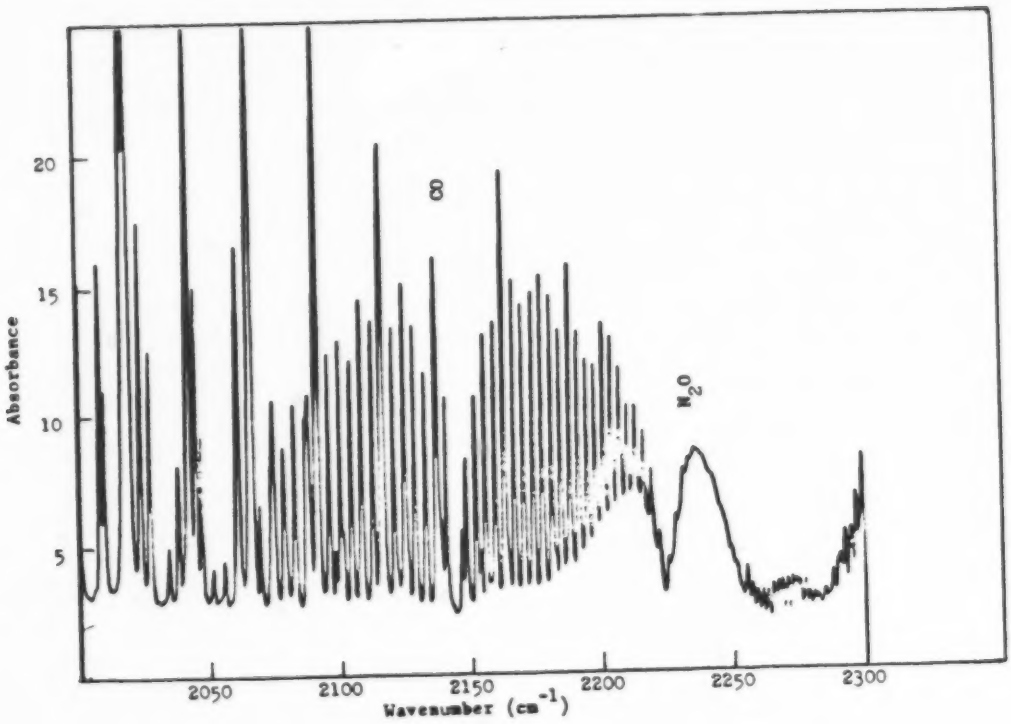

Figure 16a. InSb spectrum of formaldehyde 12-min irradiation

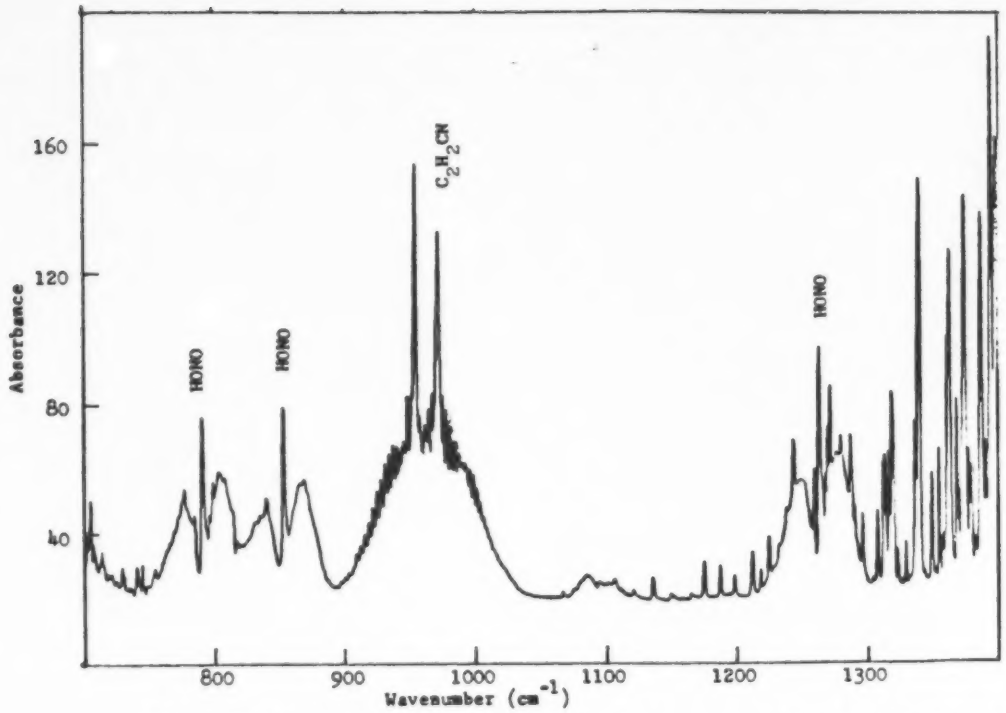

Figure 17a. MCT spectrum of reactants of acrylonitrile/HONO/NO_x run

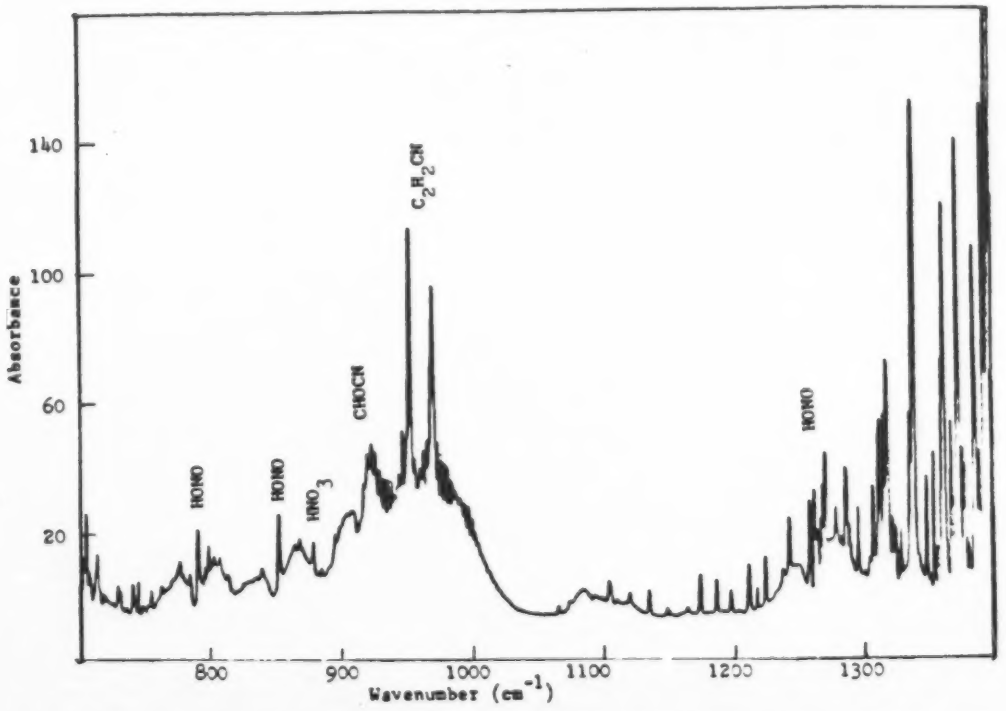

Figure 17b. MCT spectrum of acrylonitrile 20-min irradiation

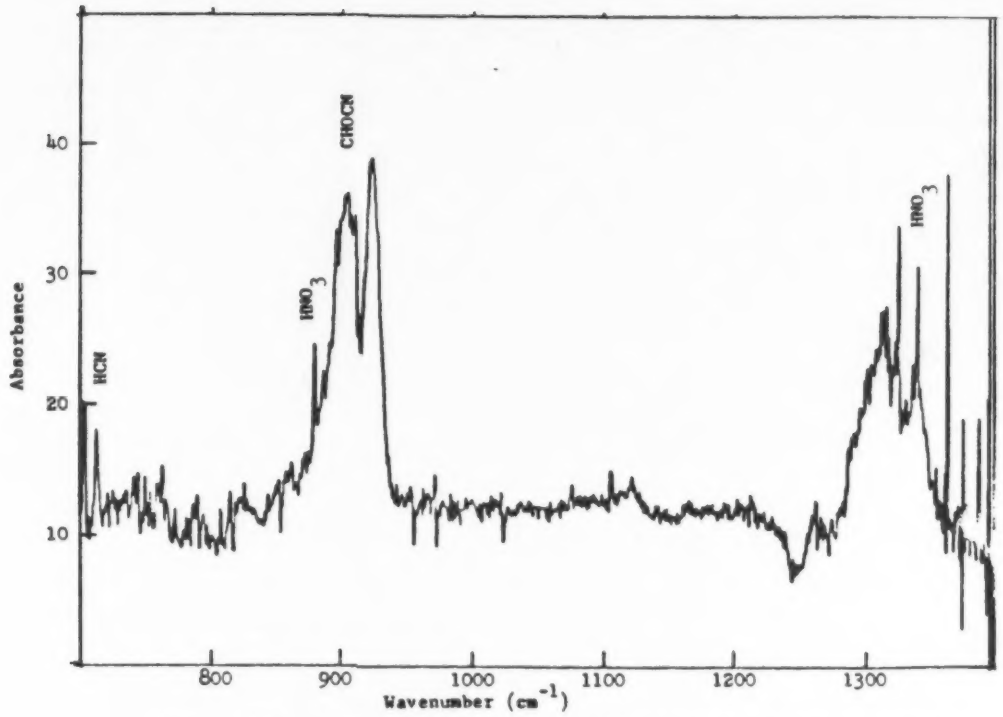

Figure 18a. MCT spectrum of acrylonitrile spectrum with HONO, acrylonitrile, and water subtracted

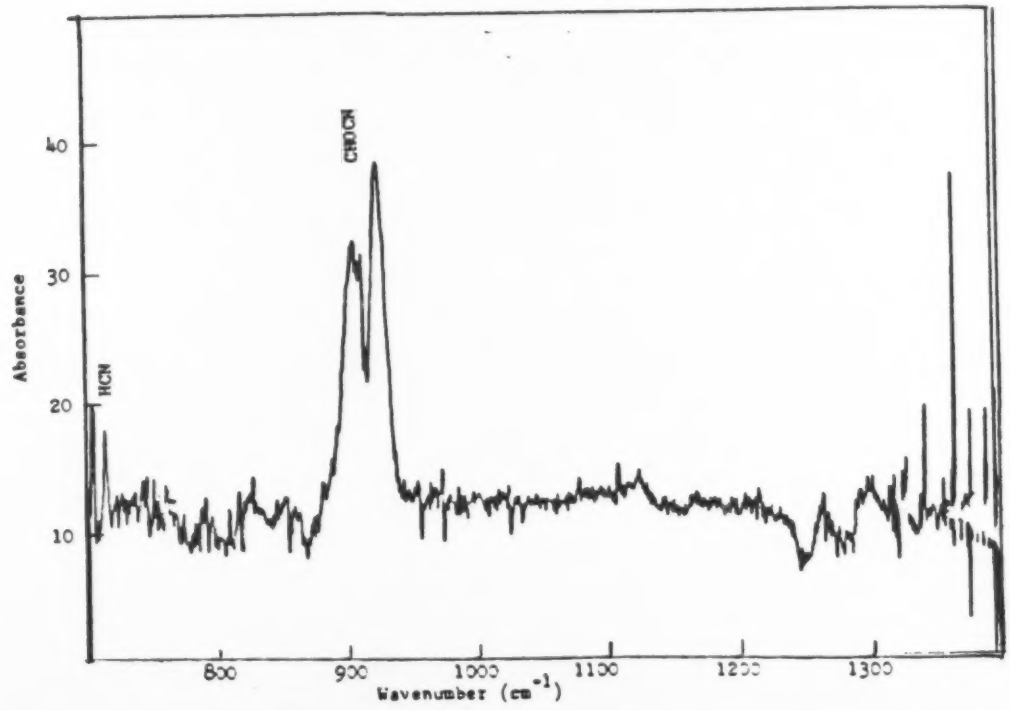

Figure 18b. Twenty-min MCT acrylonitrile spectrum with HONO, acrylonitrile, water, and HNO_3 subtracted

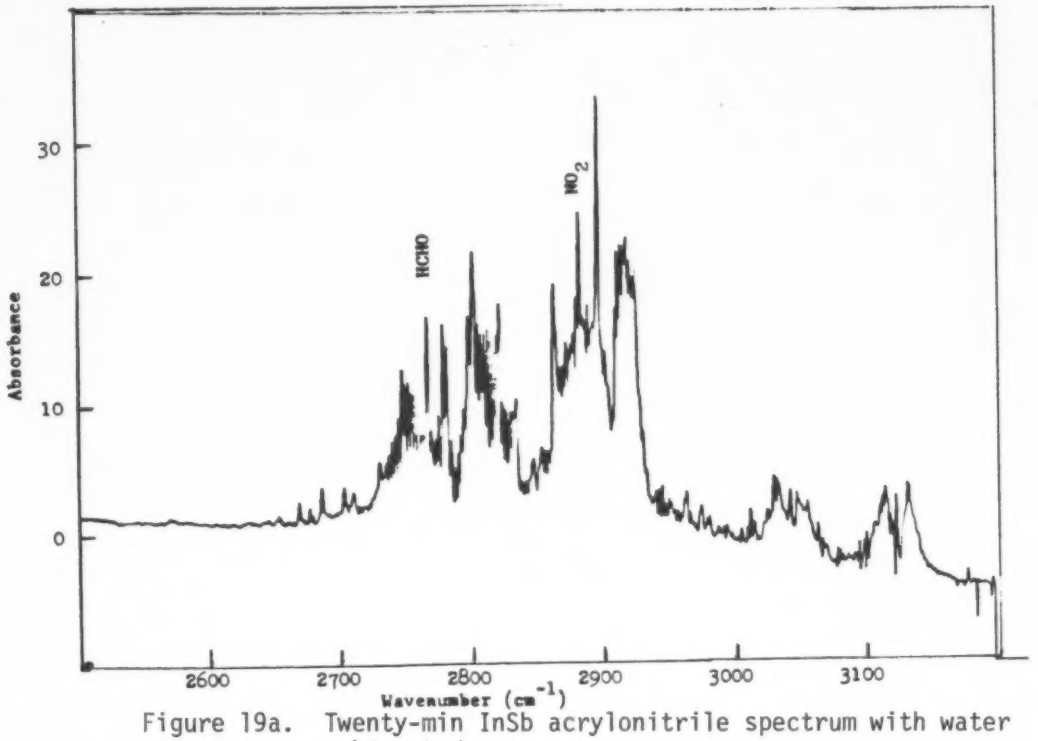

Figure 19a. Twenty-min InSb acrylonitrile spectrum with water subtracted

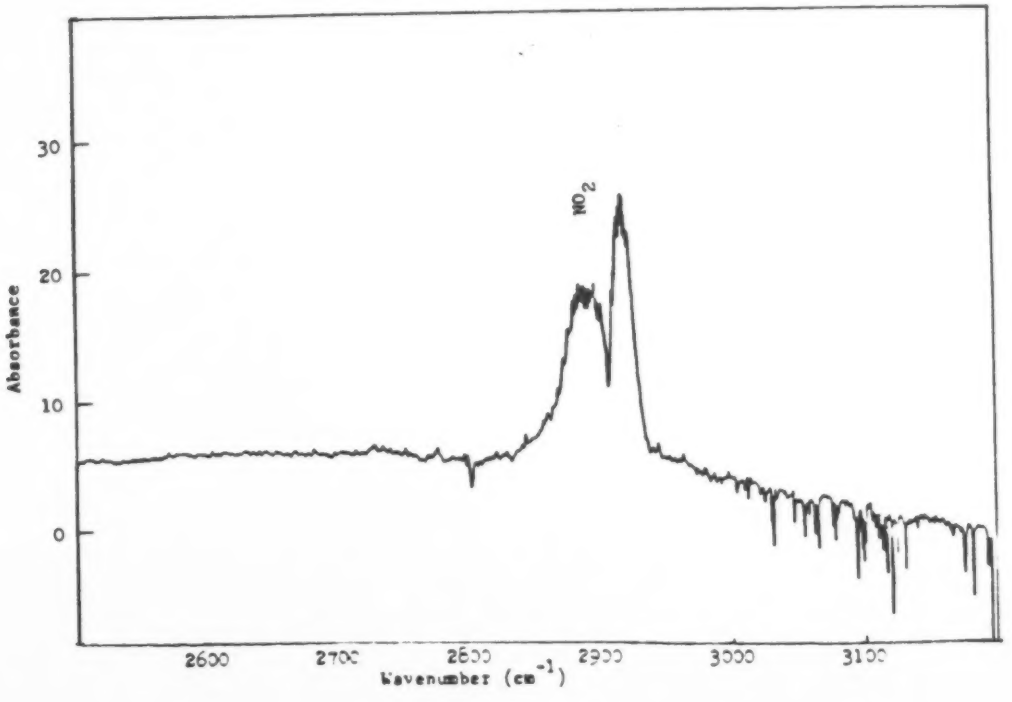

Figure 19b. Twenty-min InSb acrylonitrile spectrum with water, acrylonitrile, and formaldehyde subtracted

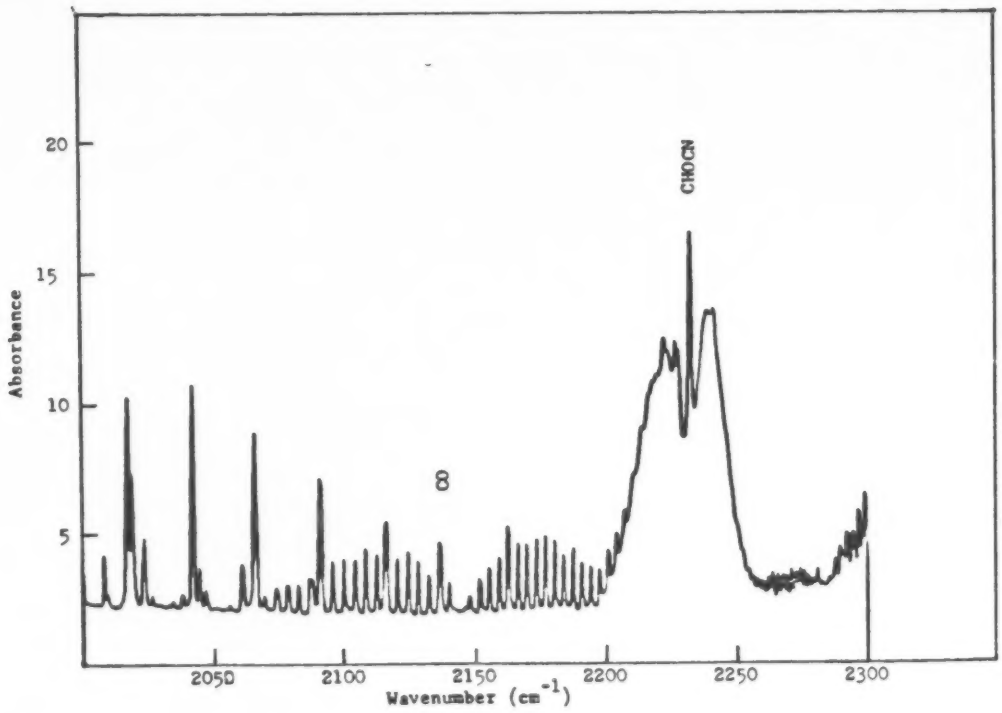

Figure 20a. Twenty-min InSb acrylonitrile spectrum with NO subtracted

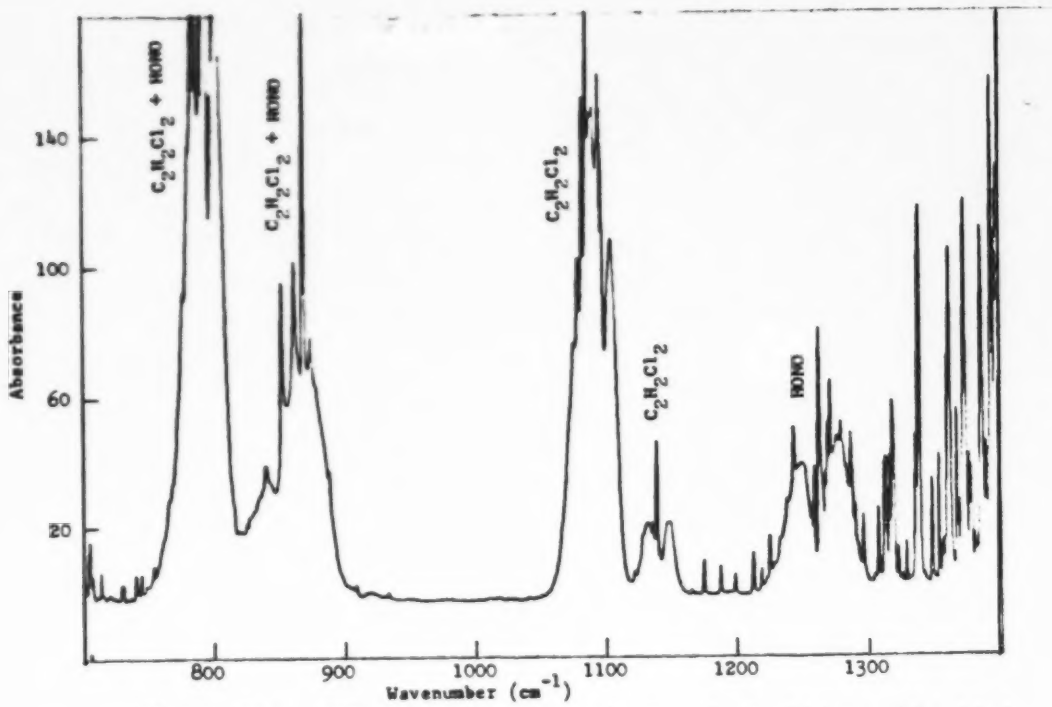

Figure 21a. MCT spectrum of reactants of vinylidene chloride/ HONO/NO_x run

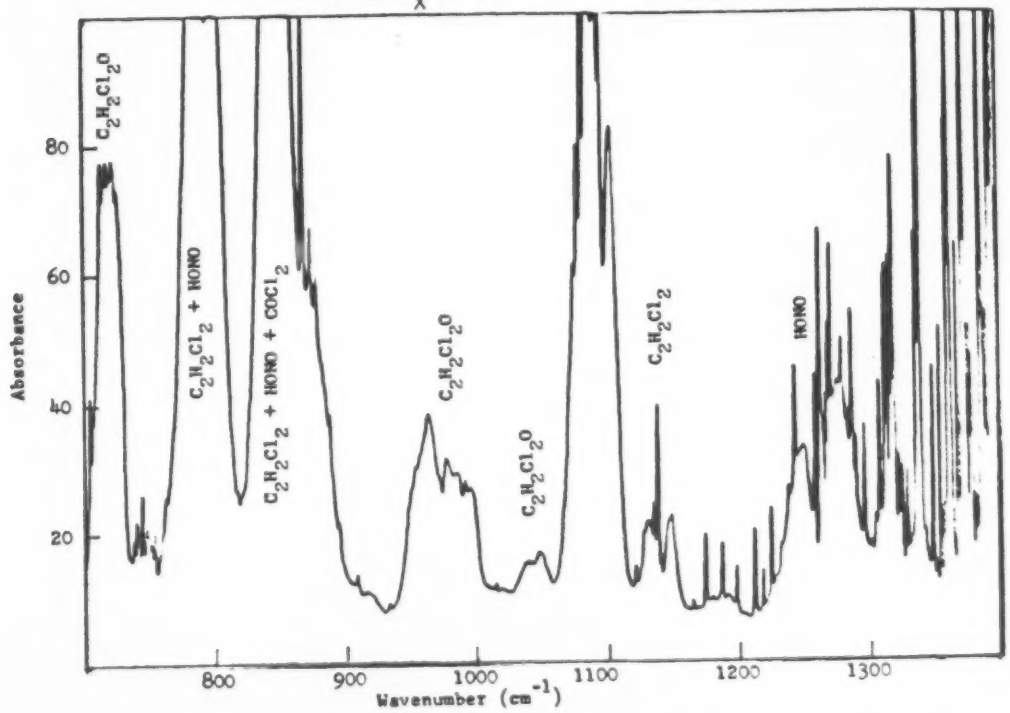

Figure 21b. MCT spectrum of vinylidene chloride 7-min irradiation

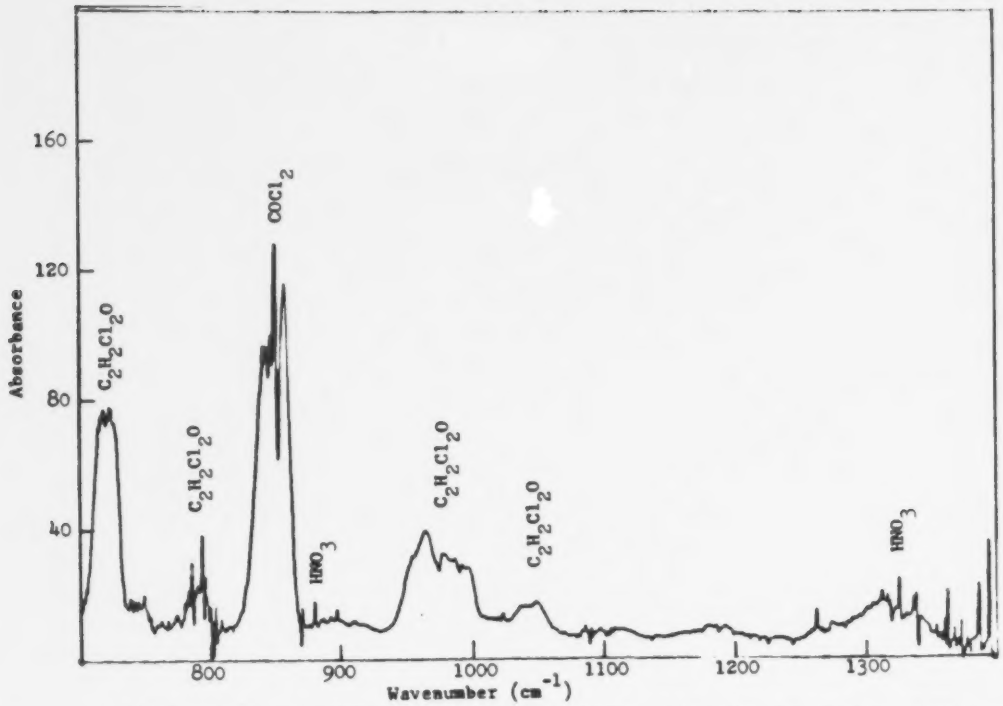

Figure 22a. Seven-min MCT vinylidene chloride spectrum with HONO, vinylidene chloride, and water substracted

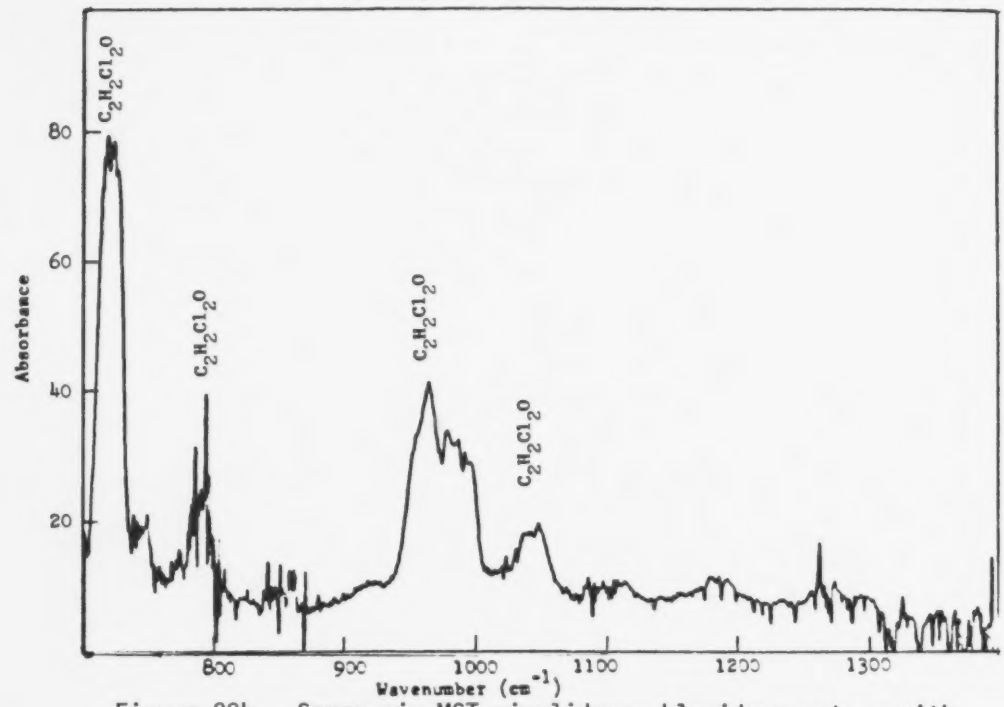

Figure 22b. Seven-min MCT vinylidene chloride spectrum with HONO, vinylidene chloride, water phosgene, and HNO_3 subtracted

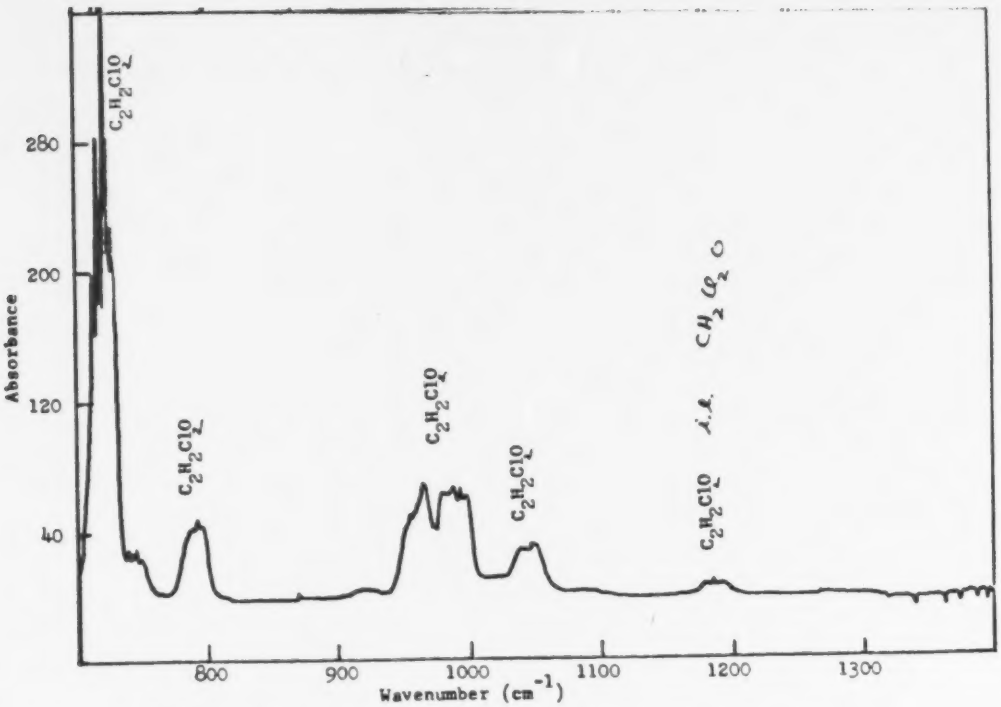

Figure 23a. MCT spectrum of chloroacetyl chloride

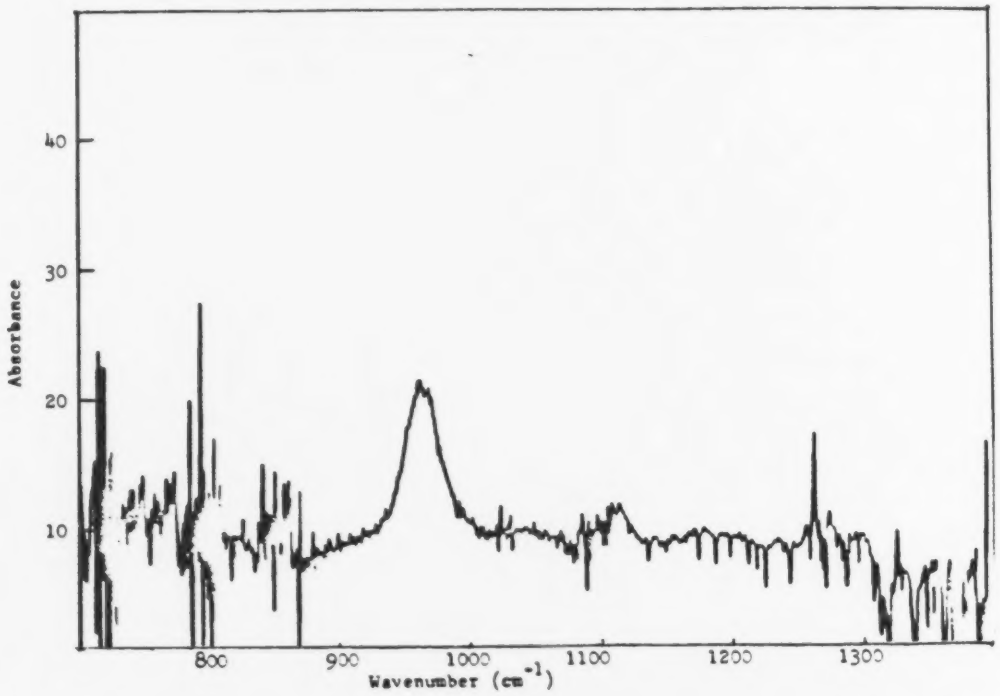

Figure 23b. Seven-min MCT vinylidene chloride spectrum with HONO, vinylidene chloride, water, phosgene, HNO_3, and chloroacetyl chloride subtracted

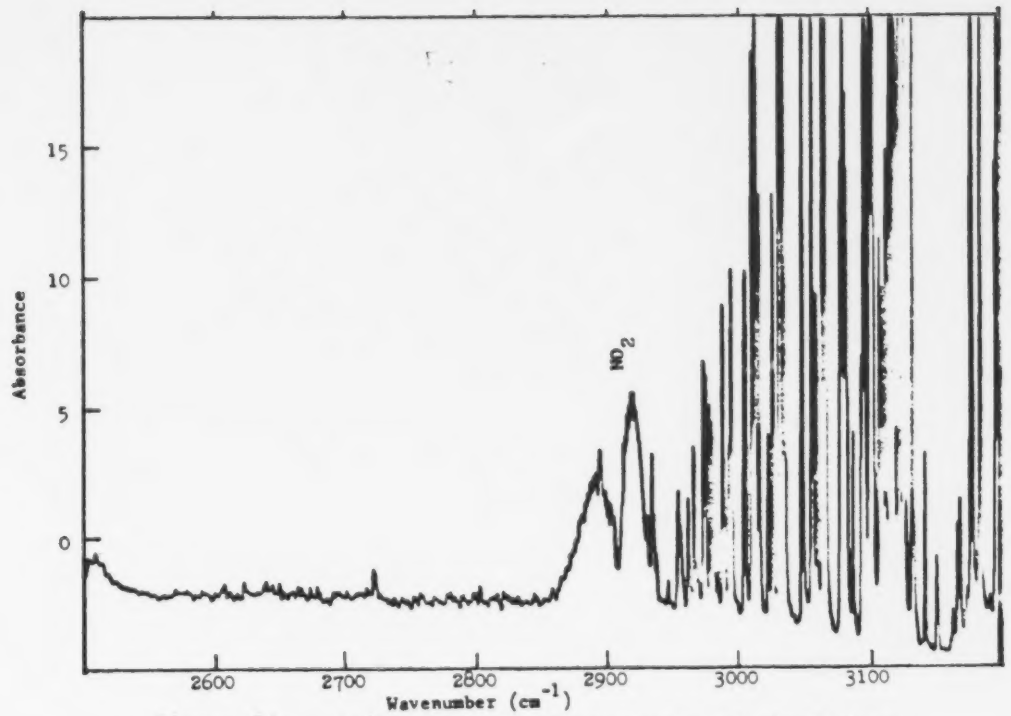

Figure 24a. InSb spectrum of reactants of vinylidene chloride/HONO/NO_x run

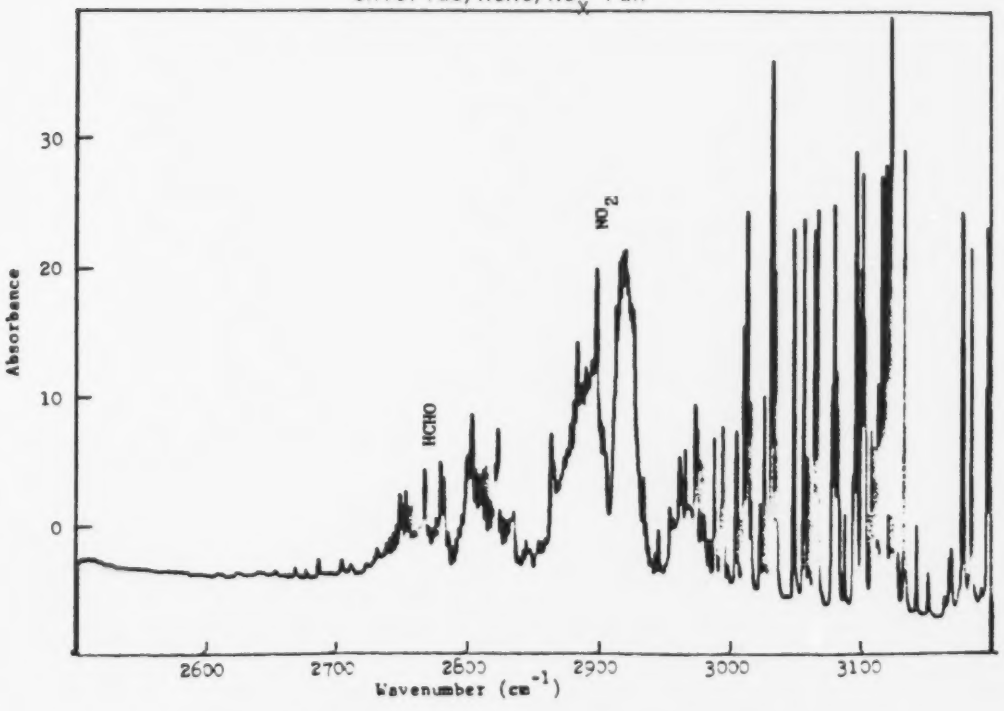

Figure 24b. InSb spectrum of vinylidene chloride 7-min irradiation

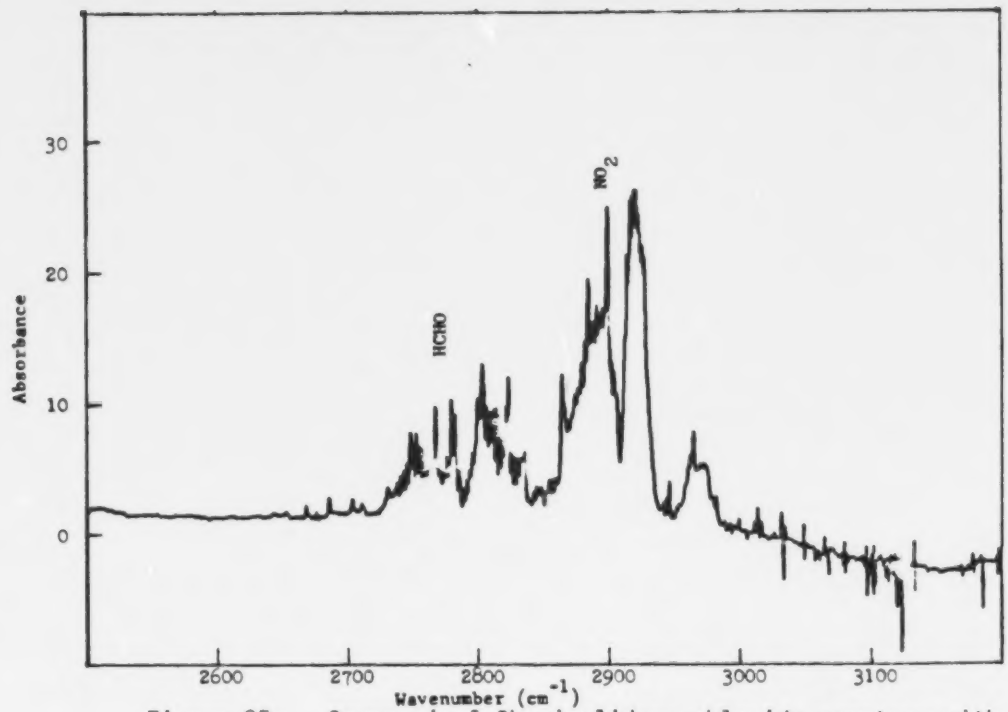

Figure 25a. Seven-min InSb vinylidene chloride spectrum with vinylidene chloride and water subtracted

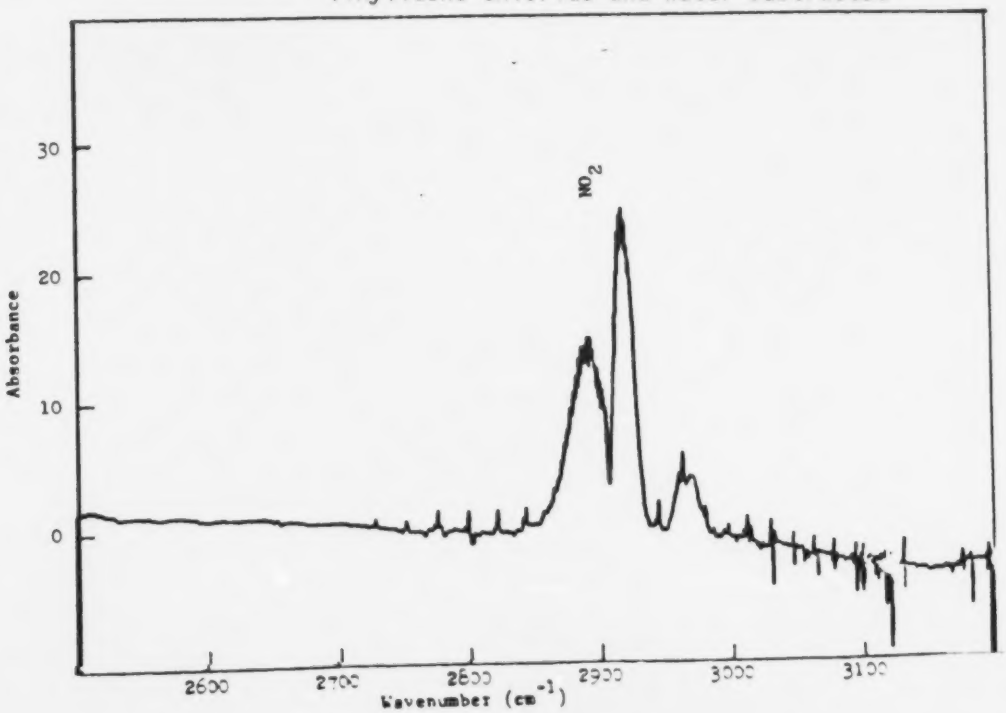

Figure 25b. Seven-min InSb vinylidene chloride spectrum with vinylidene chloride, water, and formaldehyde subtracted

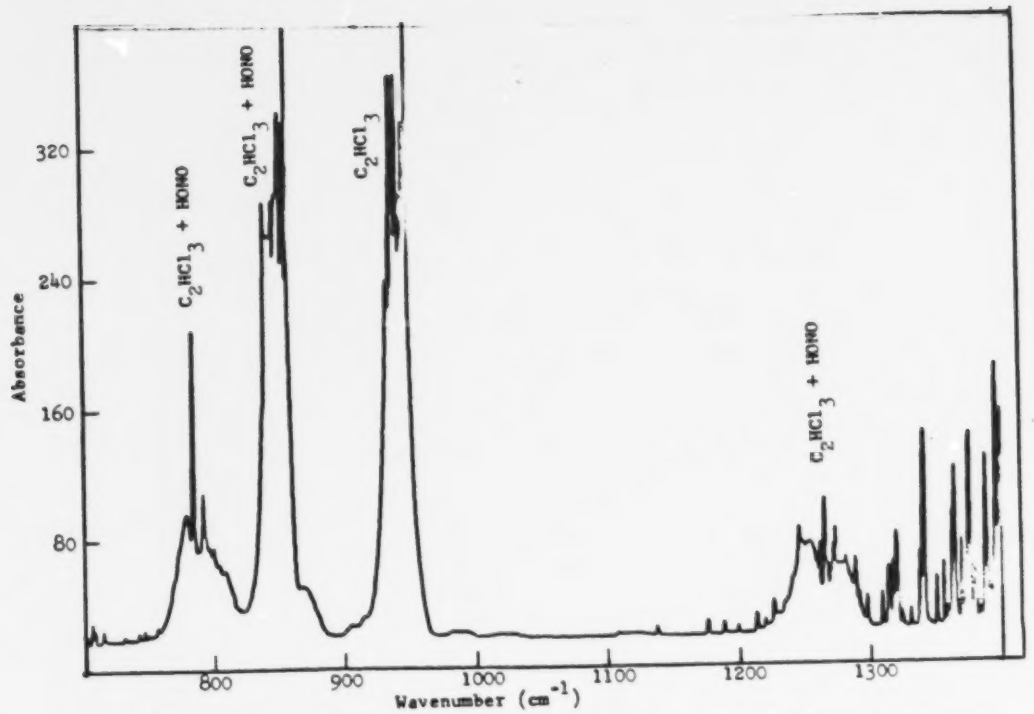

Figure 26a. MCT spectrum of reactants of trichloroethylene HONO/NO_x run

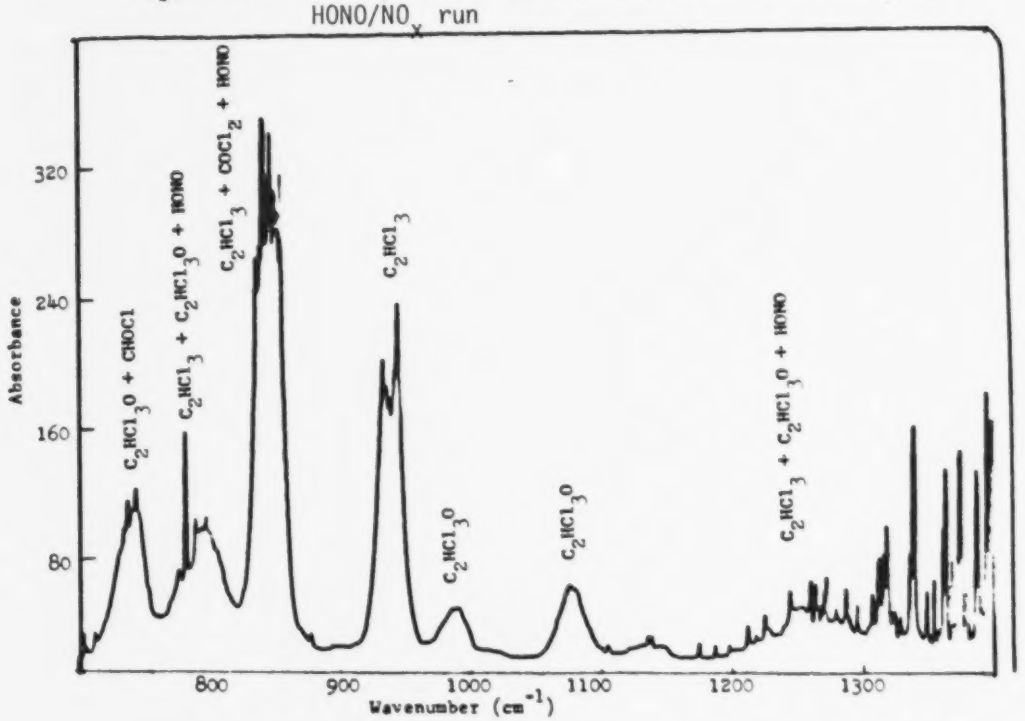

Figure 26b. MCT spectrum of trichloroethylene 15-min irradiation

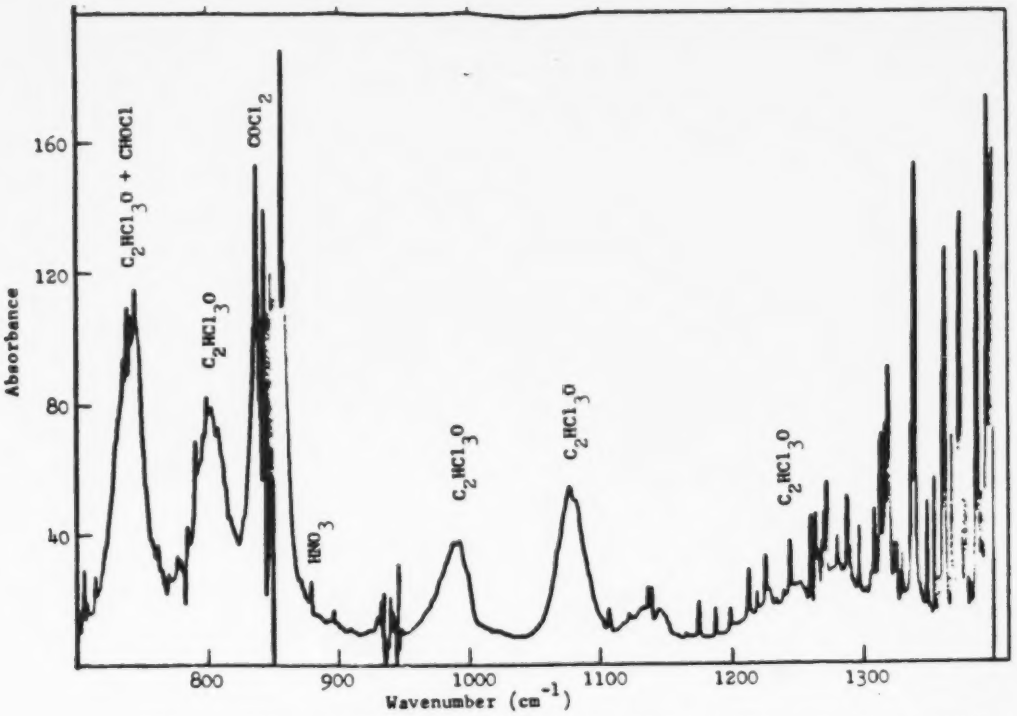

Figure 27a. Fifteen-Min MCT trichloroethylene spectrum with trichloroethylene subtracted

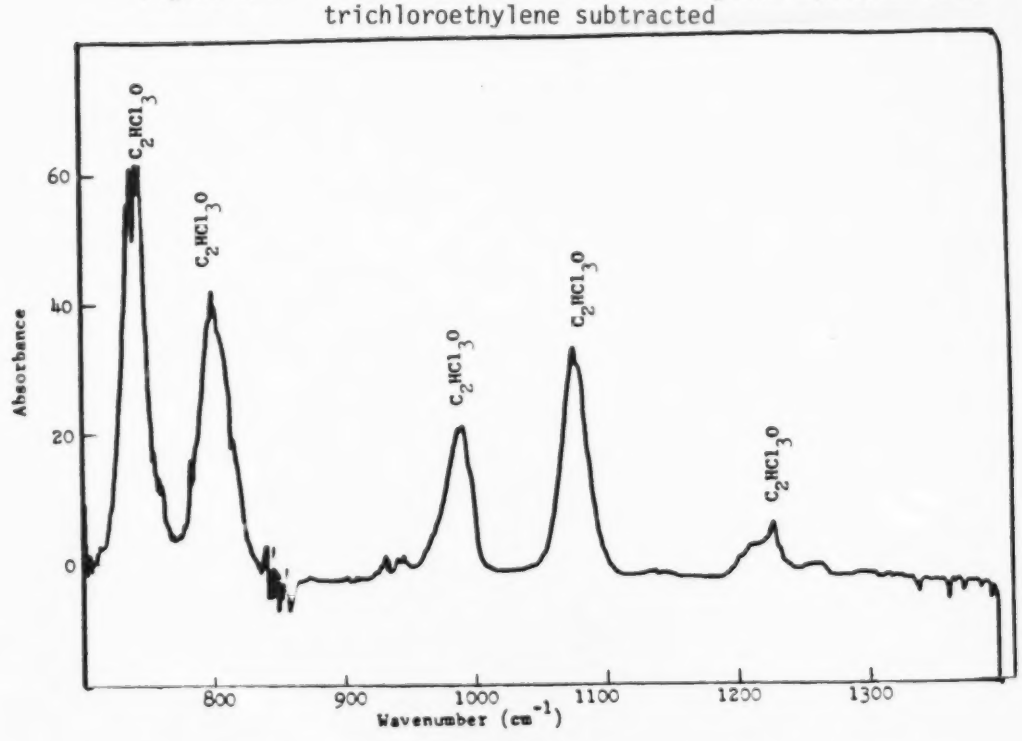

Figure 27b. MCT spectrum of dichloroacetyl chloride

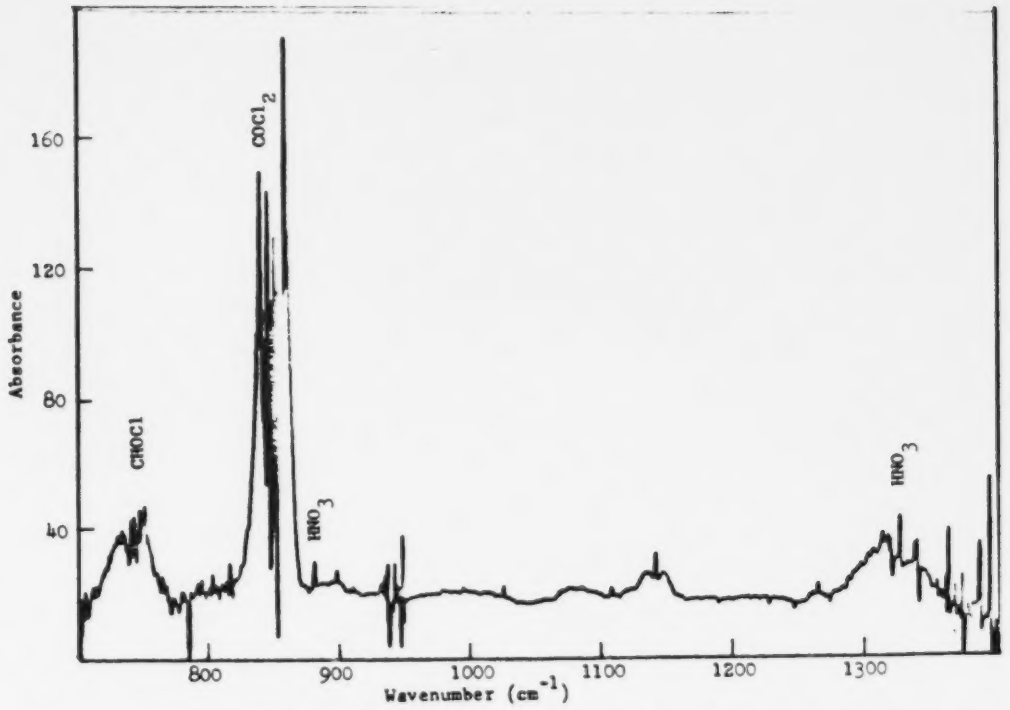

Figure 28a. Fifteen-min MCT trichloroethylene spectrum with trichloroethylene, HONO, water, and dichloroacetyl chloride subtracted

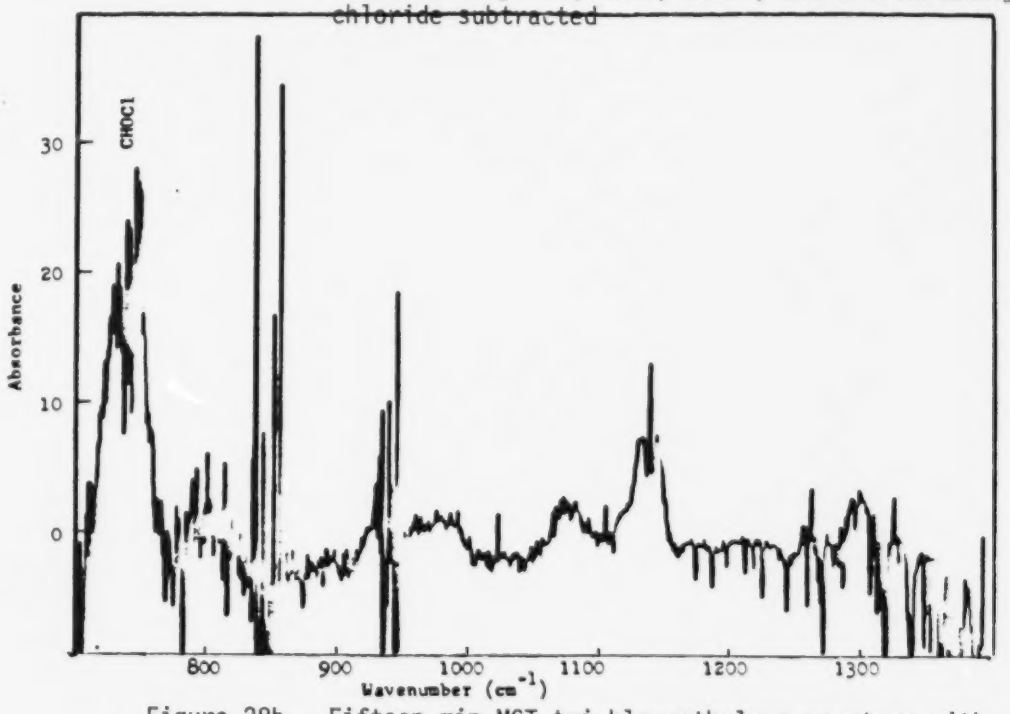

Figure 28b. Fifteen-min MCT trichloroethylene spectrum with trichloroethylene, HONO, water, dichloroacetyl chloride, and phosgene subtracted

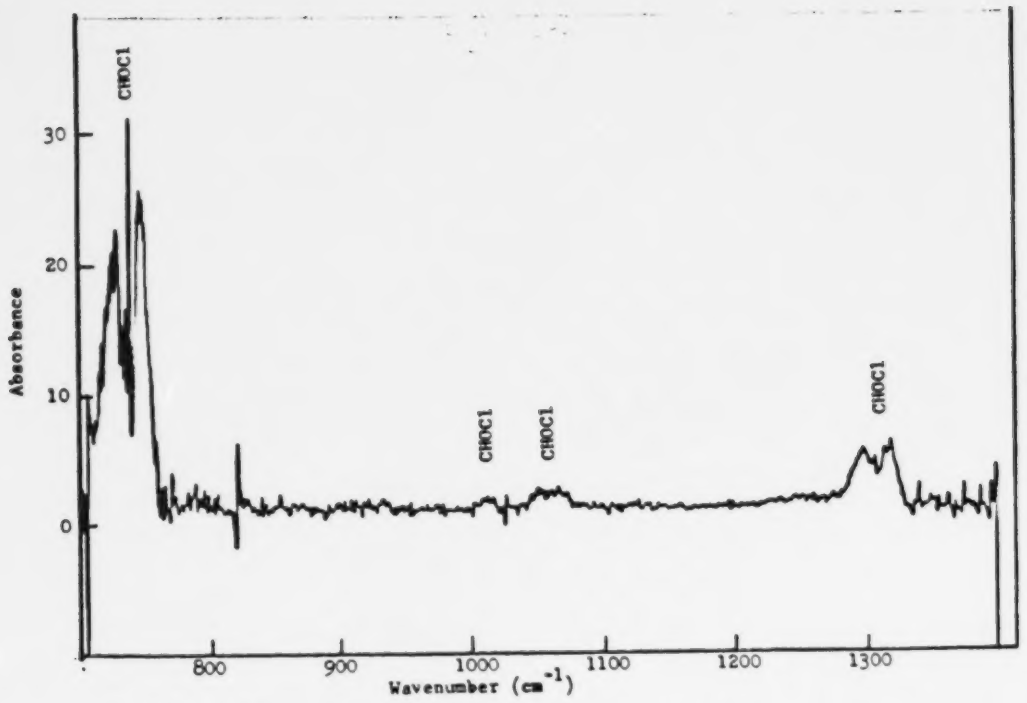

Figure 29a. MCT spectrum of formyl chloride

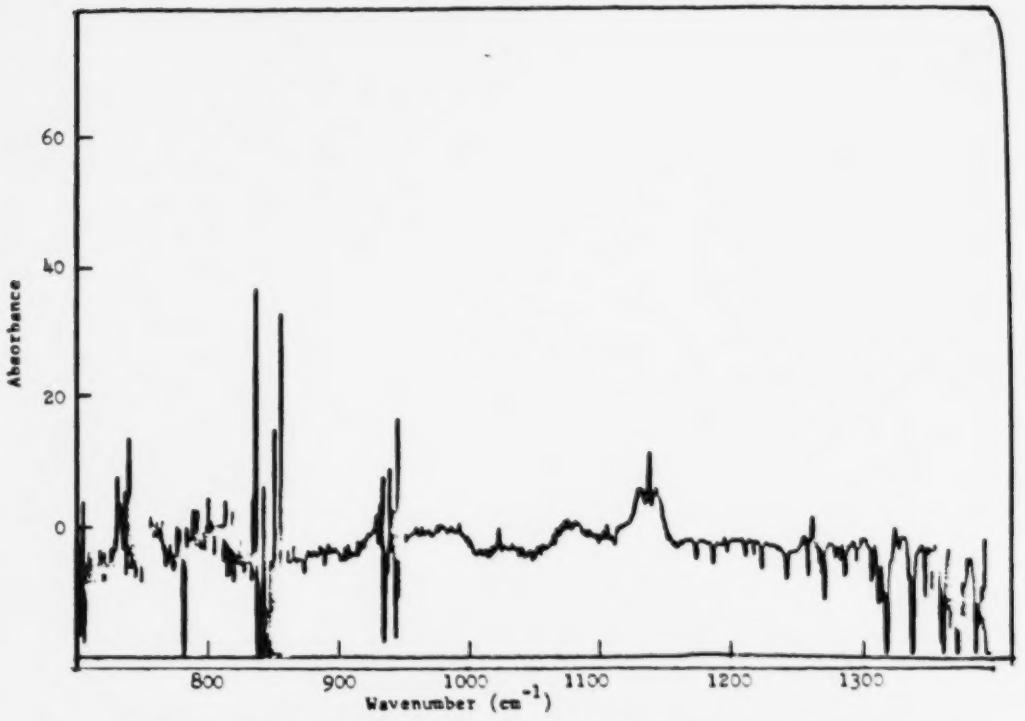

Figure 29b. Fifteen-min MCT trichloroethylene spectrum with trichloroethylene, HONO, water, dichloroacetyl chloride, phosgene, and formyl chloride subtracted

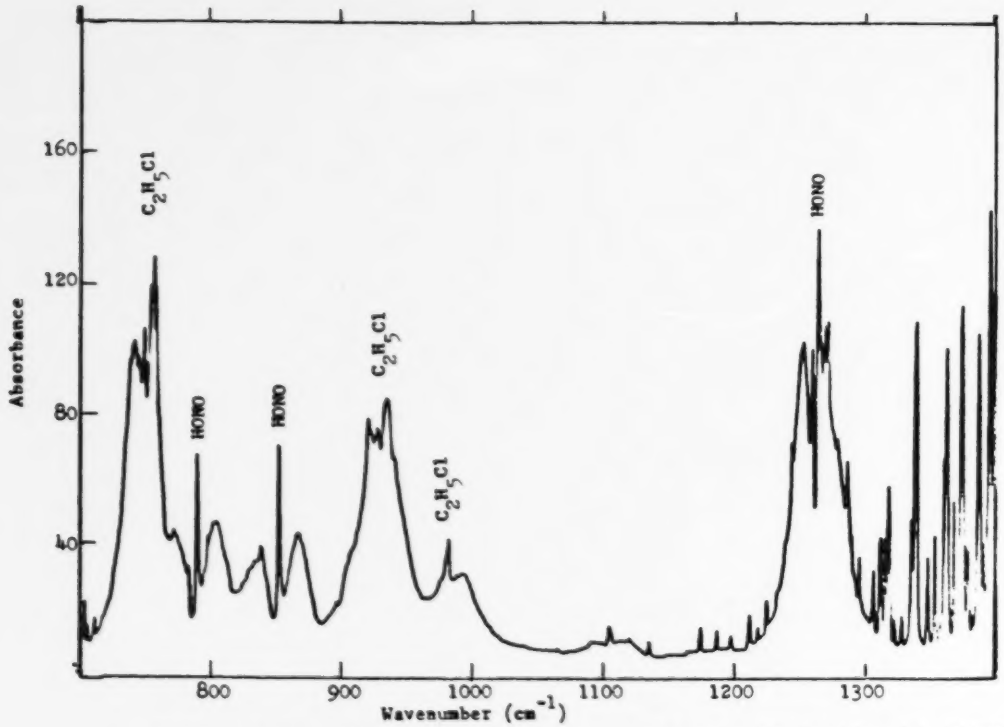

Figure 30a. MCT spectrum of reactants of allyl chloride/HONO/NO_x run

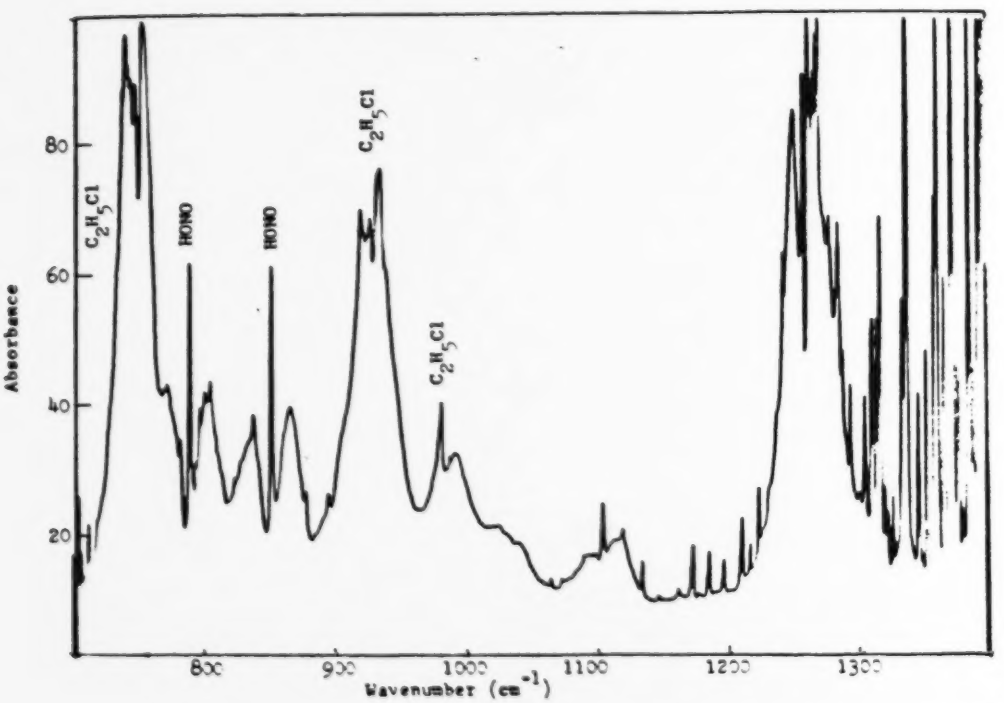

Figure 30b. MCT spectrum of allyl chloride 5-min irradiation

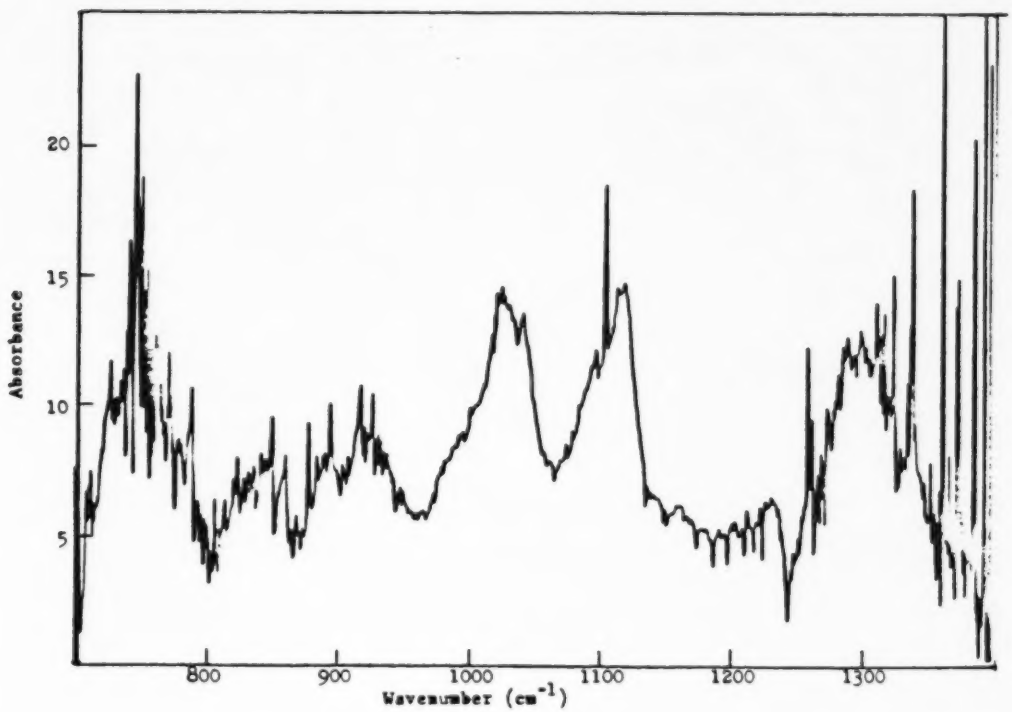

Figure 31a. Five-min MCT allyl chloride spectrum with HONO, allyl chloride, and water subtracted

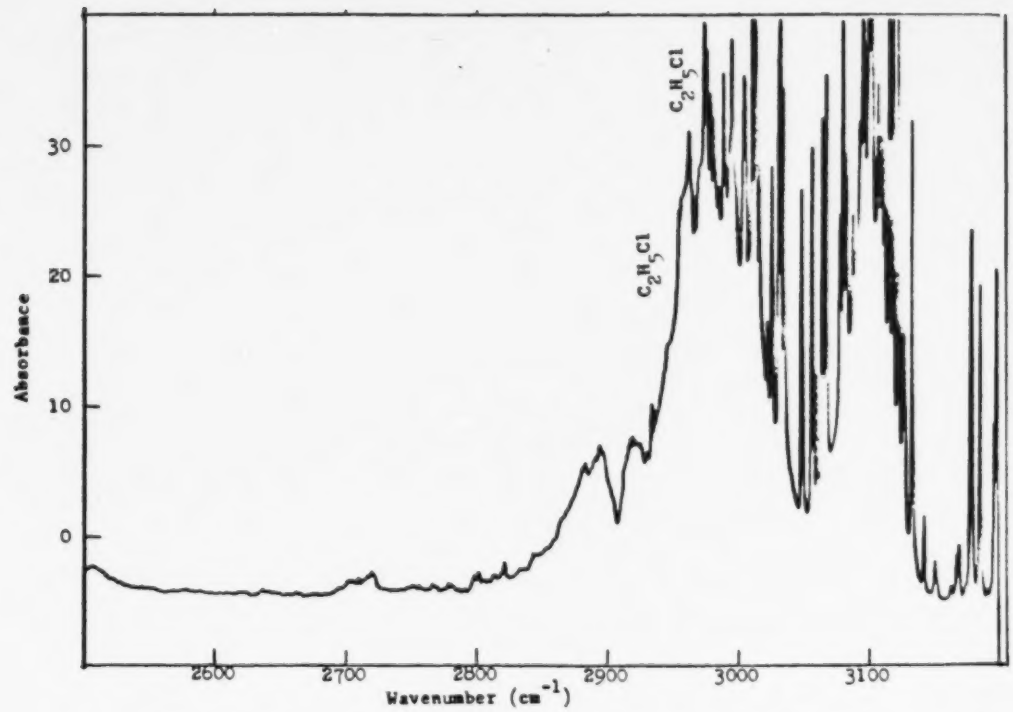

Figure 32a. InSb spectrum of reactants of allyl chloride/HONO/NO_x run

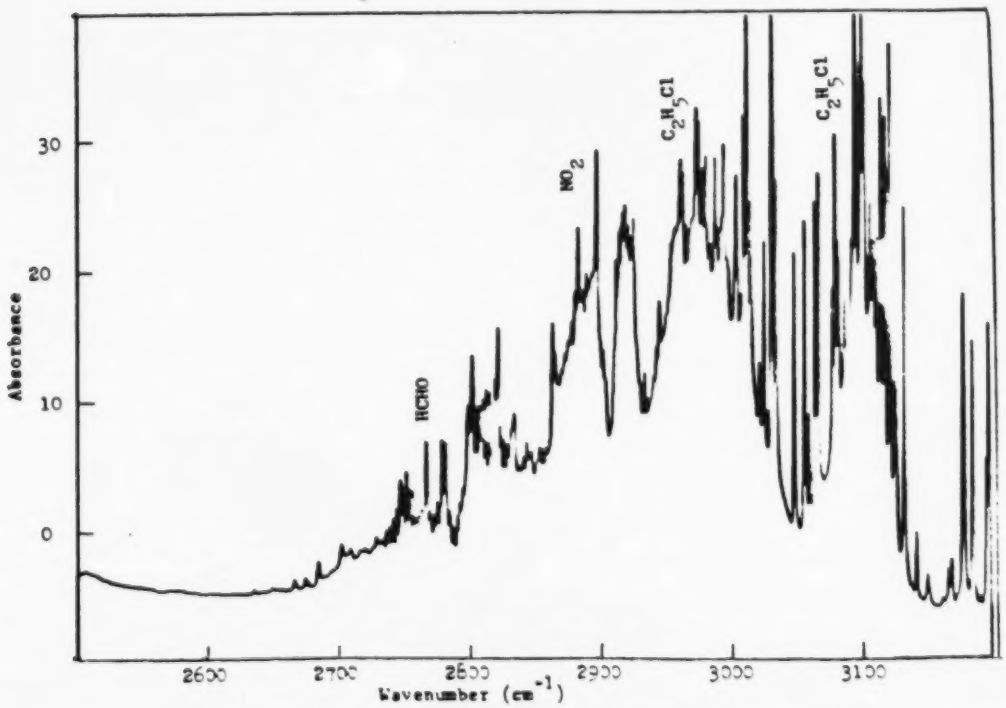

Figure 32b. InSb spectrum of allyl chloride 5-min irradiation

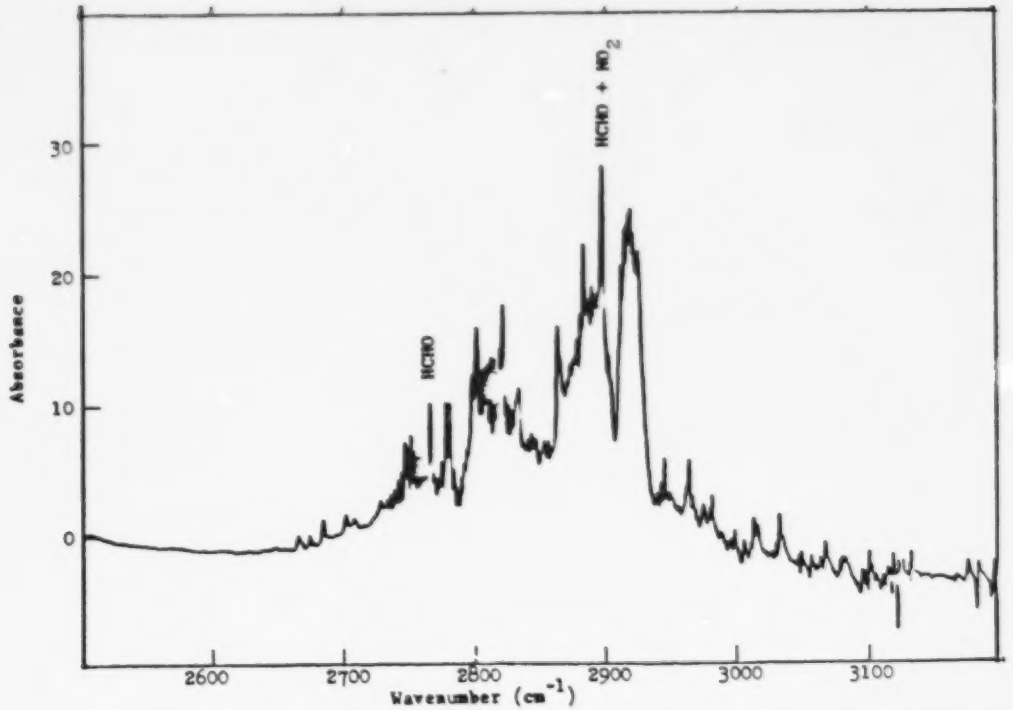

Figure 33a. Five-min InSb allyl chloride spectrum with water and allyl chloride subtracted

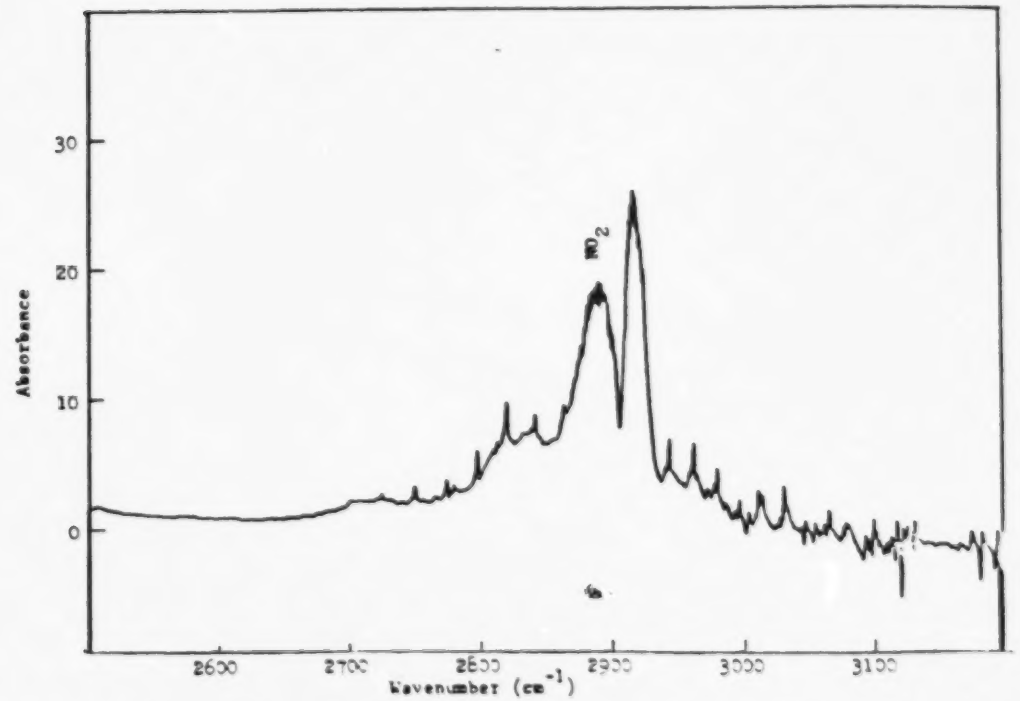

Figure 33b. Five-min InSb allyl chloride spectrum with water allyl chloride and formaldehyde subtracted

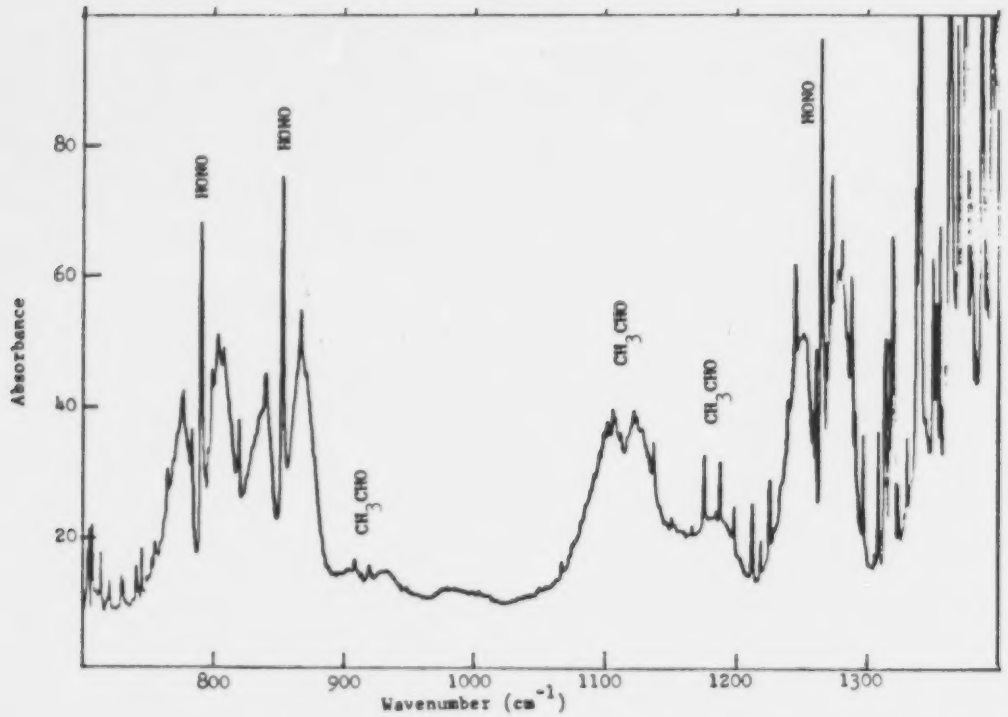

Figure 34a. MCT spectrum of reactants of acetaldehyde/HONO/NO_x run

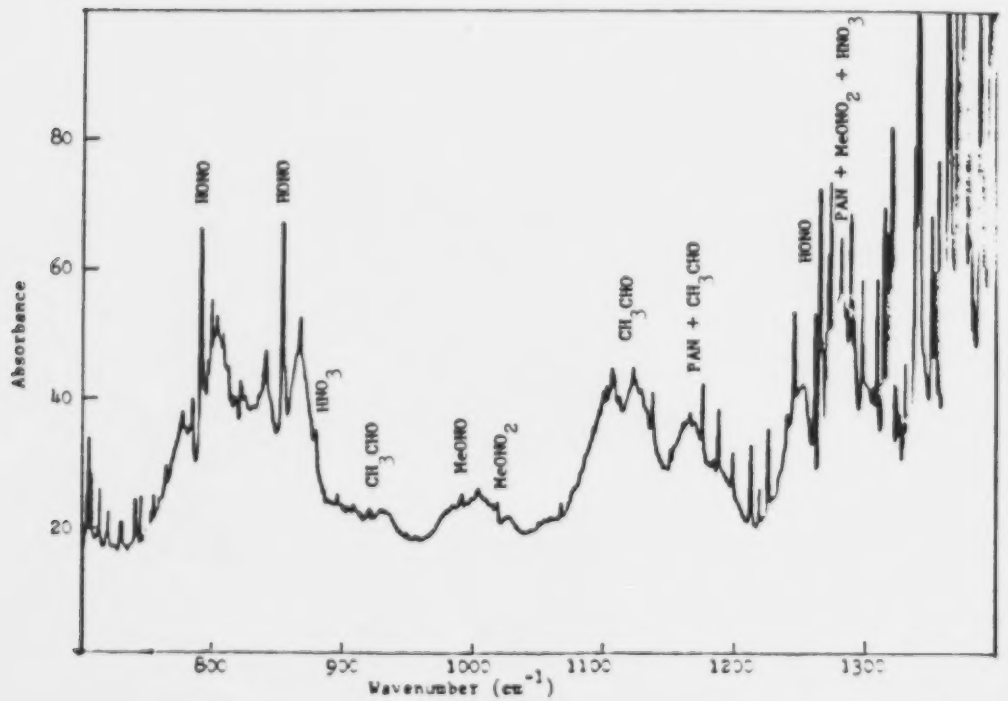

Figure 34b. MCT spectrum of acetaldehyde 10-min irradiation

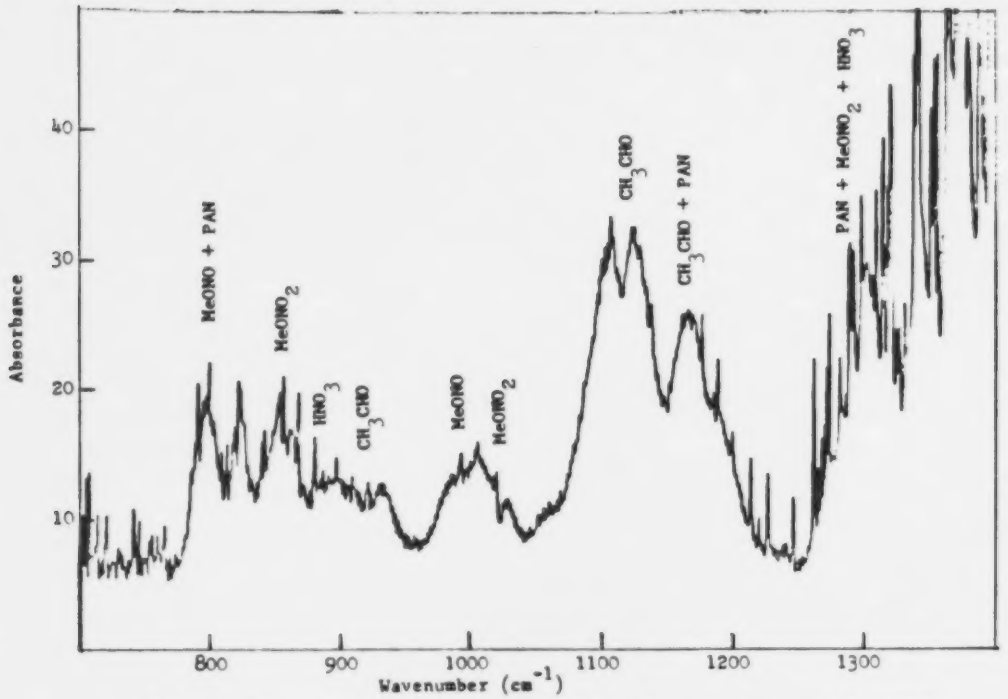

Figure 35a. Ten-min MCT acetaldehyde spectrum with HONO subtracted

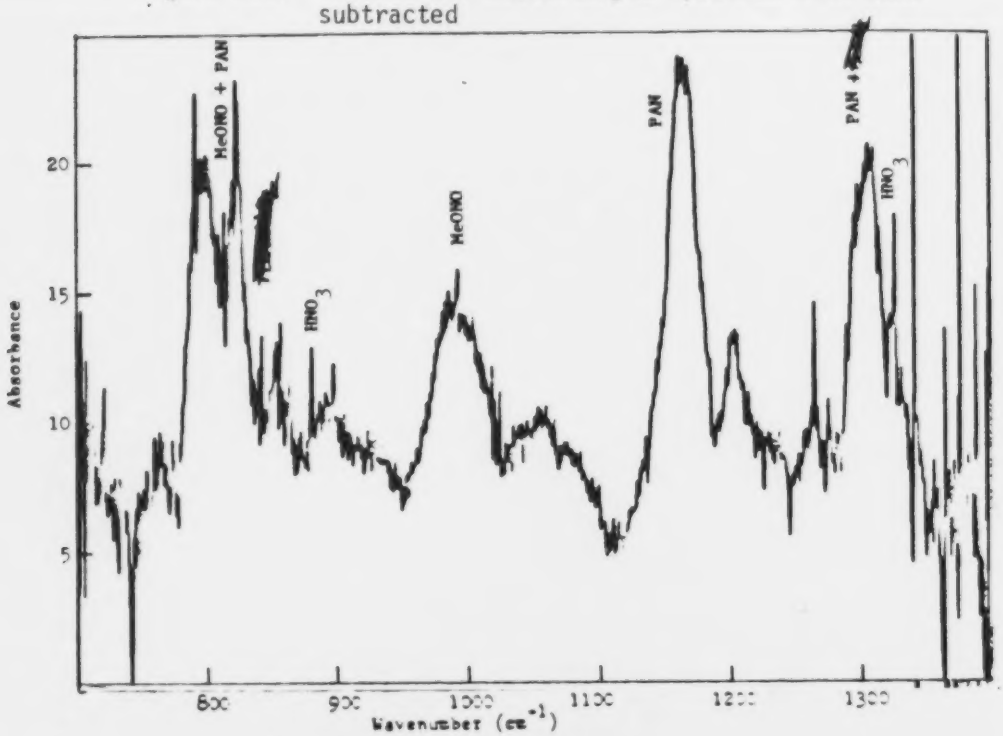

Figure 35b. Ten-min MCT acetaldehyde spectrum with HONO, methyl nitrate, acetaldehyde, and water subtracted

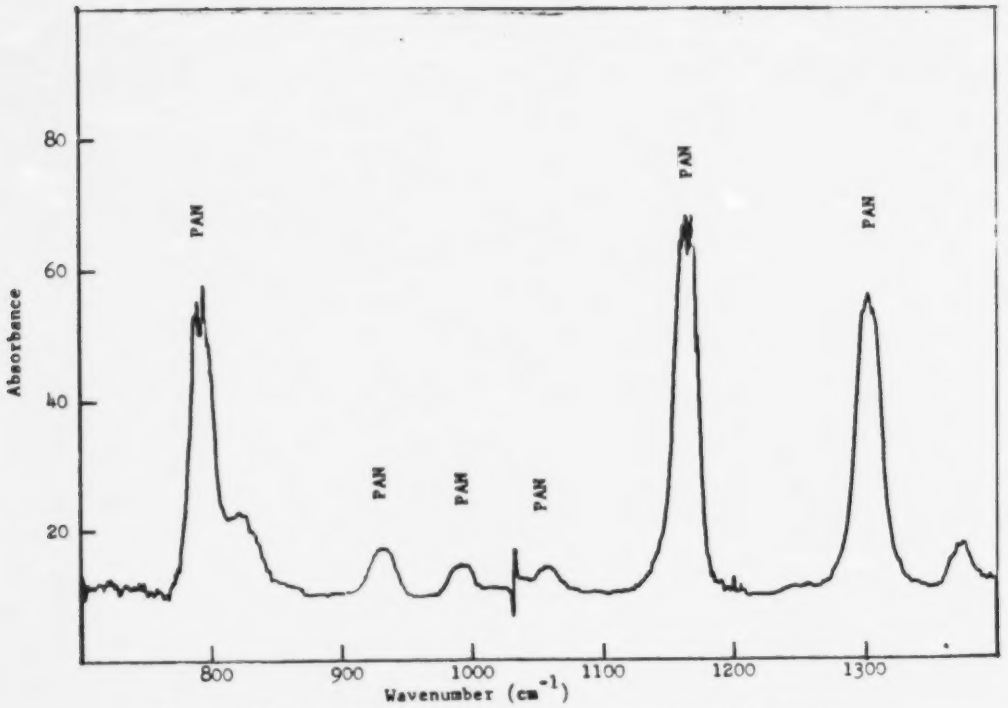

Figure 36a. MCT spectrum of peroxy acetyl nitrate

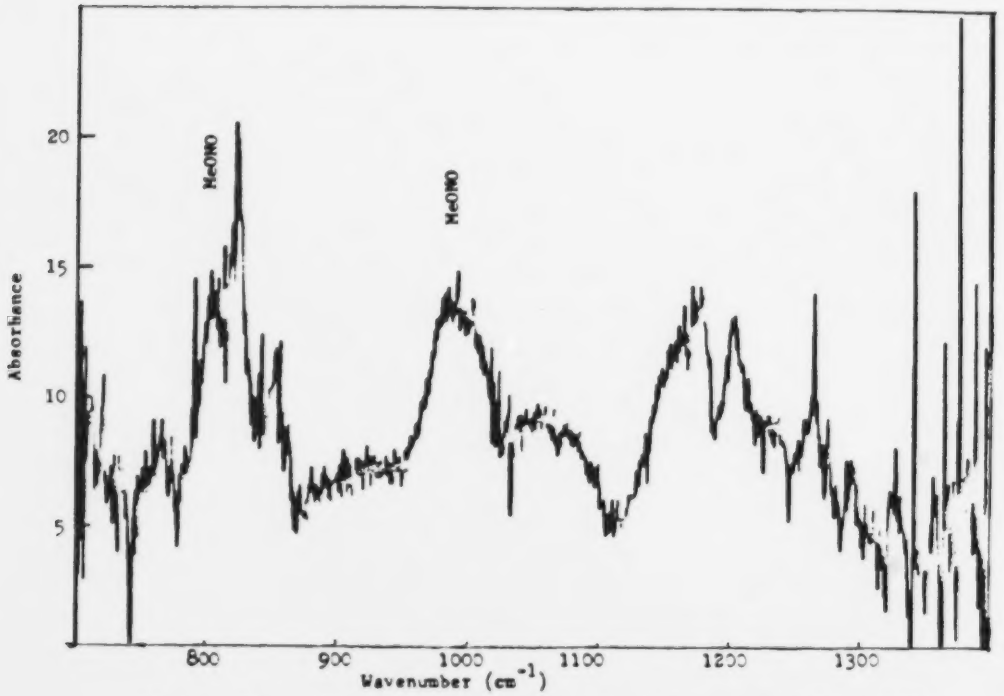

Figure 36b. Ten-min MCT acetaldehyde spectrum with HONO, acetaldehyde, water, HNO_3, and peroxy acetyl nitrate subtracted

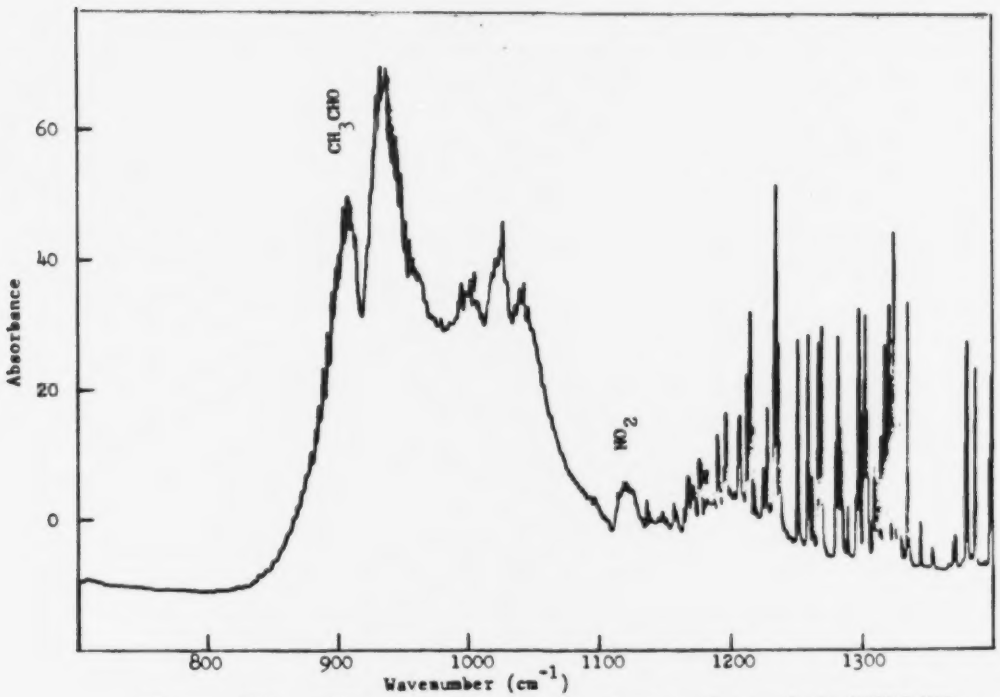

Figure 37a. MCT spectrum of reactants of acrolein/HONO/NO_x run

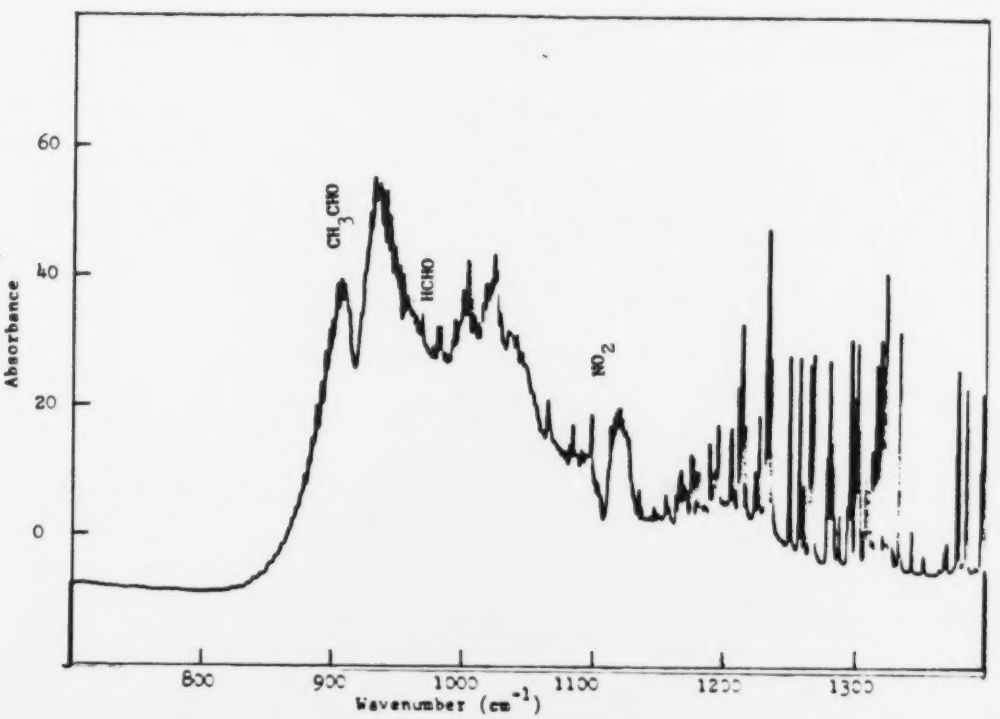

Figure 37b. MCT spectrum of acrolein four-min irradiation

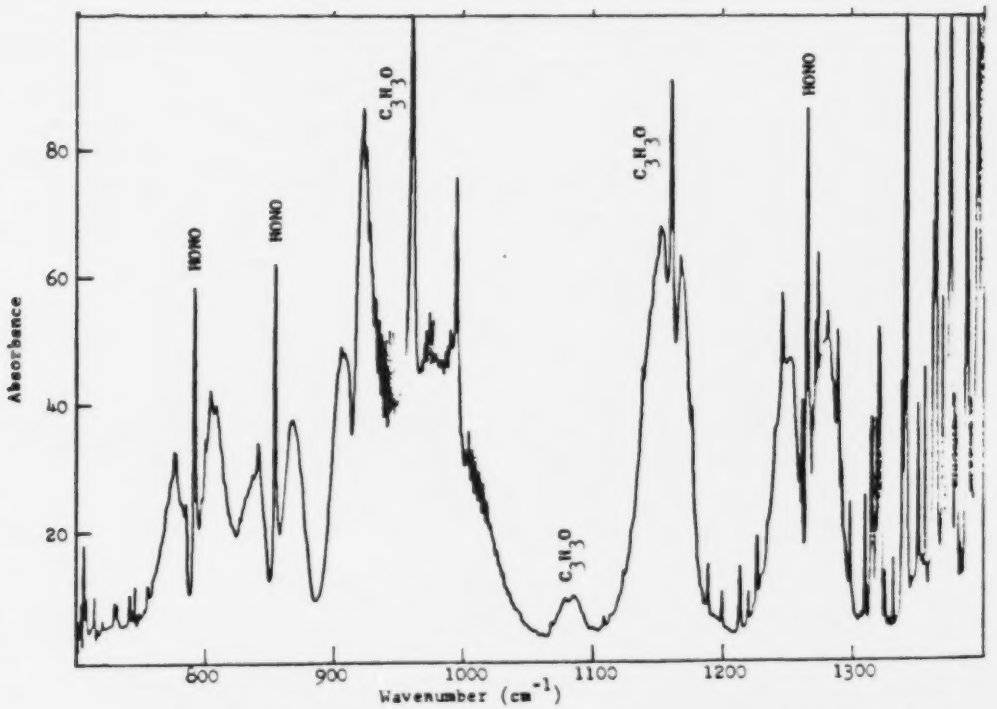

Figure 38a. Four-min MCT acrolein spectrum with acrolein, HONO, water, and HNO_3 subtracted

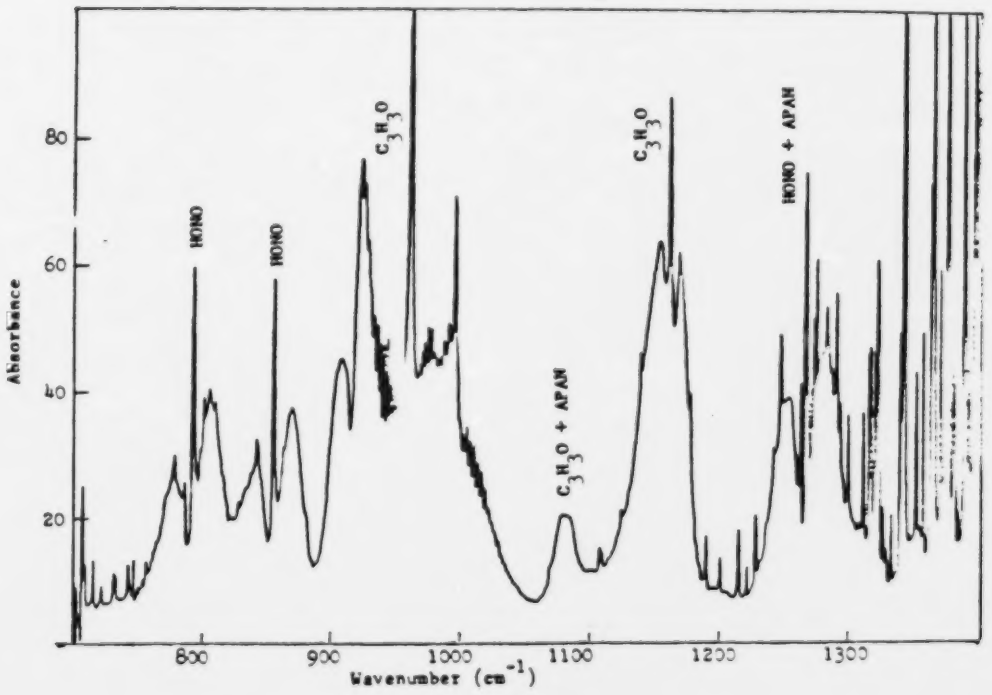

Figure 38b. MCT spectrum of APAN

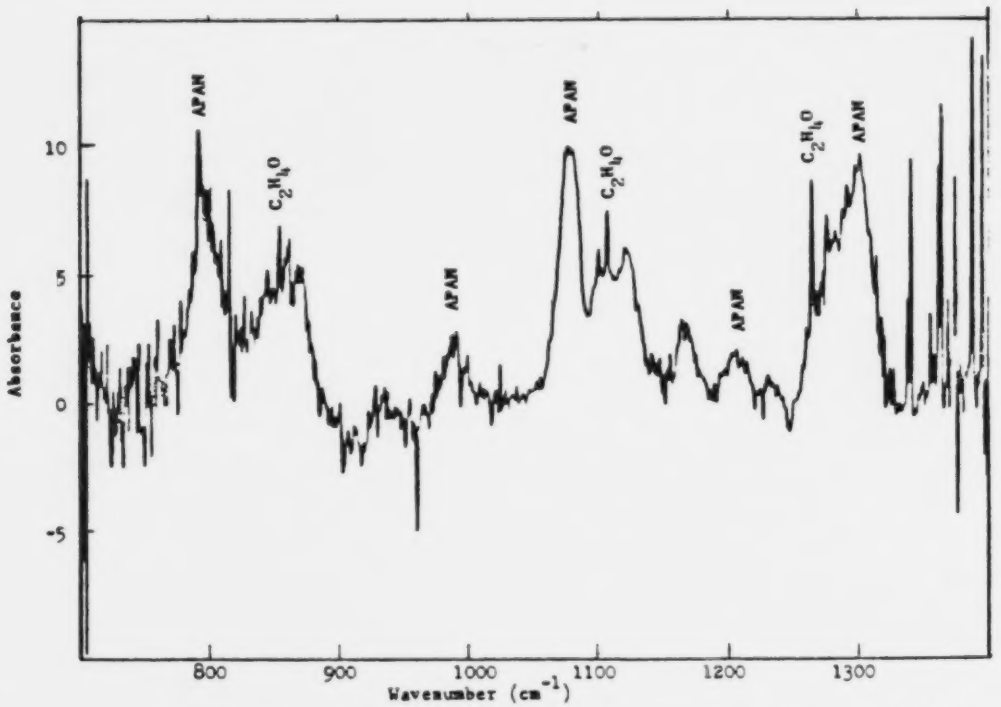

Figure 39a. Four-min MCT acrolein spectrum with acrolein, HONO, water, and HNO_3 subtracted

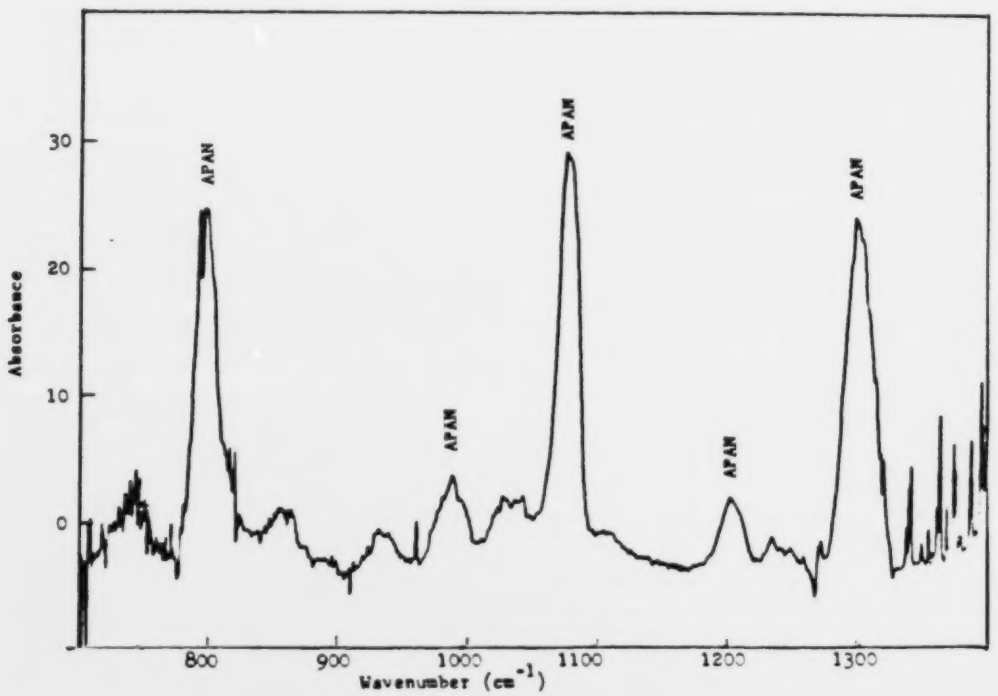

Figure 39b. MCT spectrum of APAN

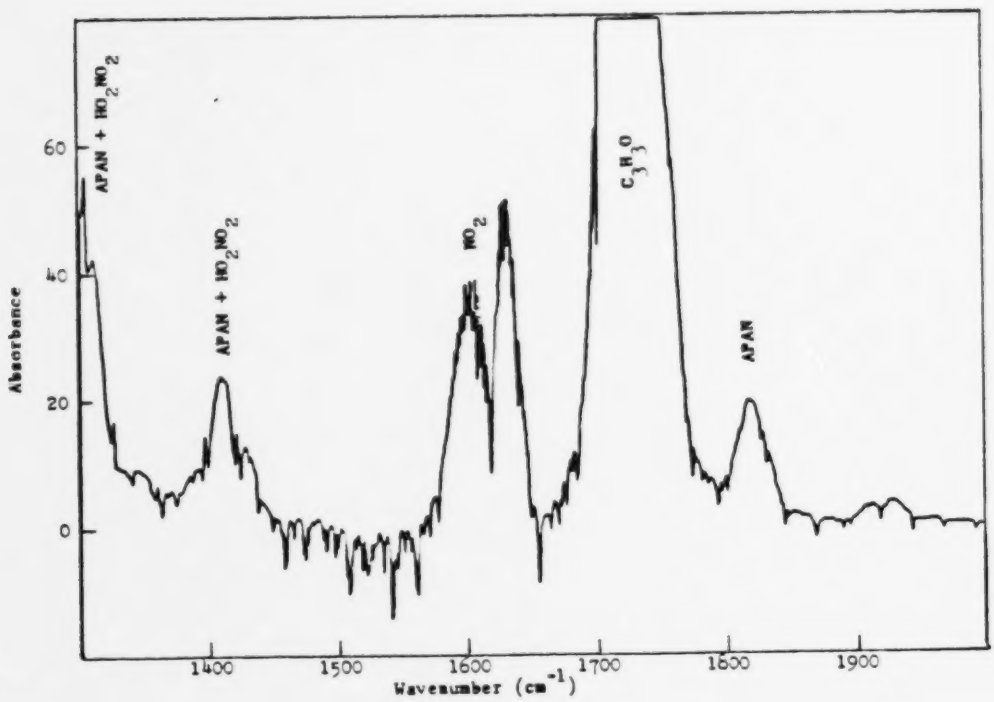

Figure 40a. MCT spectrum of APAN, acrolein, NO_2, and peroxy nitric acid

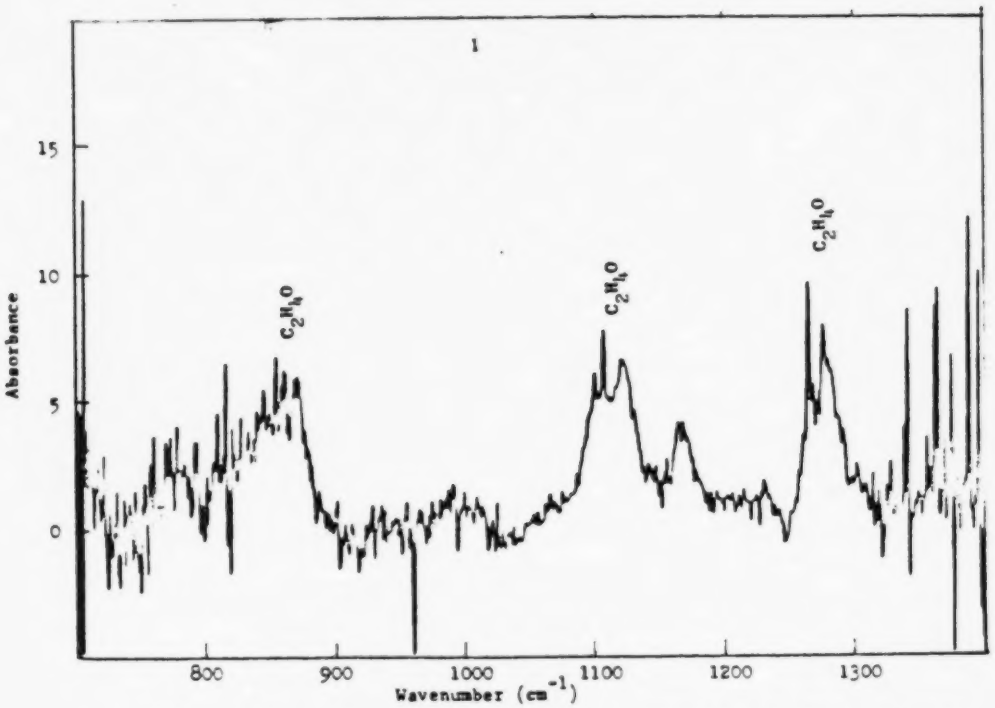

Figure 41a. Four-min MCT acrolein spectrum with acrolein, HONO, water, HNO_3, and APAN subtracted

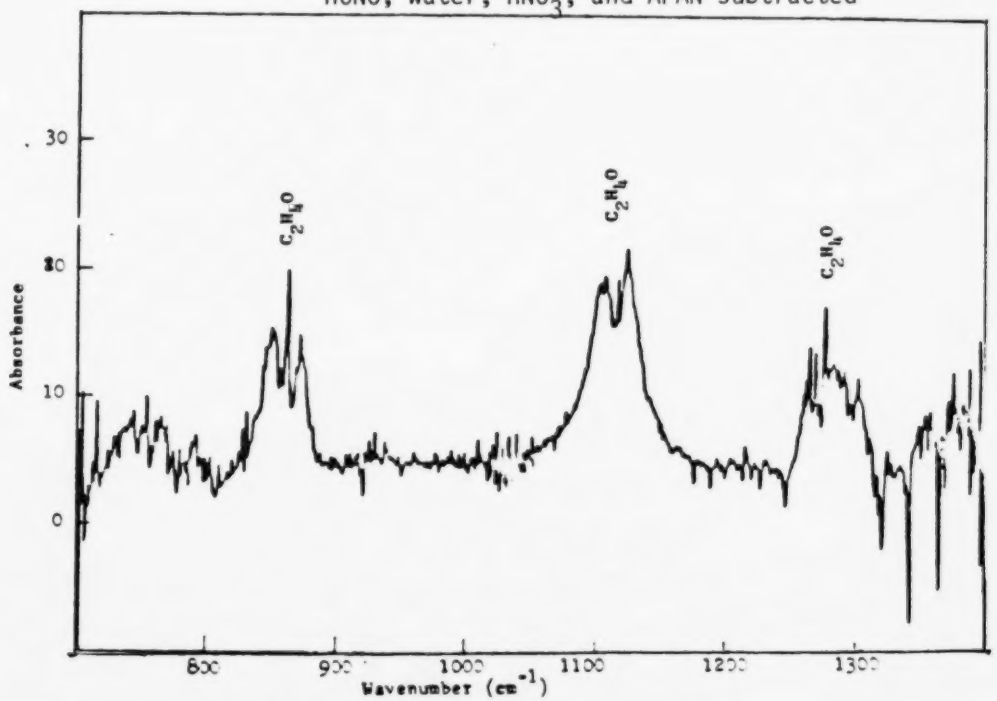

Figure 41b. MCT spectrum of glycoaldehyde

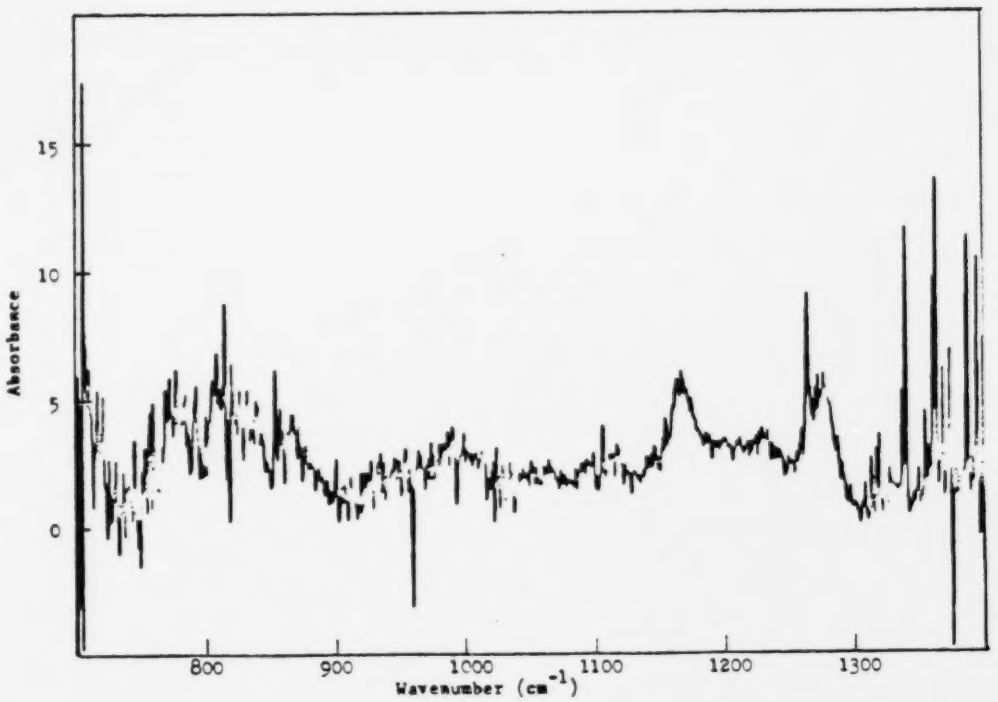

Figure 42a. Four-min MCT acrolein spectrum with acrolein, HONO, water, HNO_3, APAN, and glycoaldehyde subtracted

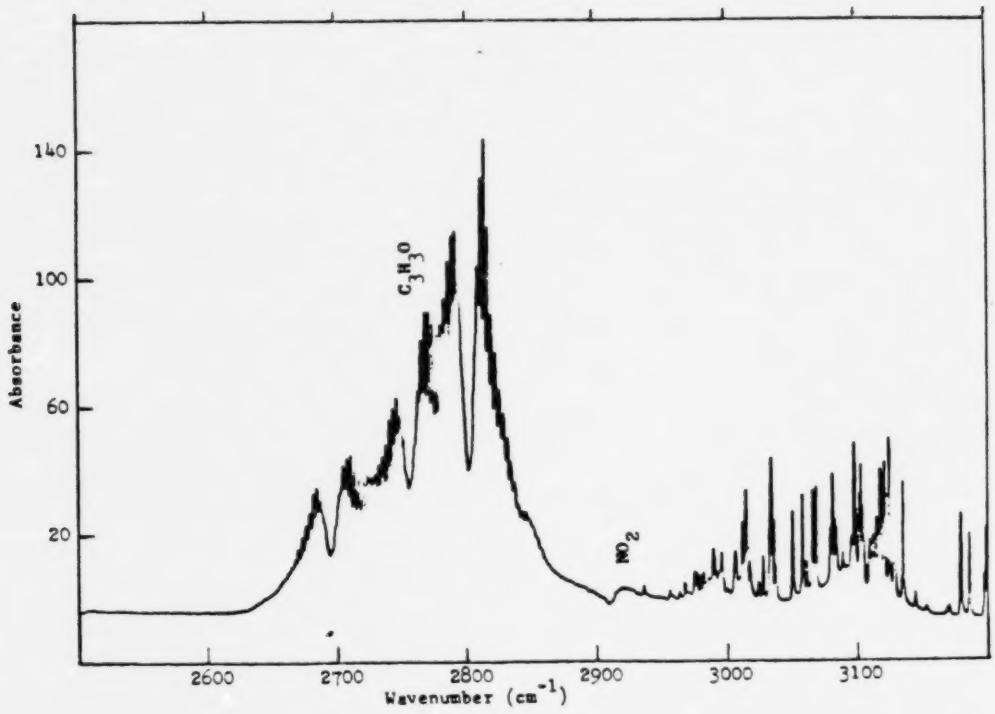

Figure 43a. InSb spectrum of reactants of acrolein/HONO/NO_x run

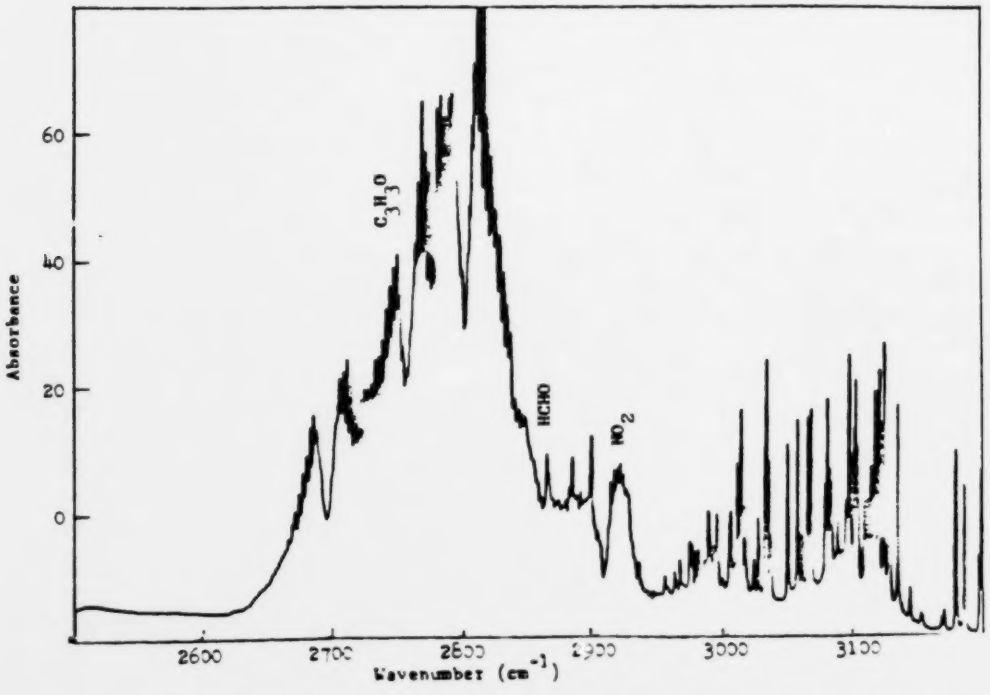

Figure 43b. InSb spectrum of acrolein four-min irradiation

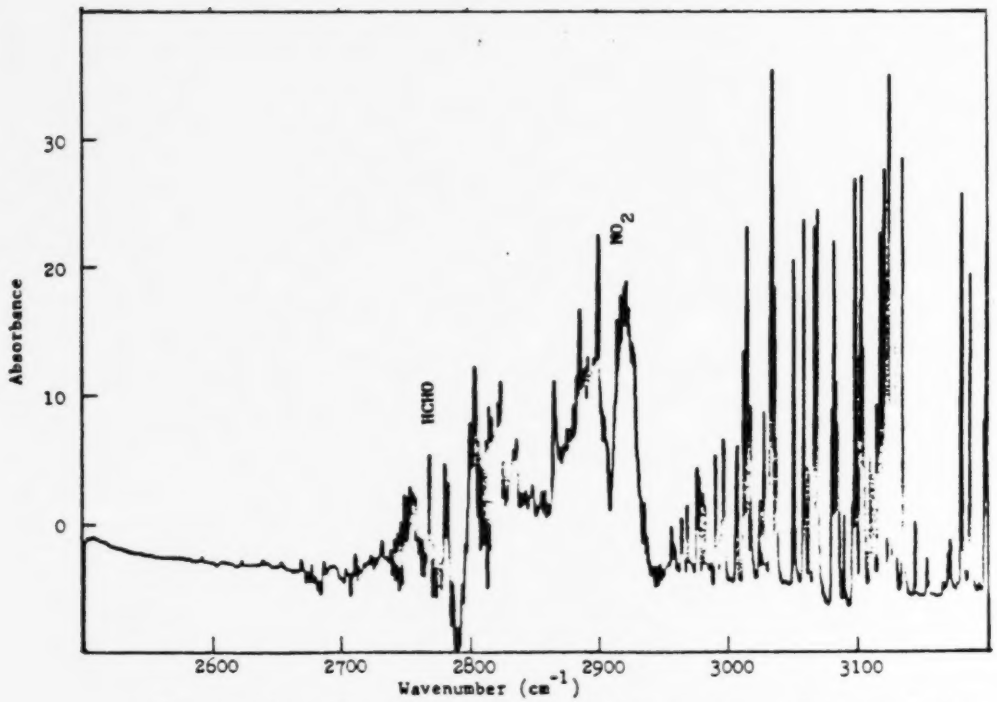

Figure 44a. Four-min InSb acrolein spectrum with acrolein subtracted

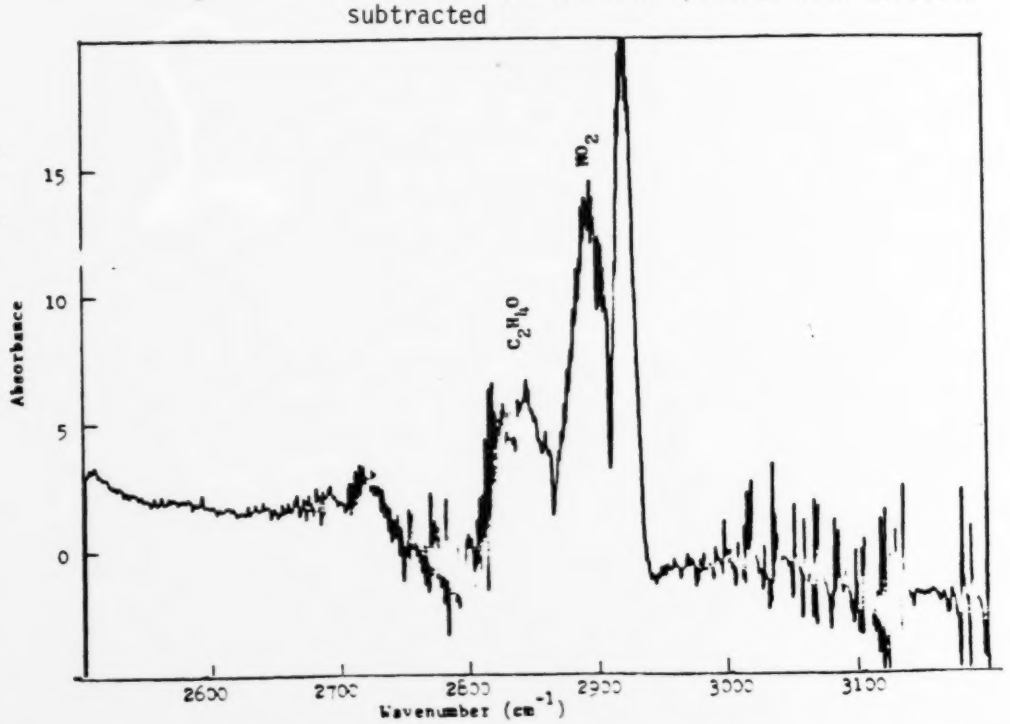

Figure 44b. Four-min InSb acrolein spectrum with acrolein, water, and formaldehyde subtracted

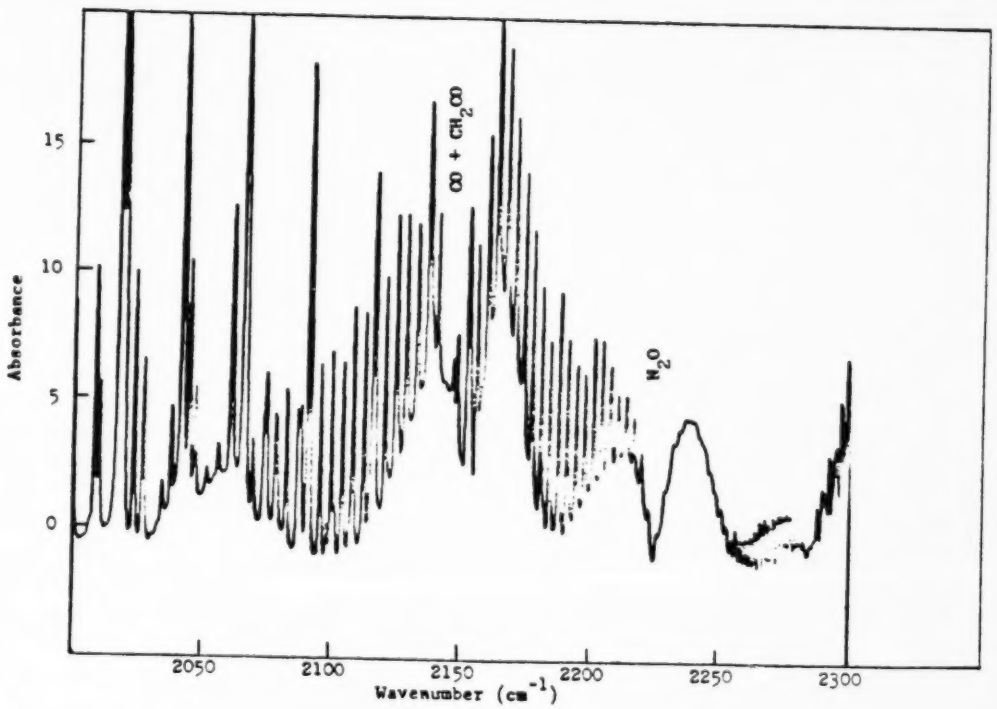

Figure 45a. InSb spectrum of acrolein four-min irradiation